IRRIGATION AREAS AND IRRIGATION WATER CONSUMPTION IN THE UPPER ILI CATCHMENT, NW-CHINA

from

THOMAS CHRISTIANSEN[1] and URSULA SCHÖNER[2]

Nr. 20, Giessen, September 2004

1 Department of Geography, Justus-Liebig-University Giessen,
Senckenbergstraße 1,
D – 35390 Gießen, Germany
http://www.uni-giessen.de/geographie/mitarbeiter/christiansen/christiansen.htm

2 Bureau for Environment Assessment, Giessen
Karl-Benner-Straße 10,
D - 35396 Gießen, Germany
http://www.uni-giessen.de/geographie/phy/akn/teiln/schoener.htm

PREFACE

The present study was compiled within the framework of the research project "*Water shortage, water use conflicts and water management in arid environments of Central Asia*". The objective of this research is to analyse the causes and the effects of the growing water shortage and the increasing deterioration of the water quality in this area. The research activities compare the situation in four inland basins of Central Asia: the Aral Lake, the Ili-Balkhash Basin, the Issyk-Kul Basin, and the Tarim Basin. The following study investigates the Upper Ili Catchment and is thus part of the research component which focuses on the Ili-Balkhash Basin. These studies are compiled and coordinated by Prof. Dr. A.A. Tursunov and Prof. Dr. Ž.D. Dostaj of the "Department of Geography" of the Kazakhian Academy of Sciences and Dr. M.Ž. Burlibaev, Director of the "Kazakhian Research Institute for Environment and Climate Monitoring". Their research results will be translated and published in a summarised form at a later point in time.

This study was mainly based on the interpretation of satellite imagery, supported by only limited field truth data. This approach had to be followed because only very little information on the Upper Ili Catchment was available to the research team. At the same time, however, detailed information on the Upper Ili Basin is essential for the overall framework of this project. The Upper Ili catchment is the main source of the water discharged to the Ili-Balkhash Basin which is mainly located on Kazakhian territory. Hence, the water balance of the Ili-Balkhash Basin crucially depends on the water supply from the Upper Ili region.

This four-year research project was made possible by a grant of the Volkswagen Foundation as part of the support initiative "Central Asia / Caucasia in the focus of science" ("Mittelasien / Kaukasus im Fokus der Wissenschaft"). I am very grateful for this support.

Giessen, September 2004 Prof. Dr. Ernst Giese
(Project Manager)

ACKNOWLEDGEMENTS

As mentioned above, the present study is a component of a larger research programme, which is funded by a grant of the Volkswagen Foundation. The authors would like to express their appreciation and gratitude for this support. We would also like to thank Prof. Dr. Ernst Giese, the project initiator and head of the research project mentioned above. Prof. Giese initiated this study and made the required resources available. He also drafted a major part of Chapter 1, including Figures 1 – 4.

Due to various constraints, we could not conduct the fieldwork for the satellite image interpretation ourselves. Instead, the required field truth data were collected by Chinese colleagues from the University Urumqi. We would like to express our gratefulness for this help and for the excellent co-operation to Prof. Dr. Hamid Yimit and his team from the College of Resource & Environmental Science, Xinjiang University / Urumqi. Their assistance was crucial for the study progress and is much appreciated. Most of the cartography of the included figures and maps was done by our cartographers, Lisett Ritter and Bernd Goecke. We would like to thank both for their efforts and their patience with the numerous corrections and modifications. We further would like to express our gratitude to Dr. H.-U. Wetzel, from the GeoForschungs-Zentrum (GFZ) Potsdam who gave very valuable advice in the initial stages of the study. Finally, we would like to thank Dipl.-Geogr. Thomas Gumm who conducted the satellite image search and part of the tedious digitizing work.

Gießen, September 22, 2004 Dr. Thomas Christiansen / Dipl.-Geogr. Ursula Schöner

Contact address:

Dr. Thomas Christiansen, Dept. of Geography, Justus-Liebig-University, D – 35390 Gießen, Germany, ☎ ++49-641-99-36290, Email: thomas.christiansen@geogr.uni-giessen.de

Dipl.-Geogr. Ursula Schöner, Büro für Umweltbewertung, Karl-Benner-Str. 10, 35396 Gießen, ☎ ++49-641-641-54716, Email: u.schoener@umweltbewertung.de

TABLE OF CONTENTS

LIST OF TABLES

LIST OF FIGURES

LIST OF PHOTOS

LIST OF ACRONYMS AND ABBREVIATIONS

BCS "Best Case Scenario"

CDS "Chinese Data Scenario"

DN Digital number (dimensionless value (usually between 0 – 255) which indicates the reflection strength in a particular satellite band)

ETM+ Enhanced Thematic Mapper (improved thematic mapper instrument onboard the Landsat 7 satellite; includes a panchromatic mode with 15 x 15 m pixels)

LCS "Likely Case Scenario"

TM Thematic Mapper (standard scanner instrument onboard the second generation Landsat satellites; 30 x 30 m pixels)

MSS Multispectral Scanner (standard scanner instrument of the first Landsat satellites (1 – 3); 79 x 79 m pixels

WCS "Worst Case Scenario"

EXECUTIVE SUMMARY

The present study investigates the water consumption for irrigation purposes in the Upper Ili region in NW-China, located between 42° - 44° north and 80° - 85° east. This report is part of an international research project which focuses on "*Water shortage, water use conflicts and water management in arid environments of Central Asia*". The project is funded by the Volkswagen Foundation (VW-Project Az: II/76927).

The Upper Ili catchment covers a triangular-formed area of about 55,000 sqkm. Two high mountain ranges, running NW-SE and NE-SW respectively, delimit the area to the north and south. The western boundary is the international border between China and Kazakhstan. The area consists of two main sub-catchments: the Tekes catchment in the southern part and the Kunes / Kash catchment in the northern part respectively. From the confluence of Kunes and Kash in the centre of the study area, the river is called "Ili" (cp. Fig. 1 and Fig. 3). The Ili area is part of the province of Xinjiang in the Uygur Autonomous Region, it includes nine counties with a total population of about two million. The main city is Yining in the north-west corner of the area.

About 150 km east of the Chinese-Kazakhian border, the Ili discharges its water into the Kapchgaj reservoir. It leaves the reservoir again at its western end and continues its course until it eventually ends in the Lake Balkhash, one of the biggest inland lakes in Central Asia.

The climate in the Upper Ili area is extremely continental: very cold, long winters and very hot, dry summers. The yearly rainfall varies between about 200 and 500 mm only, depending on the respective altitude and topographical luff / lee effects. Due to the low rainfall, crop cultivation usually depends on full-scale irrigation. The exception from this rule is the upper part of the Tekes sub-catchment, where higher elevations lead to higher rainfall which enables rainfed cultivation. Dominant crops in the Upper Ili area are wheat, soybean, rape, sunflower, and maize. Some wetland rice cultivation areas occur as well. They are concentrated in very few isolated clusters along the Ili and Kunes.

The major diminution of the discharge volume of the Ili, which results from the increasing water consumption for irrigation in the Upper Ili area, will decrease the inflow into the Kapchagaj reservoir and thus eventually into the Lake Balkhash. According to scenario calculations, in the medium run, a considerably reduced inflow would put the lake's sensitive hydrological equilibrium off balance and, in the long run, the lake could possibly suffer a similar ecological disaster as the Aral Lake.

The present study was conducted to assess the accuracy and reliability of existing data on the extension of the irrigation areas and the resulting water consumption in the Upper Ili region. The underlying background was that various Chinese and Kazakhian sources give quite different estimations of the water quantities extracted from the Ili system. The present study aimed at clarifying this situation by establishing reliable reference data which are based on a systematic and transparent survey procedure.

The survey was mainly based on Landsat 7 ETM+ satellite images from 2000/2001. The results of this survey were later compared with Landsat 2 MSS images in order to assess the expansion of the irrigation areas within the last 25 years. The remote sensing based mapping approach followed a combination of visual image interpretation and (supervised) digital image classification. In Step 1, first the exterior limits of the irrigated areas were delineated by visual image interpretation. In Step 2, the settlement areas and water bodies were filtered out from this 'gross development area', again by visual image interpretation. Finally, in Step 3, a supervised digital classification of the remaining 'net irrigation area' was conducted.

Parallel to this mapping of the presently irrigated areas, field data were compiled on the range and the spatial distribution of the (net) irrigation rates for different crops in different parts of the study area. Based on the established (presumed to be fairly accurate) data on the extension of the irrigation areas and the net irrigation rate data inquired on site, the net water consumption for irrigation could be calculated for each county. In a final step, the resulting net water consumption figures were corrected for the (estimated) water conveyance losses. This was done on the basis of irrigation efficiency rate figures quoted in the literature.

The final result of this procedure gives a fairly accurate and reliable quantification of the likely amount of water which is yearly being extracted for irrigation purposes. These figures were then compared with the respective data given by Chinese and Kazakhian literature sources.

Furthermore, the figures were compared with an assessment of the respective figures for the situation in 1976/1977.

The figures resulting from the remote sensing based study revealed the following:

- The Chinese data on the extent of irrigation land in the Upper Ili area are very inconsistent and in any case very far out of the reality. According to different Chinese sources, the irrigation area in the Upper Ili catchment totals between about 1,840 and 3,450 sqkm (including about 60 sqkm wetland rice). However, according to the remote sensing based survey, the actual extension of the irrigation area is in the order of 6,000 – 6,500 sqkm (including about 215 sqkm wetland rice)!
- Between 1976/1977 and 2000/2001, the irrigation area has increased by about 1,000 – 1,500 sqkm. This corresponds to an average yearly expansion of the irrigation area by 40 – 60 sqkm!
- While the Chinese data on the irrigation areas are definitely way off the real situation, their data regarding the overall water consumption for irrigation are surprisingly close to the study findings! As for the extension of the irrigation areas, also the figures for the amount of water, which is yearly being extracted from the Ili system, are inconsistent and oppositional. The figures which are quoted or can be calculated from other data range between 2.35 km^3 and 4.404 km^3 per year. While the lower figure cannot be taken seriously, the bigger of the two figures is quite in line with the study results! Several variants of the water consumption assessment were calculated in this study, based on three water use scenarios and four different irrigation efficiency rates. The two most likely of these calculations result in a total gross water consumption of about 3.45 – 4.15 km^3/year. The bigger one of these figures is fairly close to the above-quoted 4.404 km^3/year given in one of the Chinese sources. This figure is also well in line with realistic average (gross) water consumption rates between 5,000 – 6,000 m^3/ha.

Assuming a realistic total error of about plus/minus 10%, it can be concluded that the Chinese are at present extracting a water volume in the order of magnitude of 4.0 – 4.5 km^3/year. This water is used to irrigate an area of about 6,000 to 6,500 sqkm with an average (gross) irrigation rate of about 6,000 m^3/ha. If one adds the (almost negligible) water extraction for non-irrigation purposes (e.g. industry, drinking water), the present study, all things considered, confirms that the yearly total water extraction is very likely to be close to the 4.5 km^3 which the Chinese have always conceded! It can thus be concluded that this figure of 4.5 km^3 / year seems to be a rather reliable reference for further discussions in the ongoing dispute on the just distribution of the Ili water.

However, it should be kept in mind that the Chinese plans for new irrigation areas in the Ili catchment are not yet fully implemented. In the past, the still ongoing expansion of the irrigation projects resulted in an average increase of the water extraction rate of 40 – 60 million m^3/year. At this growth rate, the total water extraction for irrigation is bound to reach soon 5.0 km^3/year or more. The only feasible solution to resolve the problem of the dwindling water resources seems to be an increase of the low irrigation efficiency rate (at present presumably 50 – 60%). Increasing the average irrigation efficiency by just 10% would result in a water saving in the order of 0.5 km^3/year. This would be sufficient to expand the irrigation area by another 850 sqkm or 85,000 ha.

1. INTRODUCTION

The Balkhash Lake is one of the largest inland lakes of Central Asia. With 18,000 sqkm it is meanwhile larger than the dry-running Aral Lake, whose area has diminished to merely 25% of its original size of 69,500 sqkm. The Balkhash Lake is located in the Ili- Balkhash Basin in the south-eastern part of Kazakhstan (cp. Fig. 1).

Figure 1: General map of the Ili-Balkhash Basin with main rivers and administrative boundaries

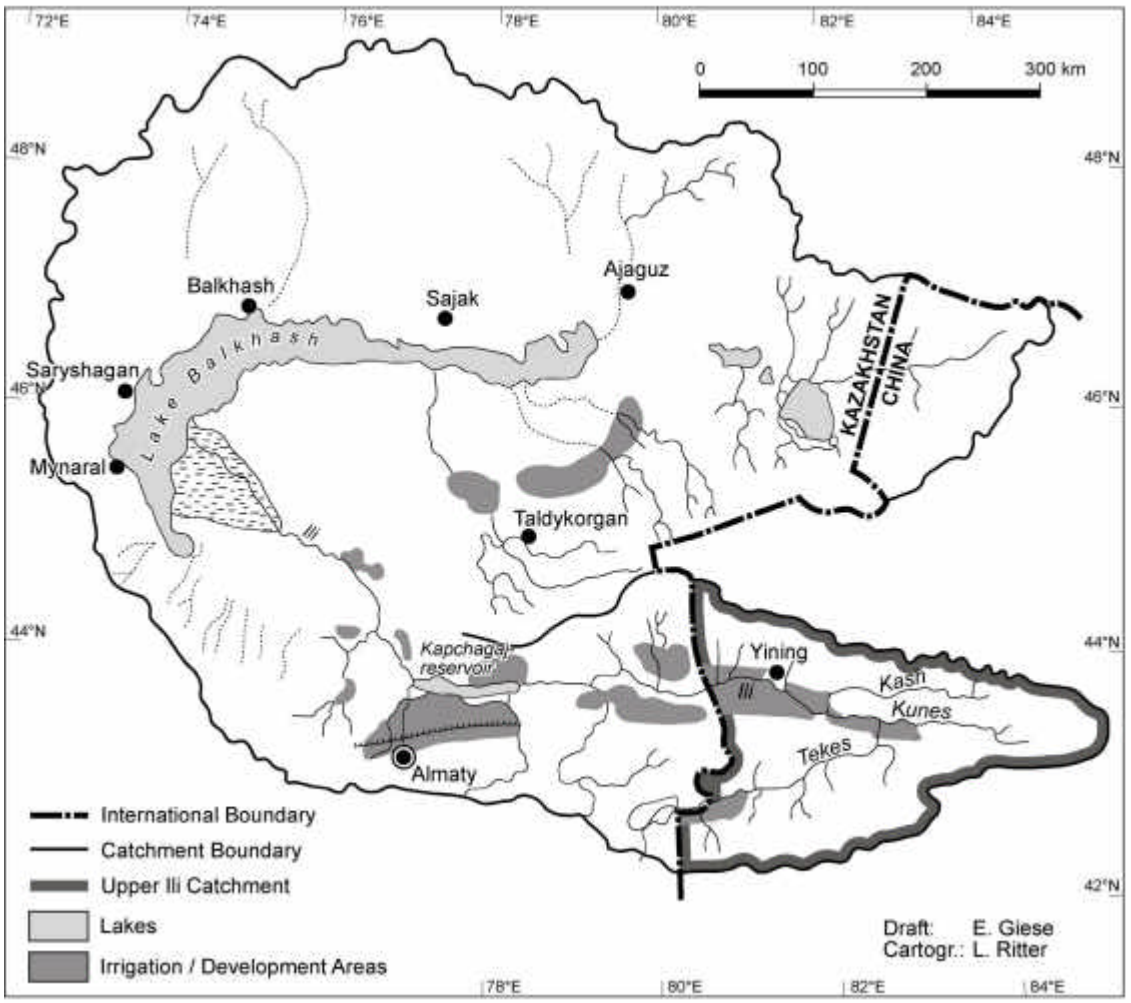

Source: Dostaj, Ż.D. (1999): Fig. 18, p.100

In the 1960s, the beginning of the recent developments, the water level of the lake varied only slightly between 342.7 and 347.0 m above NN (cp. Fig. 2). At a level of 342.0 m NN the lake covers an area of 18,480 sqkm and has a total volume of about 106 km^3. Starting from 1970 and continuing to 1987, the water level of the lake sank continuously from 347.0 to 340.7 m above NN (see Fig. 2). The main causes of this retrogression were extensive land development projects and the large-scale extension of irrigated agriculture. In the Kazakhian part of the Ili-Balkhash Basin, the irrigated areas increased from 405,000 ha to 583,000 ha (see Fig. 1) (Dostaj 1999).

Assuming an average gross water consumption of 11,000 m^3/ha (Tursunov 2002b, p. 11, 13), the inflow into the Balkhash Lake was thereby diminished by about 2 km^3 / year as compared to 1970. [1]

---

1 In the authors' opinion, this assumed water consumption rate is too high. According agricultural textbooks, the water requirements of typical irrigated crops in this area vary between about 300 and 700 mm per growing season. ILACO (1981: 475 ff), for example, quotes water requirements of 250 mm (minimum) for wheat, 600 mm for soya bean, 300 – 800 mm for sunflower, 600 – 900 mm for maize. An exception is irrigated rice ("paddy") which requires

Since 1987, the water level of the lake has recovered somewhat, in particular during the period 1998 – 2002, which was characterised by relatively high rainfall (cp. Fig. 2). However, this fact should not be misinterpreted! Despite this relatively moist interval, the Balkhash continues to be a highly endangered inland lake. At a level of 342.0 m NN, the lake totals an area of 18,480 sqkm and a volume of about 106 km^3. Due to its relatively low depth (about 5 – 8 m on average only), the Balkhash Lake has a relatively small volume, as compared to its surface. Considering the high evaporation of about 1,000 mm / year (14 km^3 / year), the lake is likely to run dry within a short time if the present inflow will be diminished considerably. At present, there are plans on the Kazakhian as well as on the Chinese side to further extend the existing irrigated areas (cp. Fig. 3). If these plans are being fully implemented, in the medium term the Balkhash will be threatened by the same gradual desiccation process which can be observed at the Aral Lake since the 1960s.

Figure 2: Water level fluctuations of the Balkhash Lake between 1880 and 2002

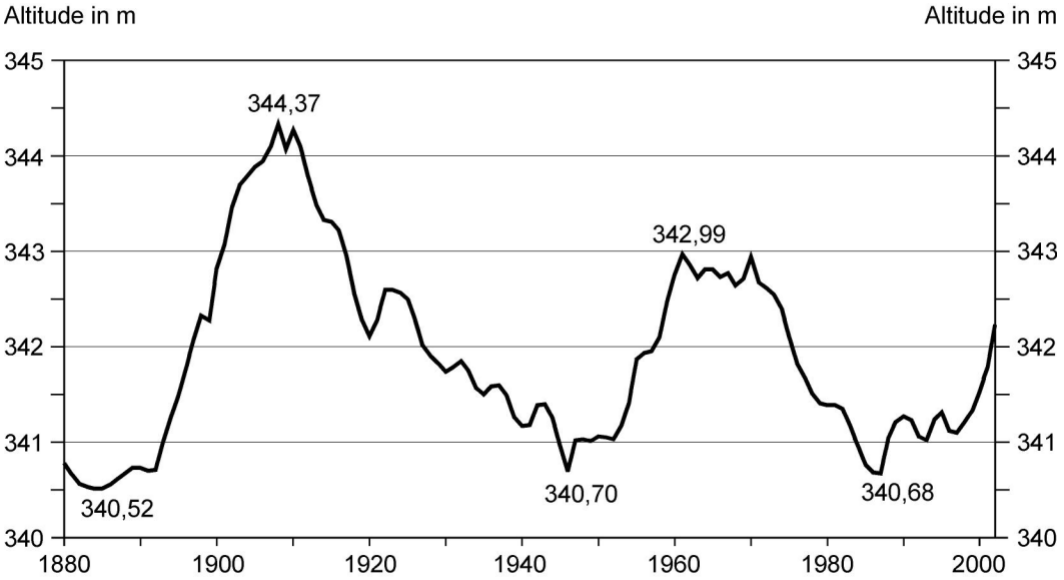

Source: Tursunov, A. A. (2002a): p. 264.

To sustain the equilibrium of this originally stable natural lake (i.e. a water level of 342.7 – 343.0 m above NN as in the 1960s), the Balkhash Lake requires an average inflow of about 15 km^3 / year. According to Kazakhian sources, the Balkhash presently receives about 11.8 km^3 of this inflow from the Ili River catchment which thus forms the main water source of the lake.[2] The remaining 3.2 km^3 stem from various smaller streams (Karatal, Aksu, Lepsy etc.) on the Kazakhian side of the border (cp. Fig. 1 and Fig. 4). Hence, in a balanced stage, the Balkhash Lake receives a total inflow of about 15 km^3, of which 79% (11.8 km^3) originates from the Upper Ili area.

1,200 to 1,800 mm (ILACO 1981: 472). Irrigated rice, however, covers a negligible fraction of the irrigated land only. In the irrigated parts of the Ili area, natural rainfall supplies between 200 – 500 mm, which leaves a water requirement gap of about 200 – 400 mm for normal crops and about 1,000 to 1,200 mm for paddy. These figures fully comply with information collected during the field check. According to information given by farmers and farm managers, the (net) irrigation rate (i.e. the amount which actually reaches the field) varies between 2,000 and 3,750 m^3/ha (i.e. 200 – 375 mm) for normal crops and 10,500 – 14,500 m^3/ha for paddy. Typical conveyance efficiency factors for poorly managed surface irrigation systems vary between 0.5 – 0.7 (ILACO 1981, p. 380). This is quite in line with figures mentioned by Ressl for the Amu-Darja delta, who quotes irrigation efficiency factors of 0.5 – 0.6 (Ressl 1999, p.156). Hence, it can be assumed that the conveyance losses are in the order of 40 – 50%. Assuming a conveyance loss of 50%, the gross water consumption per hectare is thus about twice the net irrigation rates given above! This estimation is confirmed by various other textbooks, which also quote efficiency rates of around 50% for surface irrigation systems (cp. Landon 1984, p. 338, Rogers et al. 1997). Based on these assumptions, realistic gross water consumption rates for irrigation are in the order of 400 – 800 mm respectively 4,000 – 8,000 m^3/ha. Taking a sensible average of these figures, the typical mean gross water consumption will be around 600 mm respectively 6,000 m^3/ha (or 55% of the 11,000 m^3/ha assumed by Tursunov).

2 The amount of water which the Lake Balkhash receives from the Chinese territory is a sensitive issue and heavily disputed between Kazakhstan and China. While the Kazakhian side alleges that the inflow totals 11.8 km^3 only, the Chinese side claims to discharge a volume of 13.52 km^3 to Kazakhstan (figure for 1995, Forschungsteam "Projekt 1515 des Ili-Gebietes" und Wissenschafts- und Ingenieurverein vom Ili-Gebiet (Hrsg.), 1999, pp. 37-39).

According to Kazakhian sources, more than two-third of the discharge of the Ili River are formed on Chinese territory. In the 1960s, the discharge of the (entire) Ili Catchment totalled 22.8 km^3/year. Of this amount, 17.05 km^3 (i.e. almost three quarter) were formed on Chinese territory. Of these 17.05 km^3, the major part (12.4 km^3) was discharged to Kazakhstan, while the remaining 4.6 km^3 were 'lost' on the Chinese side due to infiltration, evaporation, and water consumption.[3]

On the Kazakhian side, additional 6.4 km^3 / year were formed outside the Ili Catchment and discharged by tributaries from the Tsungarian Alatau (Karatal, Aksu, Lepsy etc.). Half of these water resources (i.e. 3.2 km^3/year) eventually reached the Balkhash Lake, the remaining 3.2 km^3 / year were used by man, again mainly for irrigation purposes (cp. Fig. 1).

At present, plans exist on both sides of the border to utilise the water resources of the Ili-Balkhash Basin even more intensively than today. The Kazakhs are planning a comprehensive extension of the Dzungarian irrigation complex. On the Chinese side there are plans to extend the existing irrigation areas along the Ili River (cp. Fig. 3). Moreover, there are also plans for a canal to divert water from the Kash, a northern tributary of the Ili, to the industrial complex around Karamay. A second canal is planned to divert water from the Keksu, a southern tributary of the Tekes, to supply water via the Chajdyk-Gol (Karasar) into the Tarim Basin (cp. Fig. 3). Furthermore, a total of 15 dam projects are under discussion for Tekes, Kunes and Kash, the three main tributaries of the Ili River.

If these plans are being implemented, a critical situation may develop as modelled by Tursunov in cooperation with Dostaj (cp. Tursunov 2002a, p. 294). Figure 4 illustrates the modelled results. The first of the two scenarios assumes that the water inflow from the western into the eastern part of the Balkhash Lake will shrink from 3.2 to about 1.0 km^3/year and that the water supply from the Ili River into the western part of the Balkhash will drop off from 11.8 to 8.95 km^3/year. The assumed declined water inflow into the Balkhash from 15.0 km^3/year to 10.0 km^3/year would induce a shrinking of the lake surface as shown in Scenario 1. According to Tursunov (2002a, p. 292), this scenario is (at present) the more likely one. The water level of the lake would drop to about 340 m NN. As a consequence, the lake would split into two smaller, separated parts with a total surface area of only 11,720 sqkm, which correspond to just about two-third of its original size in the 1960s (about 18,000 sqkm).

In case of Scenario 2, the size of the lake area would be reduced even further. The water level would drop for another 2.4 m to 337.6 m NN and the remaining lake would cover only 6,800 sqkm, respectively one-third of the original lake size. In this case, we may expect similar conditions and effects as being observed at the Aral Lake since the mid-1980s.

The data and facts outlined above demonstrate that there is a precarious uncertainty about absolutely crucial base figures for the water balance regime of the Ili river catchment as well as on the amount of water taken from the Ili for irrigation purposes. The Kazakhian side presents calculations which estimate the regeneration rate of the Ili, the main water source of Lake Balkhash at 16.6 km^3/year and the inflow from the Ili into the lake at 11.8 km^3/year (present discharge) respectively 12.4 km^3/year (figure for the 1960s). Hence, the resulting difference indicates a water extraction in the order 4.8 respectively 4.4 km^3/year on the Chinese side.

The Chinese, on the other hand, tune their calculations just the other way round! Their estimation of the regeneration rate of the Ili system is about 0.7 km^3 lower (15.87 km^3/year). At the same time, they claim to discharge 13.32 km^3/year (cp. Forschungsteam "Projekt 1515 des Ili-Gebietes" und Wissenschafts- und Ingenieurverein vom Ili-Gebiet 1999: 37 -39) which is about 1.1 – 1.7 km^3/year more than the quantities given by the Kazakhian scientists (11.8 respectively 12.4 km^3/year). According to their calculation, the Chinese side merely extracts 2.345 km^3/year, about 2 km^3/year less than in the Kazakhian calculation.

---

[3] As mentioned in the preceding footnote, the quantities given by Chinese scientists differ from the Kazakhian figures. According to the results of the "Forschungsteam "Projekt 1515", in 1995 the water volume formed in the (entire) Ili Catchment totalled 16.459 km^3. Of this total 15.865 km^3 (96%) are formed on the Chinese part of the catchment and only 0.594 km^3 (3,6%) are formed on the Kazakhian side (Forschungsteam "Projekt 1515 des Ili-Gebietes" und Wissenschafts- und Ingenieurverein vom Ili-Gebiet (Hrsg.), 1999, pp. 37 -39). As mentioned above, the Chinese claim to transmit 13.52 km^3 (i.e. 85%) of the water formed on their side to Kazakhstan. According to these figures, the Chinese would use just 2.345 km^3 of the Ili water. This figure, however, is contradicted by other figures of the same report, through which the Chinese themselves concede to use 4.377 km^3 Ili water for irrigation purposes (figure for 1995, Forschungsteam "Projekt 1515 des Ili-Gebietes" und Wissenschafts- und Ingenieurverein vom Ili-Gebiet (Hrsg.), 1999, pp. 37 -39)

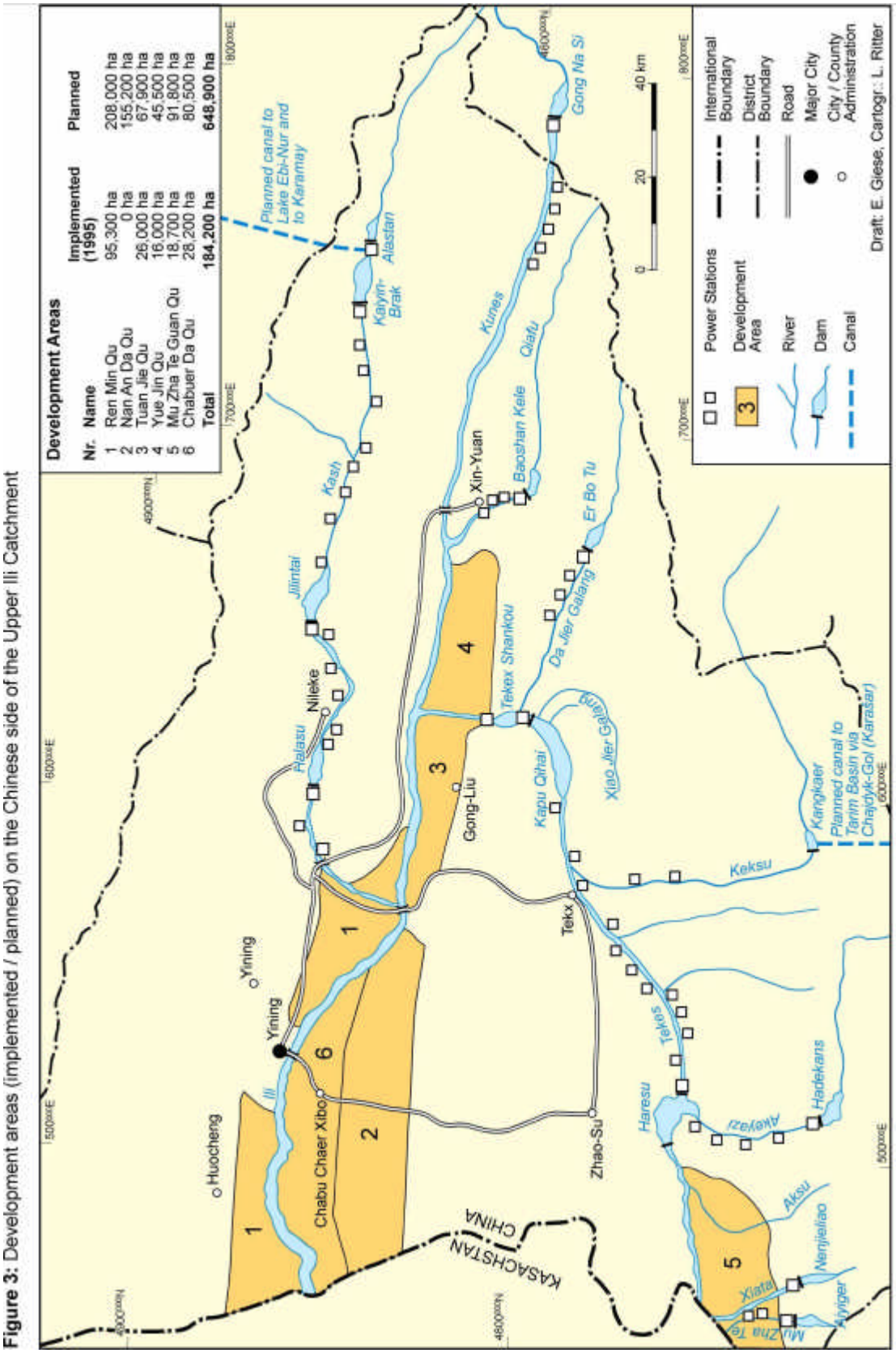

Figure 3: Development areas (implemented / planned) on the Chinese side of the Upper Ili Catchment

Source: Forschungsteam "Projekt 1515 des Ili-Gebietes" und Wissenschafts- und Ingenieurverein vom Ili-Gebiet (Hrsg.) (1999): Forschungen zur Erschließung des Ili- und Irtysch-Einzugsgebietes (Yili He e Erqisi He Liuyu Kaifa Yanjiu). Xinjiang Renmin Verlag, Urumqi.
(Remark: The original map was translated into English and somewhat modified and supplemented.)

However, these figures are contradicted by other data given in the same report! According to those figures, the Chinese consume a total water volume of about 4.4 km^3/year for irrigation (3.407 km^3/year by 'normal' farming plus 0.97 km^3/year by 'state farms', cp. Forschungsteam "Projekt 1515 des Ili-Gebietes" und Wissenschafts- und Ingenieurverein vom Ili-Gebiet 1999: 37 -39).[4]

Figure 4: Scenarios of the future development of the Balkhash Lake

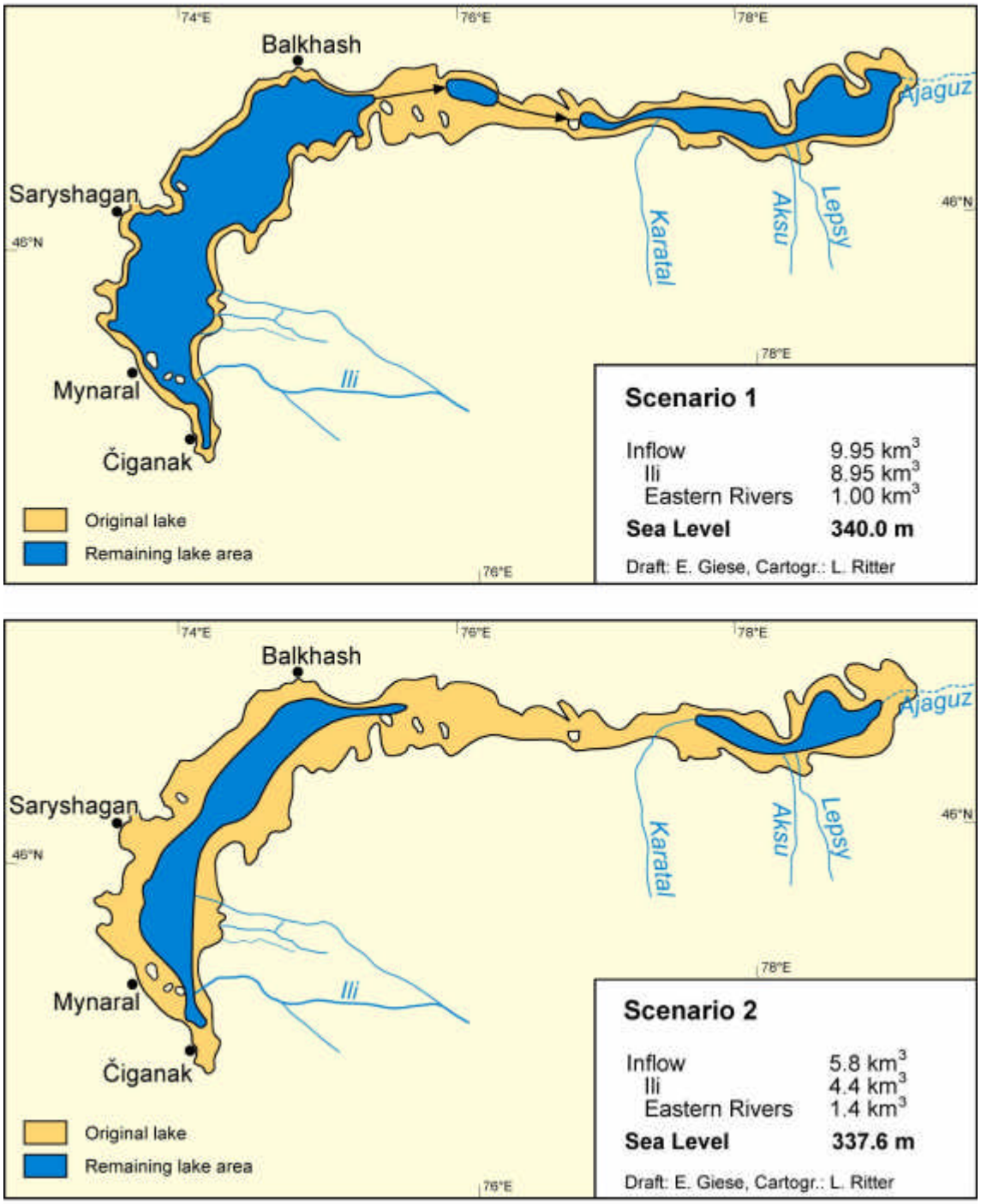

Source: Tursunov, A. A. (2002a): p. 294.

[4] It should be noted that according to Chinese sources irrigation consumes almost 98% of the total extracted surface water. Hence, other water uses are negligible! It should also be noted that the use of groundwater for irrigation purposes is likewise almost negligible! Just 2 – 4 % of the irrigation water originates from groundwater sources (Forschungsteam "Projekt 1515 des Ili-Gebietes" und Wissenschafts- und Ingenieurverein vom Ili-Gebiet (Hrsg.), 1999, pp. 37 -39).

Yet not only the water-related figures are highly uncertain and questionable, but also the figures given by Chinese sources regarding the extension of the irrigated areas! According to the "Project 1515" report, in 1995, a total area of 3,400 sqkm was under irrigation (Forschungsteam "Projekt 1515 des Ili-Gebietes" und Wissenschafts- und Ingenieurverein vom Ili-Gebiet 1999: 37 -39). However, according to the map of development areas (cp. Fig. 3) within the same report (!) the implemented irrigation areas total only 1,842 sqkm (1995). A third figure – again different - is given by the official Chinese statistics (Statistical Bureau for Xinjiang (Ed.), 2002) which quote a total irrigation area of 2,229 sqkm.

The present study aims at clarifying this chaos of widely differing figures. It focuses on the analysis of the water consumption for irrigation land on the Chinese side of the Ili Basin and the development of this water consumption between 1976 and 2001. In order to estimate the water consumption for irrigation within the study area, two key figures have to be established:

- First, the irrigation areas have to be mapped and measured as exactly as possible. Since different crops require different quantities of irrigation water, also the respective land use / crop cultivation types should be discriminated as far as feasible.
- Second, average water resource requirements per area unit have to be identified. If and where possible, inaccurate 'rules of thumb' figures of water requirements for 'irrigated land' should be replaced by more accurate crop- and cultivation-specific water requirement data.

Given these two key data - area totals and crop-specific water requirements - the water quantities used for irrigation can be assessed fairly accurately.

In theory, crop-specific land use data down to the county level should be easily available from official Chinese statistics. In practise, however, these land use data are difficult to validate and verify. The study will demonstrate that the official land use statistics for the Ili area are highly unreliable and virtually useless as a reference for the assessment of the water consumption.

Due to this data problem as well as due to the restricted access to the area, the present study relied largely on remote sensing. The irrigated areas for two different 'time slices' (1976/77 and 2000/2001 respectively) were mapped and measured from Landsat satellite imagery. The respective net and gross irrigation rates per hectare were established through personal information during a field check. This field survey was carried out by Chinese counterparts of the University of Urumqi. Based on these figures, the desired (approximate) water consumption was estimated.

The present report is structured as follows:

- **Chapter 2** summarises background information on the study area and the data which were available for the project (maps, satellite images etc.).
- **Chapter 3** outlines the general study approach and describes in detail the various working steps.
- **Chapter 4** presents the analysis results. The chapter starts with the assessment of the total irrigation areas in the mid 1970s and in 2000/2001. The second subchapter analyses the present land use (i.e. in 2000/2001) according to individual crops and crop groups. The third and last subchapter estimates the (approximate) total water consumption for irrigation, based on the results of the foregoing subchapters.

The report ends with general conclusions, given in **Chapter 5** and the usual literature list.

2. BACKGROUND INFORMATION

2.1 THE STUDY AREA

Fig. 3 presents a first overview over the study area, which covers the upper part of the Ili Catchment between about 42° and 44° north and 80° and 85° east. The Upper Ili Catchment has the form of an eastward-pointing triangle. In the north and south, the study area is bordered by high-rising mountain ranges. To the west, the limit of the study area is demarcated by the international boundary between China and Kazakhstan.

The study area covers approximately 55,130 sqkm. Its maximum extension in north-south and west-east direction totals 250 km and 350 km respectively. The Upper Ili Catchment consists of two major sub-catchments: The catchment of the Tekes (also called Tekx) in the south-western part of the area and the Kunes (also called Gong Na Si) and Ili Catchment in the north (cp. Fig. 3). The Kash (also called Kazu) which runs north of and almost parallel to the Kunes also belongs to this northern sub-catchment.

Tekes and Kunes meet somewhat north-east of Gong-Liu in the centre of the study area to form the Ili River. Besides these major tributaries, about 120 smaller streams and rivers drain the area. The entire river system is largely fed - directly or indirectly – by rainfall and melt-water from the high-rising mountain ranges which form the exterior boundaries of the study area to the north and south.

Relief and altitude of the study area vary strongly. The altitudes range between about 720 m and 6,450 m NN. The areas of special interest for this study, i.e. the agricultural areas, extend along the river plains at altitudes between 700 m in the north-west (Yining) to 900 m in the north-east (upper Kunes) and 1400 - 1600 m (Tekes sub-catchment).

The yearly rainfall in the study area ranges from 200 - 500 mm in the valley areas to 1000 mm in the mountain ranges (Hamid 2003a, 2003b). According to "The Climate of China" (cp. Domrös & Gongbing 1988, pp. 256 ff) the study area belongs to the arid ("D") variant of the "middle temperate zone" of China. This climate is characterised by (generally) low rainfalls with a summer maximum which, however "*becomes weaker or is nearly extinguished in Northwest China*" (Domrös & Gongbing 1988, p. 262). Temperatures in this zone show extreme annual variations, ranging from –10°C to –12°C in January to +20°C to +24°C degrees in July (Domrös & Gongbing 1988, p. 262). Hence, the winters in the study area are long, dry and cold while the summers are short and hot.

Fig. 5 illustrates the strongly continental character of the study area. The figure shows a climate diagram for Yining according to the Walter-Lieth-Method. The diagram was calculated on the basis of monthly data of the Bureau of Water Resources for Yining City for the period 1951 - 2002. Surprisingly, the calculated average rainfall differs considerably from figures given by Domrös & Gongbing (1988, p. 150). While the latter give an average yearly rainfall for Yining of only 177 mm / year (cp. Fig. 5, dotted line), our own calculations result in a considerable higher figure (273 mm).[5]

The yearly mean temperature for Yining totals 8.7 degrees Celsius, with an extremely strong variation from –9.1°C for January and +22.9°C for July. The temperature curve is characterised by a remarkably steep increase from Feb (-6.1°C) to April (12.3°C) and a similarly steep decrease from September (17.0°C) to October (9.4°C) and November (1.4°C) The temperature curve shows that the vegetation period is limited to the months April – September / October, of course with a certain variation from year to year.

While the total rainfall increases somewhat to the east and south of Yining, the general characteristics of the rainfall distribution remains the same. There is a relative maximum during the months April, May, June and a second smaller maximum during October / November. However, the low monthly minimum values indicate that the rainfall is erratic and unreliable. Hence, crop cultivation requires irrigation in most parts of the study area.

---

[5] Domrös & Gongbing's data of course do not cover the period after the textbook publication (1988) and are thus not directly comparable to the given data period. Nevertheless, this does not explain sufficiently a difference of more than 50%! The climate diagram uses figures which were calculated from the original data directly, the figures according to Domrös & Gongbing have been added as additional information (dotted line).

Rainfed agriculture is limited to the cooler areas at the higher altitudes of the upper Tekes sub-catchment in the southwestern part of the project area. Due to the considerably higher altitude, this region also receives a somewhat higher yearly rainfall (about 500 mm/year and more).

Figure 5: Climate diagram for Yining (Walter-Lieth method)

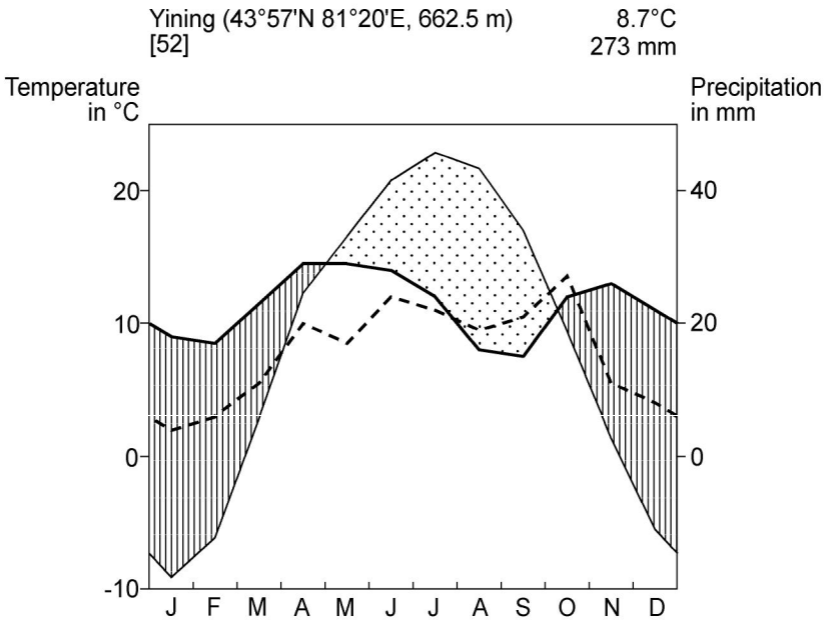

	Jan	Feb	March	Apr	May	June	July	Aug	Sep	Oct	Nov	Dec	Year
Temp. (°C)	-9.1	-6.1	2.9	12.3	16.6	20.8	22.9	21.7	17.0	9.4	1.4	-5.5	8.7
Precip. (mm)	18	17	23	29	29	28	24	16	15	24	26	22	273

Source: Bureau of Water Resources, Urumqi, based on monthly data 1951-2002. For comparison, the dashed line indicates the rainfall values given by Domrös & Gongbing 1988, p.101 and 150. The temperature values from Domrös & Gongbing do not differ significantly from the values of the Bureau of Water Resources, and were therefore not indicated.

Administratively, the area is subdivided into nine counties and 1 city. In year 2000, the study area had a total population of 2,000,000 (Hamid 2003a). Table 1 summarises the key data of the study area.

Table 1: Key data of the Upper Ili Catchment

Data type	Data	Remarks
min. X-coordinate	80°10' East 431,774 East	geographical co-ordinate UTM co-ordinate (Zone 44)
max. X-coordinate	85°00' East 826,529 East	geographical co-ordinate UTM co-ordinate (Zone 44)
min Y-coordinate	42°16' North 4,680,718 North	geographical co-ordinate UTM co-ordinate (Zone 44)
max. Y-coordinate	44°35' North 4,936,820 North	geographical co-ordinate UTM co-ordinate (Zone 44)
max. west-east extension	about 350 km	
max. north-south extension	about 250 km	in the centre of the study area

Data type	Data	Remarks
		about 180 km only
lowest point of the study area	≈ 720 m NN	
highest point of the study area	≈ 6,450 m NN	
total size of the area	about 55,130 sqkm	calculated by ArcView
relief distribution	mountains 63%, hills 10%, valley plains 27%	Source: Hamid 2003a
Agricultural area (total)	14,834 sqkm	= 27% of total area
of this: crop land (mainly irrigated)	6,428 sqkm	= 39% of total agricultural area
oft this: animal husbandry	8,406 sqkm	= 61% of total agricultural area
total population	about 2,000,000	Source: Hamid 2003a
population density (sqkm)	about 36	calculation based on figures given by Hamid 2003a
population density / sqkm agricultural area	about 131	calculation based on figures given by Hamid 2003a
average yearly rainfall	about 200 – 1000 mm	Source: Hamid 2003a
months with highest rainfall	April, May, June	Source: own data, Domrös & Gongbing 1988
average yearly temperature	between 3° and 9° C in the valley, considerably colder in the mountains	Source: Hamid 2003a; Domrös & Gongbing 1988
administrative structure	one urban agglomeration, nine counties,	Source: Hamid 2003a: City: Yining Counties: Yining County, Ili Valley, Chabuchaer, Huocheng, Gongliu, Xinyuan, Zhaosu, Tekex, Nileke
main crops	soya bean, wheat, rape, maize, (paddy) rice	Source: Hamid 2003b

Source: Hamid 2003a; Domrös & Gongbing 1988, own data extracted from various topographic maps

2.2 AVAILABLE DATA

Table 2 gives an overview over the data which were available for the study area or which were made available during the course of the project. The following sub-chapter briefly describes the data and comments on their quality and topicality.

Table 2: Available data for the Upper Ili Catchment

Data	Data Type	Scale / Resolution	Source / Acquisition	Remarks
Satellite Images				
Landsat 2 MSS	satellite data	79 m	Gesellschaft für Angewandte Fernerkundung (GAF)	3 scenes taken in 1976 / 77: Path / Row / Date: 157/030 (17-08-1977) 158/030 (18-07-1976) 158/029 (25-06-1977) Scenes do not cover the entire area.

Data	Data Type	Scale / Resolution	Source / Acquisition	Remarks
Landsat 7 ETM+	satellite data	30 m (multi-spectral), 15 m (pan)	Gesellschaft für Angewandte Fernerkundung (GAF)	4 scenes taken in 2000 / 2001 Path / Row / Date: 147 / 030 (27-05-2001) 147 / 029 (27-05-2001) 146 / 030 (05-06-2001 145 / 030 (27-06-2000)
Maps				
Tactical Pilotage Chart	analogous map	1 : 500,000	ILH Stuttgart / US Defence Mapping Agency Aero-space Center St. Louis	Revision stage 1985 and 1989; maps were scanned and georeferenced (UTM Zone 44, WGS 84)
Russian topo-graphic maps 1 : 200,000	analogous map	1 : 200,000	Gesellschaft für Angewandte Fernerkundung (GAF)	Revision stage: 1978/80. Maps were supplied on CD as non-georeferenced RGB-Scans in GIF-format. Available maps cover the entire project area, but only 9 sheets (covering the central parts of the study area) were purchased.
Russian topo-graphic maps 1 : 100,000	analogous map	1 : 100,000	Gesellschaft für Angewandte Fernerkundung (GAF)	cp. topographic maps 1 : 200,000 (see above) Just one map sheet was purchased for evaluation purpose.
'Map' of new 'development areas'	Sketch map with-out scale, grid and coordi-nates	about 1 : 1,200,000	Wissenschafts - und Ingenieur-Verein vom Ili-Gebiet (Eds.) (1999)	Sketch map in a Chinese publication, showing six planned 'development areas'. A translated and modified English version of the map is given by Fig. 3.
Digital Vector Data				
Administrative county boun-daries	digital data	1 : 1,000,000	CITAS (China in Time and Space Project, Univ. of Washington, distributed by CIESIN (Con-sortium for Inter-national Earth Science Informa-tion Network9	Cartographic base is the Digital Chart of the World, developed by the US Defence Mapping Agency in coopera-tion with various agencies in Australia, Canada and the U.K.; Revision stage: Sept. 1994 URL: www.citas.csde.washington.edu/data/cntybnd/overview.htm
River network	digital data	1 : 1,000,000	CITAS / CIESIN (cp. county boundaries)	Details as county boundaries (see above)
Digital Elevation Model				
GTOPO30-DHM	digital data	1 : 1,000,000 (30-arc-sec-onds, ca. 1 x 1 km)	U.S. Geological Survey, EROS Data Center, Sioux Falls, South Dakota	worldwide available low resolution digital elevation model; URL: http://edcdaac.usgs.gov/gtopo30/Readme.html

Source: own compilation

2.2.1 Satellite Data

The selection of the "best"[6] satellite data was based on the following criteria:

- no or low cloud-cover (as much as possible),
- good data quality (no or few defect lines),
- recording month (as late as possible in the growing season)
- recording time correlation (scenes taken at about the same time),
- price

Based on these criteria, a comprehensive data search was conducted to identify suitable satellite scenes for two different 'time slices'. The first set of data should reflect the situation in the mid-1970s, the second should be as recent as possible. For cost-saving reasons, only Landsat data were considered. The data search used the U.S. Government Data Catalogue (http://edcsns17.cr.usgs.gov/EarthExplorer/). As usual, the search results could not fully satisfy all selection criteria. The scenes finally selected represent a 'best compromise' between the selection criteria and the actually available data as listed in the catalogue.

Landsat 2 MSS

Fig. 6 illustrates the area of the three purchased satellite scenes, Table 3 summarises their principal data. The data quality of these early Landsat images is rather limited, but cloud-free scenes with a better data quality were not available for the required time windows (May – August, 1975 – 77). Unfortunately, the selected scenes were taken far later in the growing period than the respective images for the time-slice 2000 / 2001.

Figure 6: Coverage of the Landsat 2 MSS images (1975 / 1976)

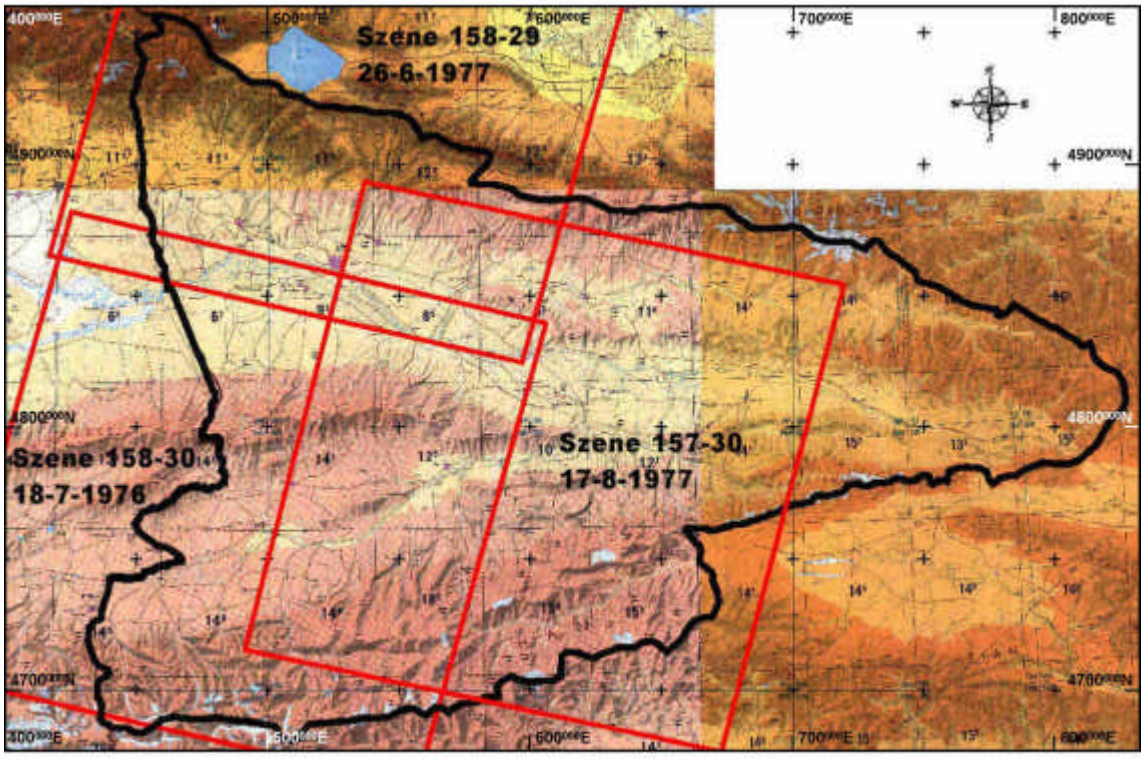

Source: Own compilation, based on Tactical Pilotage Chart 1 : 500,000 and the satellite image frame data

[6] "Best satellite data" should here be understood as a 'relative' term. The principal target of the data search was to identify satellite data which provided a reasonable trade-off between technical requirements and reasonable data costs. If costs had not been an important selection criterion, other satellite data might have been a (technically) better choice.

Table 3: Principal data of the selected Landsat 2 MSS images

Path	Row	Entity-ID	Date	Cloud Cover	Upper left corner	Upper right corner	Lower left corner	Lower right corner	Centre
158	**29**	2158029007717690	25.06.1977	10-19%	45° 32' N 80° 34'E	45° 09' N 82° 52'E	43° 56' N 79° 58'E	43° 34'N 82° 12' E	44° 33' 00" N 81° 24' 00" E
158	**30**	2158030007620090	18.07.1976	10-19%	44° 05' N 80° 04' E	43° 42' N 82° 19' E	42° 29' N 79° 29' E	42° 07' N 81° 41' E	43° 06' 00" N 80° 53' 00" E
157	**30**	2157030007722990	17.08.1977	10-19%	44° 06' N 81° 26' E	43° 43' N 83° 42' E	42° 30' N 80° 52' E	42° 08' N 83° 04' E	43° 07' 00" N 82° 16' 00" E

Source: own compilation

Landsat 7 ETM+

Fig. 7 shows the area covered by the four Landsat 7 scenes which were bought as base data for the assessment of the present land use. Table 4 summarises the principal data of the images used. These newer satellite images are of a much better quality than the old images.

The four selected scenes are largely cloudless in the areas of interest as well as free of major data errors. Only scene 147 / 029 has a few faulty lines, which are, however, largely outside of the area of interest. Three of the four scenes were taken at a fairly early phase of the growing period, which starts in April and ends in August / September. The optimal recording phase would have been mid-July to early August. Unluckily, for this growing stage suitable cloud-free, high-quality scenes recorded in 2000 or 2001 were not available. [7]

Figure 7: Coverage of the Landsat 7 ETM+ images (2000 / 2001)

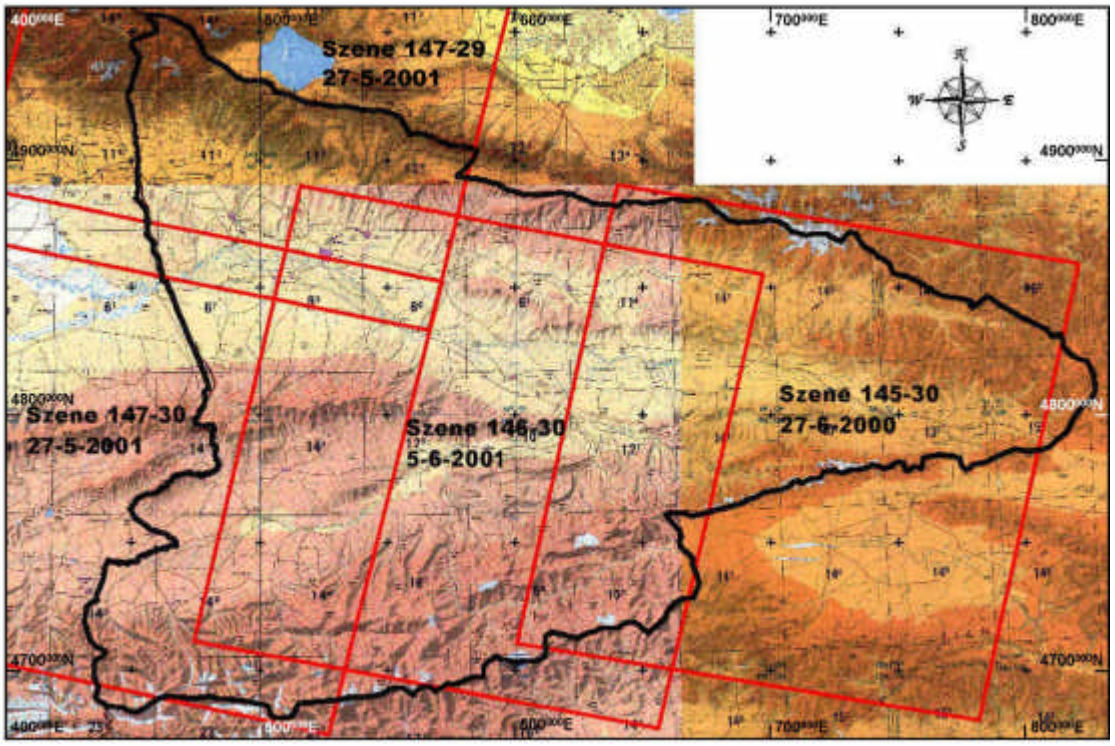

Source: Own compilation, based on Tactical Pilotage Chart 1 : 500,000 and the satellite image frame data

[7] The early recording of these new images limited the comparability with the 1975 / 1976 images which were taken between end of June and mid-August. Moreover, it also limited the discrimination potential for different crops during the supervised classification. For details see Chapter 3 and 4.

Table 4: Principal data of the selected Landsat 7 ETM+ images

Path	Row	Entity-ID	Date	Cloud Cover	Upper left corner	Upper right corner	Lower left corner	Lower right corner	Centre
145	**30**	71450300000 17950	27.06.2000	10-19%	44°09"21" N 82°41'18" E	43°48'53" N 85°01'44" E	42°32'17" N 82°10'07" E	42°12'21"N 84°26'58" E	43°11'10" N 83°35'06" E
146	**30**	71460300001 15650	05.06.2001	10-19%	44°09'28" N 81°08'57" E	43°49'05" N 83°'29'23" E	42°32'14" N 80°37'41" E	42°12'23" N 82°54'32" E	43°11'10" N 82°'02'40" E
147	**29**	71470290001 14750	27.05.2001	0-9%	45°34'57" N 80° 03'58" E	45°14'02" N 82°27'49" E	43°57'49" N 79°'31'33" E	43°37'30" N 81°51'33" E	44°36'36" N 80°58'47" E
147	**30**	71470300001 14750	27.05.2001	10-19%	44°09'27" N 79°35'21" E	43°49'03" N 81°55'48"E	42°32'15" N 79°04'07" E	42°12'23" N 81°'20'59" E	43°11'10" N 80°29'06" E

Source: own compilation

2.2.2 Topographic Maps

Existing Chinese topographic maps of border areas are restricted and thus not easily available to foreigners. Even if they were available, the language problem would have posed a major constraint for their utilisation. Hence, the project team had initially to fall back on international small scale maps which are world-wide available.

Tactical Pilotage Chart (1 : 500,000)

Figure 8: Index map of the Tactical Pilotage Chart (TPC 1: 500,000) map sheets

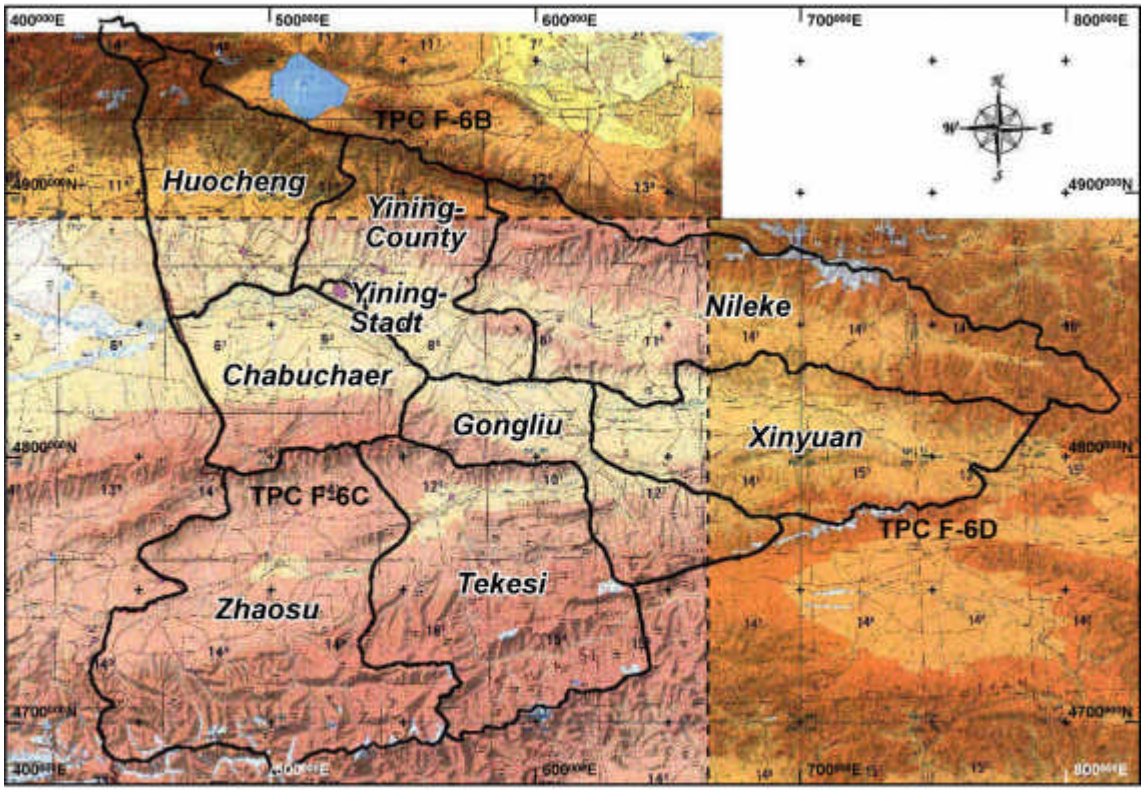

The map shows the sheet index of the three used TPC sheets and the delimitation of Upper Ili Basin project area. The black lines within the area indicate the administrative sub-division (county boundaries).

Source: Own compilation, based on Tactical Pilotage Chart 1 : 500,000.

The map series with the largest scale available for the entire world is the so-called Tactical Pilotage Chart (1 : 500,000) of the US Defence Mapping Agency Aerospace Center in St. Louis,

USA (cp. Fig. 8).[8] The project area is covered by parts of the map sheets TPC F-6A, TPC F-6B, and TPC F-7D.

As the name indicates, the TPC map series has been compiled for air traffic navigation. Hence, topographic details, such rivers, roads and settlements are fairly limited in this map, as illustrated by Fig. 9. Due to lack of alternatives, in the beginning this map formed the only available base map which covers the entire project area at a (more or less) useful scale. Fig. 8 shows the location of the three TPC-sheets used and the exterior limits of the Upper Ili Basin project area. The black lines within the area indicate the administrative sub-division (county boundaries). The county boundaries were downloaded as digital vector data from an Internet source (CIETAS, cp. data list in Table 2). The project area covers eight "counties" and one urban agglomeration:

- City Area: Yining
- Counties: Yining County, Ili Valley, Chabuchaer, Huocheng, Gongliu, Xinyuan, Zhaosu, Tekex, Nileke

Figure 9: Map example of topographic details in the Tactical Pilotage Chart (TPC) 1 : 500,000

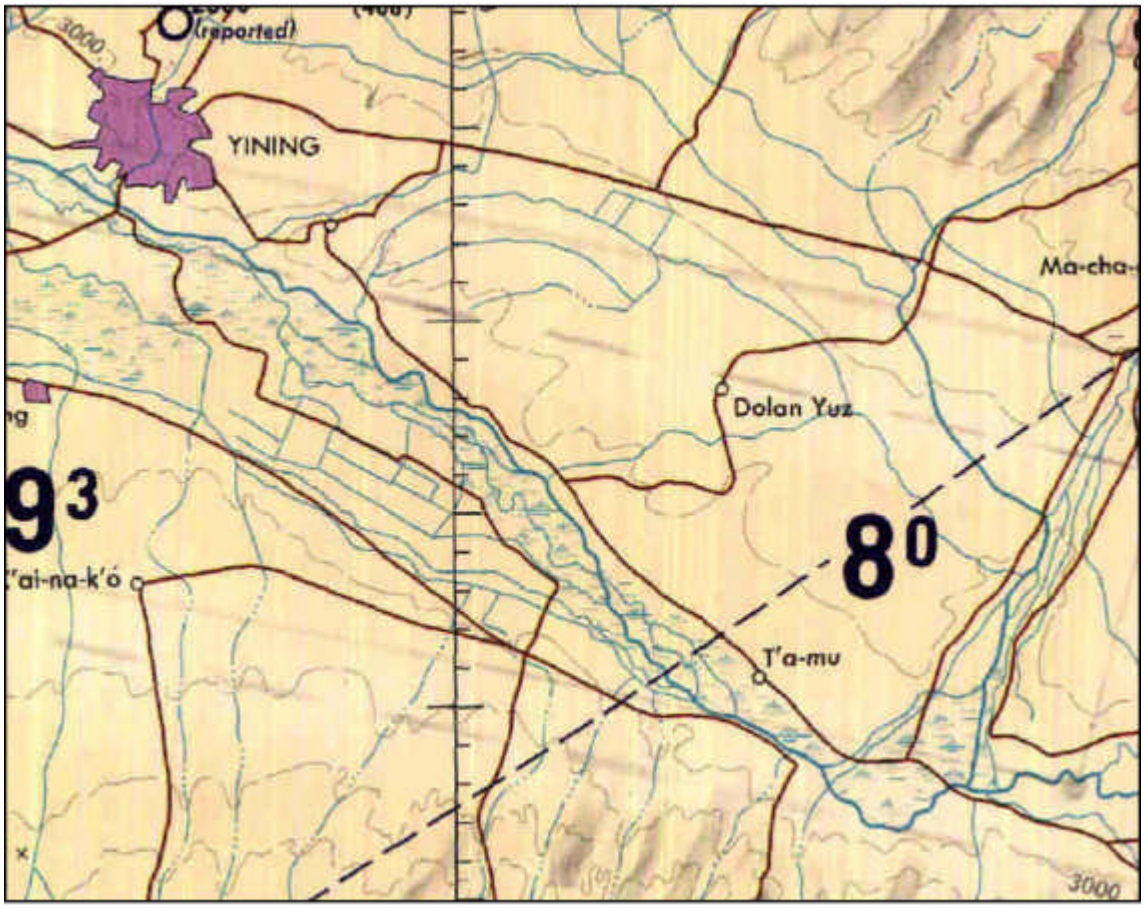

Source: TPC 1 : 500,000, own compilation

[8] At map scale 1 : 500,000, the TPC map can be purchased by everbody . A second, more detailed version at scale 1 : 250,000 is available for internal use of US institutions only.

Russian Topographic Maps 1 : 200,000 and 1 : 100,000

Figure 10: Index map of the used map sheets of the Russian Topographic Map 1 : 200,000

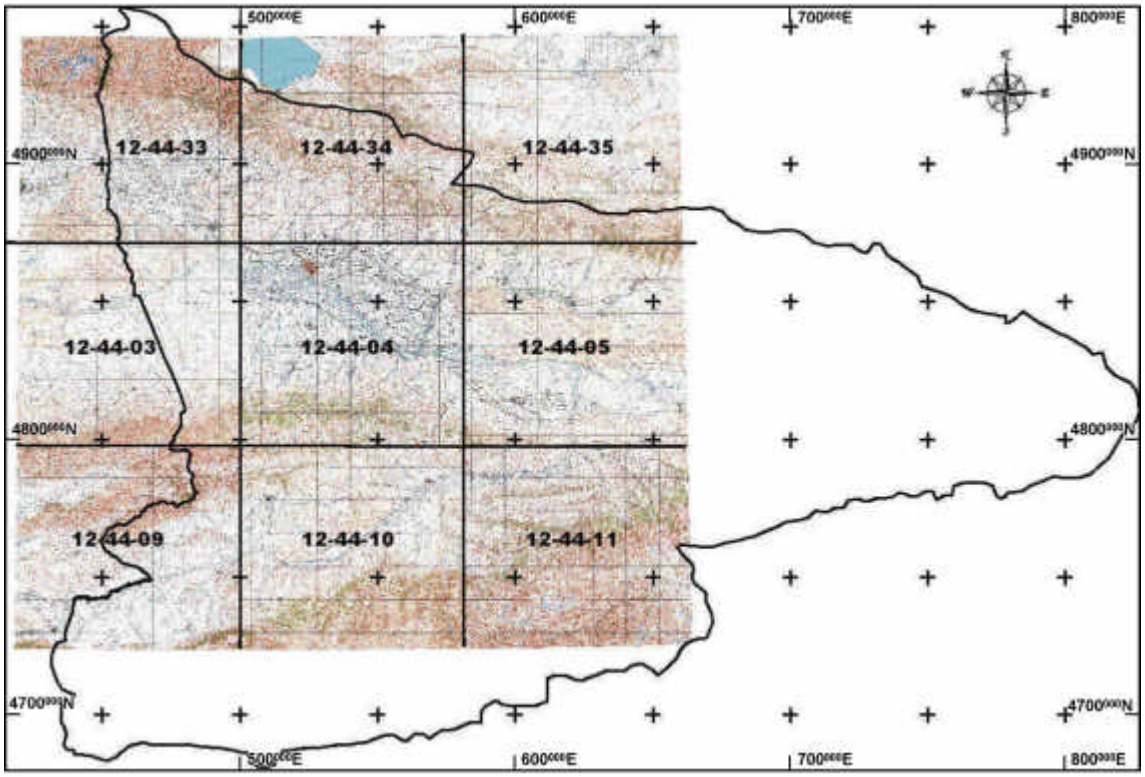

Source: own compilation

Figure 11: Map example of topographic details in the Russian Topographic Map 1 : 200,000

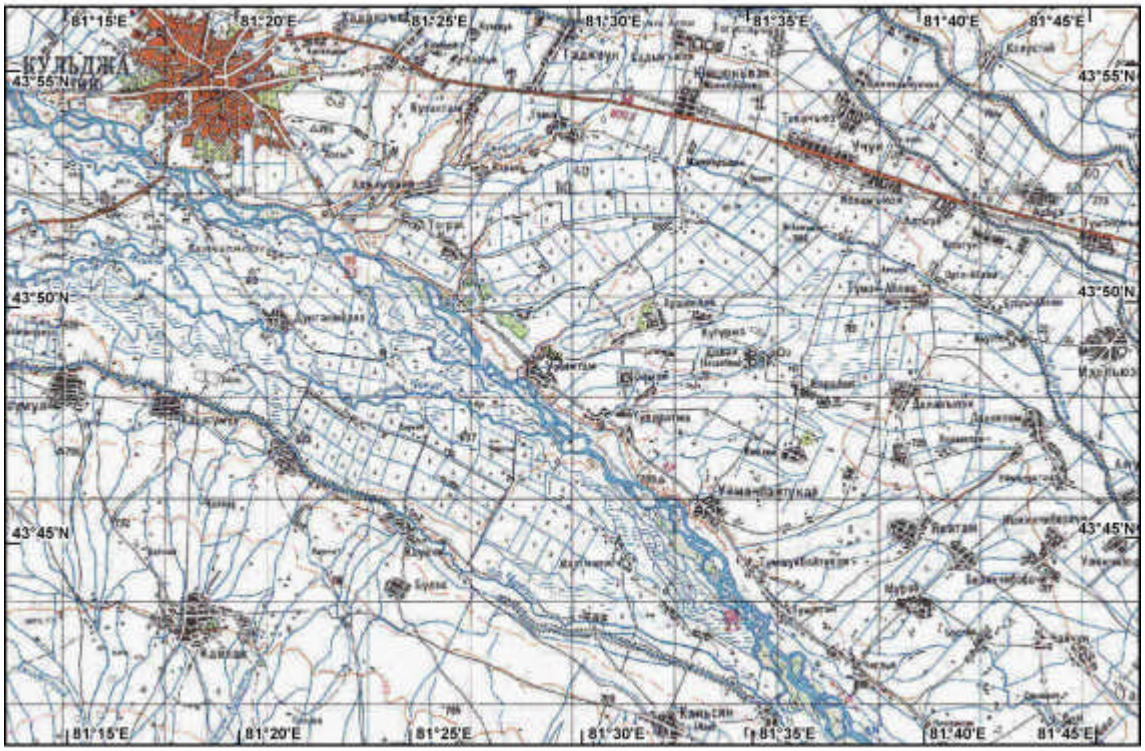

Source: own compilation

During the course of the project it became known that in Russia topographic maps at scales 1 : 100,000 and 1 : 200,000 are available for the study area. Although the revision date of these maps date back to 1978 / 1980, they nevertheless give much more topographic information than the Tactical Pilotage Chart 1 : 500,000. Maps would have been available for the entire project area, but for cost saving reasons just nine sheets of the 1 : 200,000 series were purchased (sheets L-44-33 to 35, K-44-3 to 5, K44-9 to11) (cp. Fig. 10). These map sheets cover most of the central part of the Upper Ili Catchment. An example of the topographic detail of this map series is illustrated by Fig. 11.

The topographic detail of the 1 : 100,000 map series was fairly similar to the 1 : 200,000 maps. Hence, only one sheet of this map series 1 : 100,000 was purchased for evaluation purpose.

2.2.3 Map of 'Development Areas'

Another very important information source was a sketch map of 'development areas' published by a team of Chinese scientist who investigated the Ili area and its development potential (Wissenschafts- und Ingenieurverein vom Ili-Gebiet (Hrsg.) 1999). Fig. 12 shows the original Chinese Map taken from this publication. This map was translated and redrawn into the map shown by Fig. 3. The map original illustrates that this 'map' is actually more a sketch than a real map. There is neither a co-ordinate grid, nor a scale bar, nor any information on the used map projection.

Figure 12: Original version of the (sketch) map showing implemented / planned 'development areas' in the Upper Ili Region.

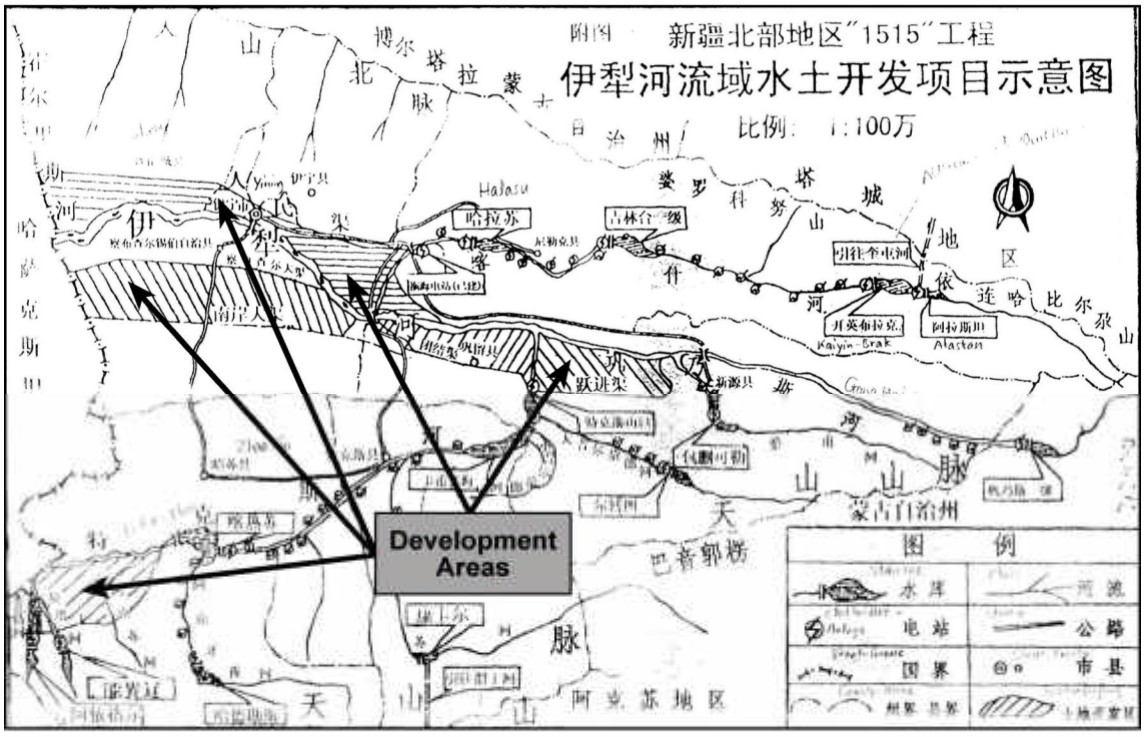

Source: Forschungsteam "Projekt 1515 des Ili-Gebietes" und Wissenschafts- und Ingenieurverein vom Ili-Gebiet (Hrsg.) (1999): Forschungen zur Erschließung des Ili- und Irtysch-Einzugsgebietes (Yili He e Erqisi He Liuyu Kaifa Yanjiu). Xinjiang Renmin Verlag, Urumqi, p. 48/49

Despite these shortcomings, the development areas could eventually be integrated into the GIS database. However, to achieve this task, a couple of technical 'detours' and tricks were required. Since the sketch map shows only rudimentary topographical details, the 'map' could not be geo-referenced in the usual manner. Instead, the marked boundaries had first to be correlated with specific topographic landmarks (mainly rivers, roads) on already georeferenced maps and satellite images. Once the respective landmark was identified, the boundary could be registered by screen-digitizing. Finally, the digitized lines were transformed into polygons, which were later used for the area measurements. Since, the boundaries of the development areas

usually followed roads and rivers, this indirect map compilation was nevertheless reasonably accurate.

2.2.4 Digital Vector Data for the County Boundaries

Administrative boundaries could be downloaded from the Internet. Digital boundaries for the whole of China are available as vector data sets from CITAS (China in Time and Space) a spatial data base compiled as part of a project of the University of Washington. [9]

The county boundaries for China were downloaded and those parts relevant for the study area were cut out. After correction of some obvious digitizing errors along the exterior limits of the study area, the lines were transformed into polygons.

2.2.5 Digital Vector Data for Streams and Rivers

The CITAS database for China (s. above) includes numerous other digital datasets for various features. Apart from the county boundaries, also the dataset for the drainage network seemed to be a promising information source for the present study. Hence, also the stream and river lines were downloaded and cut out in the above-described manner. However, this dataset turned out to be fairly useless. A digital overlay of these lines on top of the georeferenced maps and satellite images showed that this data set was digitised very poorly. Consequently, the CITAS river data were discarded and not used further. [10]

2.2.6 Digital Elevation Model

The third internet-based spatial data source for the study area was the digital elevation model (DEM) of the so-called GTOPO30. GTOPO30 is a global digital elevation model of the U.S. Geological Survey. The horizontal grid spacing of the elevation values is 30-arc seconds (0.008333 degrees), corresponding to a data spacing of about 1 x 1 km. The horizontal coordinate system is decimal degrees of latitude and longitude referenced to WGS84. The vertical units represent elevation in meters above mean sea level. The data have to be downloaded in large tiles. The data tile which includes the study area (ID-code E060N90) covers the entire area between 40° to 90° N and 60° to 100° E.[11]

After downloading, the data required for the study area were clipped and transformed into the coordinate system and projection used as project standard (UTM Zone 44 N, WGS 84). Fig. 13 shows the resulting DEM for the study area. The black line indicates the boundaries of the study area. In the north and south, these lines correspond to main water divides, the western boundary is formed by the international boundary between China and Kazakhstan.

Due to the course spatial resolution, the usability of this DEM is limited. The DEM facilitated the screen digitizing of the catchment divides (cp. Chapter 3). Later, the DEM was used for display purposes, in particular to visualise the study results in form of three-dimensional maps of the project area.

---

[9] Cp. CITAS (China in Time and Space Project, University of Washington (Sept. 1994), distributed by CIESIN (Consortium for International Earth Science Information Network 9). The original cartographic source of these digital boundaries is the Digital Chart of the World (1 : 1,000.000) developed by the US Defense Mapping Agency in co-operation with various institutions in Australia, Canada and the United Kingdom. URL: www.citas.csde.washington.edu/data/cntybnd/overview.htm.CITAS. The map revision date of the boundaries represent the situation in 1990 – 1994.

[10] Instead, a completely new river dataset was compiled by screen digitizing the major streams and rivers from the 2000/2001 satellite images. Since the river network is only required for orientation and display purposes, the digitizing was confined to major rivers, i.e. Ili, Tekes, Kunes, Kash and their main tributaries.

[11] For detailed information see data documentation under http://edcdaac.usgs.gov/gtopo30/README.html#h2. The data can be downloaded in tiles of 50 degrees latitude and 40 degrees longitude. X- and Y-valus are given as geographical coordinates, the Z-value (elevation) is given in (full) meters above sea level. The data are free of charge.

Figure 13: Digital elevation model of the study area

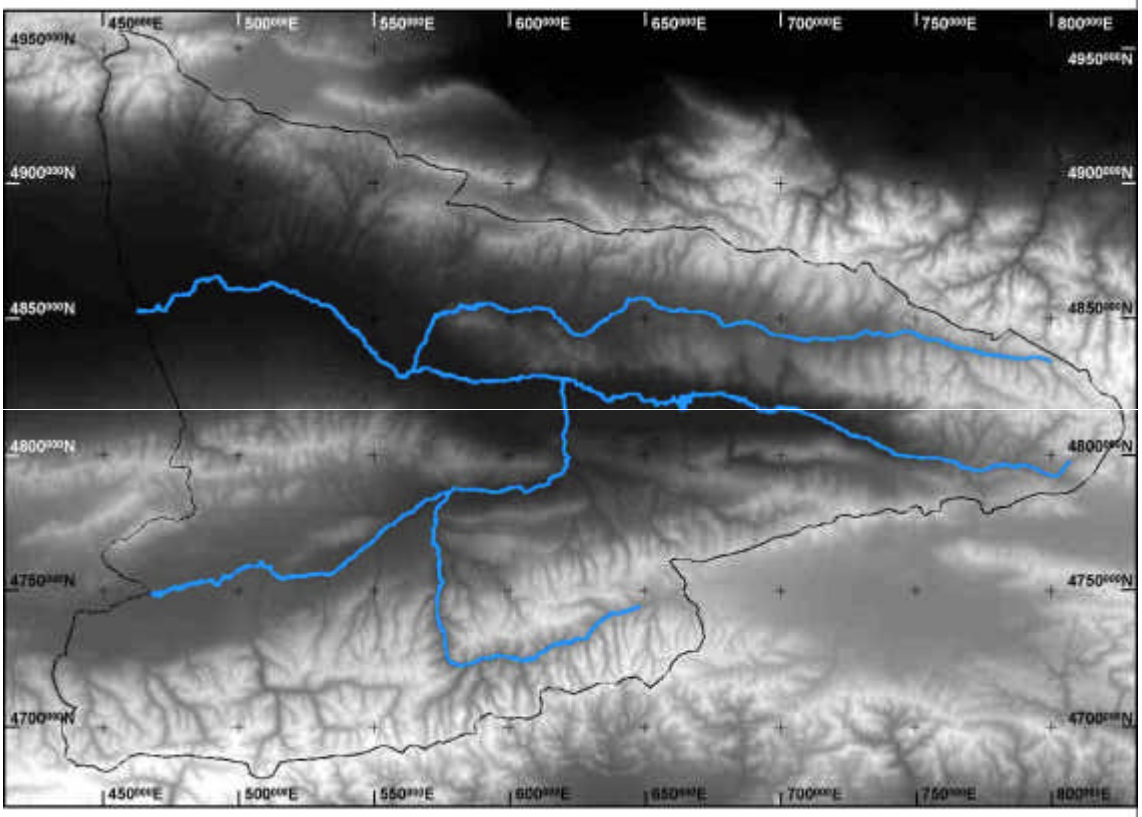

Source: GTOPO30 database, http://edcdaac.usgs.gov/gtopo30/README.html#h2.

3. STUDY APPROACH AND METHODOLOGY

3.1 GENERAL APPROACH

The working steps of the study are illustrated by the schematic flow chart shown in Fig. 14. In general terms, the study approach is based on a combination of conventional methods (i.e. visual image interpretation) and digital image classification techniques. In the following, the different working steps and their respective tasks will be described in more detail.

The main software used for the project activities - especially for the image processing tasks - was ER-Mapper 6.2. Certain vector-based tasks and some of the final map compilations were performed with MapInfo, ArcView 3.2 and ArcGIS/ArcView 8.2. DXF was used as exchange format for data transfer between ERMapper and the GIS software packages.

3.2 DATA ACQUISITION

The first step included the selection and the acquisition of the various data sets described in Chapter 2. The satellite images were selected using the USGS Earth Explorer Database (US Geological Survey)[12]. The satellite data were purchased from Gesellschaft für Angewandte Fernerkundung (GAF), Munich[13]. The map sheeet of the Tactical Pilotage Chart 1 : 500.000 were ordered as hardcopies via GeoCenter (Internationales Landkartenhaus), Stuttgart[14]. The Russian Topgraphical Maps 1 : 200:000 and 1 : 100:000 were purchased via GAF, which ordered them from a vendor in Russia. The maps were supplied as color scans in GIF-format on CD-ROM. The selected digital vector data and the digital elevation model were both downloaded from the respective internet pages of CITAS and GTOPO30 (cp. Chapter 2). Both types of data are free of charge.

3.3 DATABASE COMPILATION

The database compilation consisted of the following main activities:

- The three TPC-maps 1 : 500.000 were scanned as high resolution TIFF-files. To reduce the data volume for day-to-day work to a more convenient file size, the scans were then resampled with a lower resolution. Subsequently, the scanned maps were georeferenced to UTM Zone 44 North as standard co-ordinate system and WGS 84 (World Geodetic System) as reference ellipsoid. To reduce the file size even further, the maps were thereafter clipped to those parts which are actually required to cover the project area.
- The Russian topographic maps, which were already supplied as digital scans, were georeferenced in their original co-ordinate system (Gauss-Krüger) and then converted into the database standard UTM 44 N / WGS 84.
- The digital vector data and the DEM were supplied with geographic coordinates and then converted into UTM 44N / WGS 84 too.
- The Landsat 7 satellite images were provided by GAF as rectified and georeferenced images (UTM 44 N / WGS 84) with an (average) spatial accuracy of about 50 m. To achieve this accuracy, GAF post-processed the ordered images with a special rectification technique which uses data from the global GTOPO30 digital elevation model to compensate relief-induced distortions and data from the so-called ephemeris file[15]. This improves the usual spatial accuracy of Level 1G data from 150 m to about 50 m. The Landsat 2 images from 1976/77 were later fit into the database by means of 'image-to-

[12] http://edcsns17.cr.usgs.gov/EarthExplorer/

[13] http://www.gaf.de/

[14] http://www.geocenter.de/

[15] The ephemeris file records the deviations between the theoretically planned and the actual course and movement of the spacecraft. By reversing the image errors which are caused by these deviations the spatial accuracy of the results of the image rectification process can be improved considerably.

image' rectification, using the fairly accurately geocoded Landsat 7 images as reference. The 'nearest neighbour' option was used in all resampling procedures.

Figure 14: Flowchart of the study approach

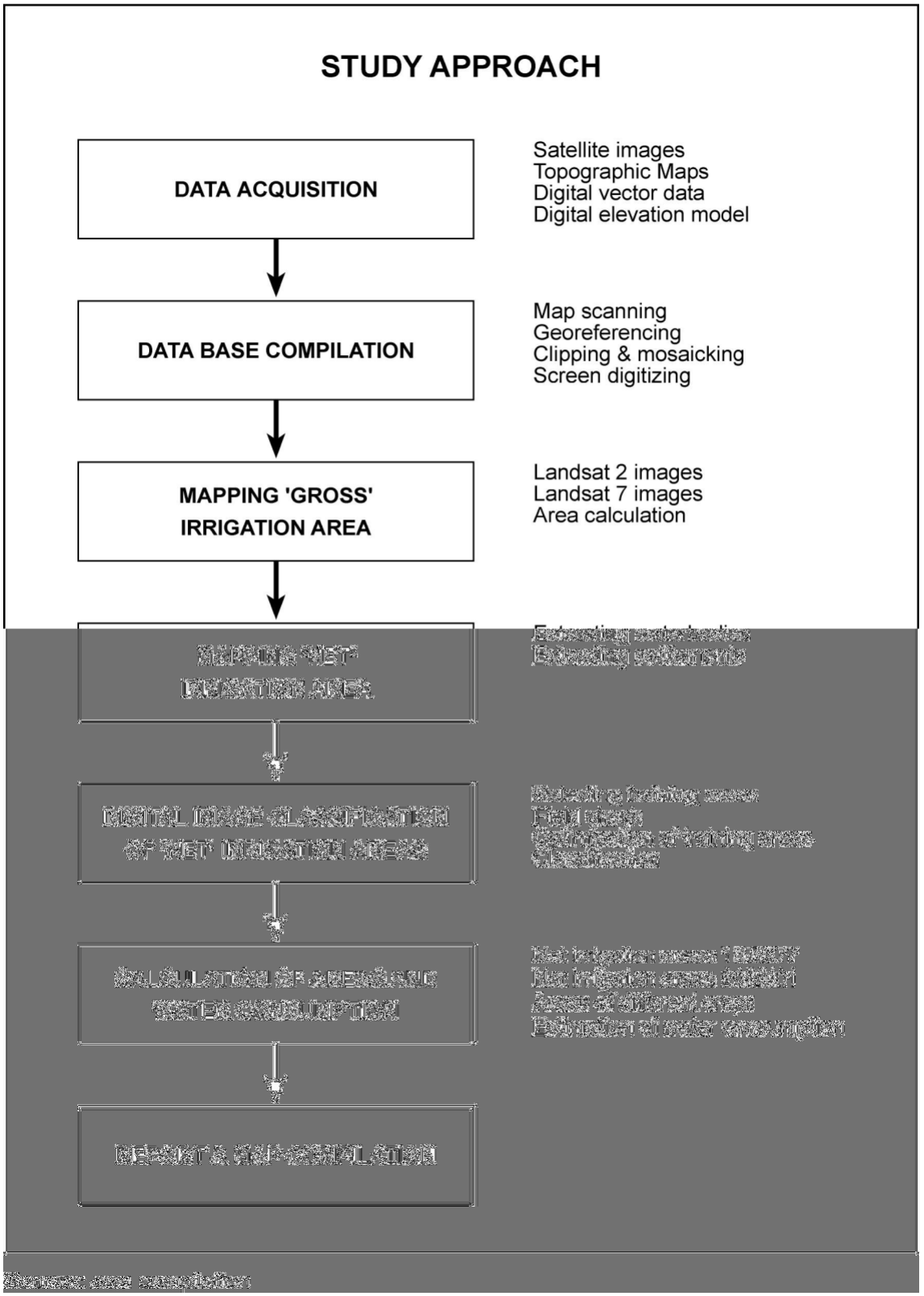

- The last two steps of the database compilation consisted of the delineation of the limits of the study area and (for display and orientation purposes only) the mapping of the main

river system. The northern and southern boundary of the project area was defined by screen-digitising the water divides of the mountain ranges in the north and south. These divides separate the Ili Basin from the adjacent catchments. The western boundary of the project area is formed by the international boundary between China and Kazakhstan, which was screen-digitised as well. For both digitising tasks, the TPC 1 : 500,000 served as base map. During the digitising of the divides, the DEM was used as additional topographic reference to double-check and verify the correct location of the digitised boundaries. Regarding the main river system, it was initially intended to use the digital vector data downloaded from the CITAS database. However, these data were poorly digitised and did not fit well to the rectified satellite images. Hence, the main river network was digitised again from the scratch, using the Landsat 7 images as reference map.

Finally, some auxiliary vector data sets were digitised in order to facilitate the orientation on the satellite images. These auxiliary data include the frames of the four Landsat 7 images and the three Landsat 2 images (cp. Fig. 6 and Fig 7).

3.4 MAPPING THE GROSS DEVELOPMENT AREA

As outlined in Chapter 1, the main task of the study was to map and measure the total irrigation areas at two different points in time in order to estimate the surface water consumption for irrigation purposes. According to information from local experts, in daily practice the consumption of irrigation water is (more or less) similar for all kinds of crops cultivated in the area, except for wetland rice, which needs about four to five times as much as a 'normal' crop. Hence, a detailed land use map which specifies the extension of individual crops would have been nice, but was not crucial to achieve the study objective. As a result of these and other considerations, a mixed-technology approach was followed which filtered out the areas of interest and refined the desired information in a step-by-step procedure.

The first step in this approach was to discriminate the irrigated land from the surrounding non-irrigated areas (fallow and pasture land, shrubs and forest). Already a glance at the satellite images reveals that the irrigated areas form large, consolidated and fairly easily recognisable blocks of land along the Ili River and its major tributaries Tekes, Kunes, and Kash.

Due to the aridity of most parts of the Ili Basin, the boundaries between irrigated and non-irrigated lands are rather sharp and thus easy to delineate, at least in most parts of the project area. As illustrated in Fig. 15 and 16, this holds true not only for the Landsat 7 images, but also (to some lesser extent) for the old Landsat 2 images with their lower data quality and lower spatial resolution. Fig. 15 shows an irrigation area along the Ili River in the northwest of the project area using a so-called Tasseled Cap (Kauth-Thomas) transformation of the Landsat 7 data. Tasseled Cap turned out to be particularly well-suited to display the irrigation areas.[16] Figure 16 illustrates the sharp boundary between irrigated and non-irrigated land on a standard false colour composite representation.

Due to the low rainfall in most parts of the project area, it can be assumed that cultivated land is usually irrigated. The field check showed that this assumption holds true for most of the project area with the exception of some areas along the upper Tekes River in the southwest section of the study area. In this part, higher elevations result in lower temperatures and higher yearly rainfall of up to 500 mm and more. These conditions allow large-scale rainfed cultivation of rape and wheat. According to the Chinese colleagues who conducted the field check, rainfed agriculture (locally called "glebe") is the by far dominating land use type in this area.

Downstream the Tekes River elevation and rainfall decreases and cultivation gradually changes to full irrigation. The higher rainfall in the upper Tekes region also shows up clearly on the satellite images. Due to the increased rainfall and the lower temperatures the vegetation cover on the non-cultivated lands is more pronounced and the boundary between irrigated and non-irrigated land becomes somewhat blurred and more difficult to delineate.

However, apart from this section and (possibly) some smaller areas in the extreme east of the upper Kunesh, the limits of the irrigated areas could be mapped fairly well by simple screen

---

[16] The tasseled cap transform of Landsat TM data defines a new coordinate system whose axes represent "brightness", "greenness" and "wetness" of the pixel. For details see Mather 1999, p. 124 ff.

digitising. The result of this procedure forms the so-called 'gross development area'. The term 'gross area' has been selected for this first step, because these consolidated irrigation areas along the Ili, Tekes and Kunesh still include various 'impurities', i.e. areas which are not used for the cultivation of irrigated crops. The major part of these non-irrigated areas within the irrigation land consists of water bodies and settlements.

The following Chapter 3.5 describes the procedure which was used to mask out these settlement and water areas in order to extract the actual so-called 'net irrigation area'. The respective area figures for the 'gross' and 'net' areas and the two types of excluded subunits are presented in Chapter 4 'Analysis Results'. It should be noted that this step does not yet exclude any fallow plots or other non-irrigated areas from the consolidated irrigation belt along the rivers. The 'fallow problem' has been considered and taken care of at a later stage of the procedure (cp. Chapter 3.6 and Chapter 4)!

Figure 15: Landsat 7 Data: Example of clear boundary between irrigated and non-irrigated land

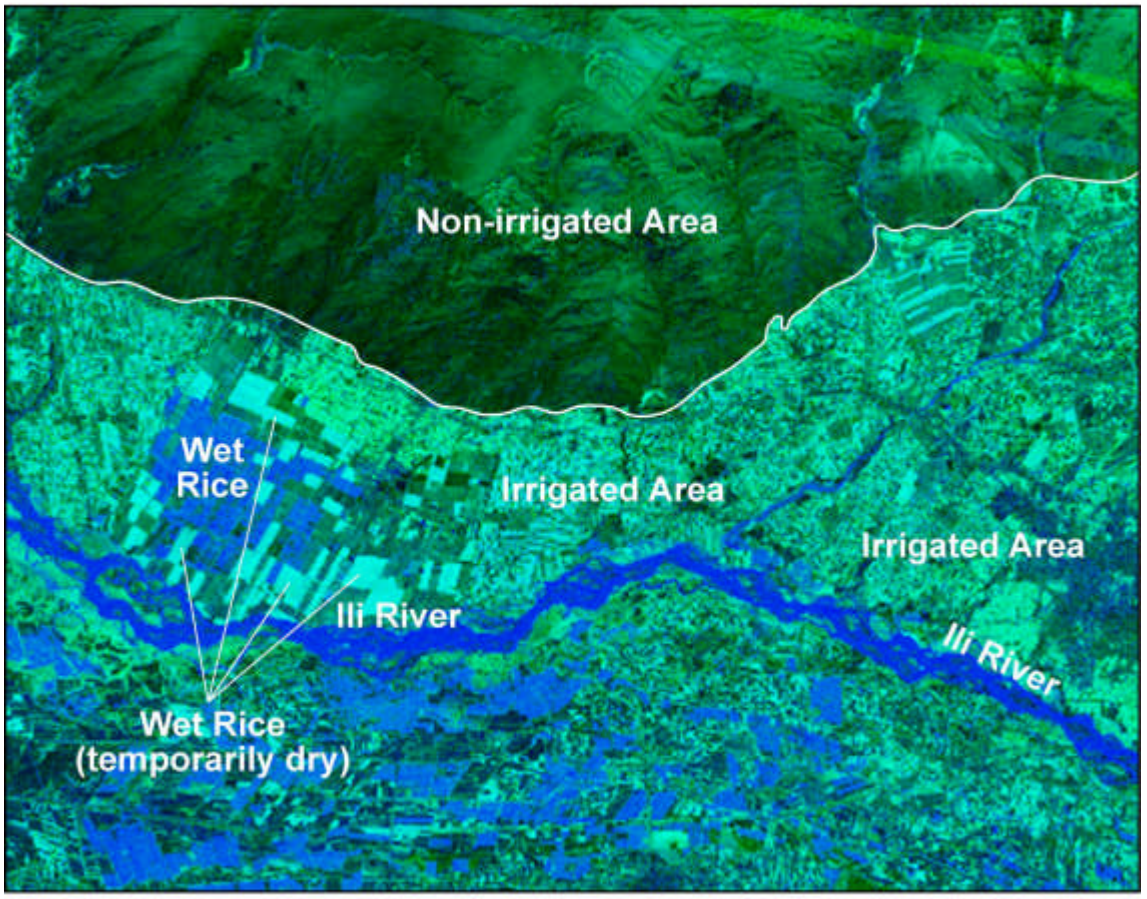

Source: own compilation

Figure 16: Landsat 2 Data: Example of clear boundary between irrigated and non-irrigated land

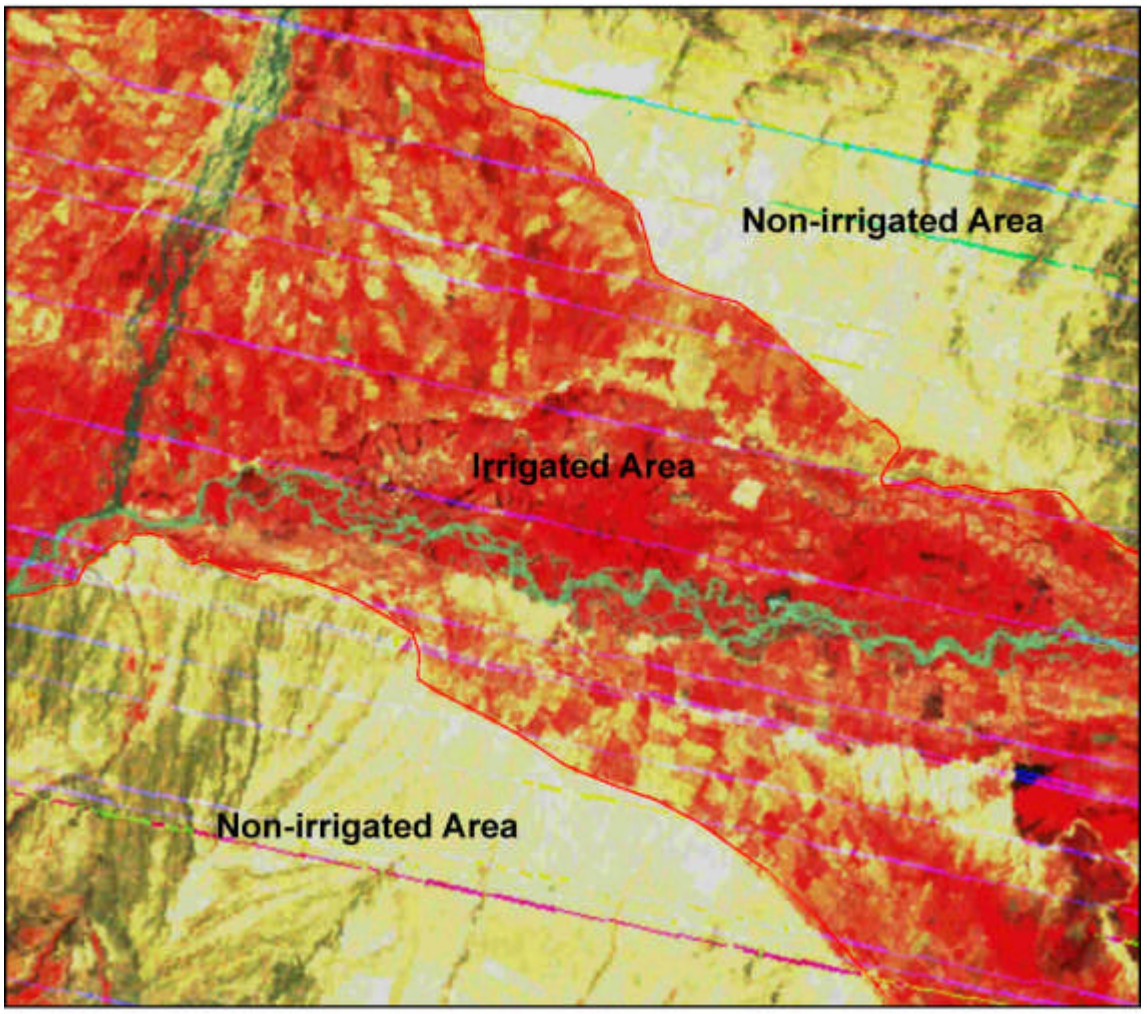

Source: own compilation

3.5 MAPPING THE NET IRRIGATION AREA

Two major types of non-irrigated land had to be mapped and extracted from the gross development area:

- areas covered by water bodies (excluding flooded wetland rice fields),
- areas covered by settlements.

A combination of digital and visual interpretation methods was used to filter out these areas. The result of this refinement procedure is the so-called 'net irrigation area':

Net Irrigation Area = Gross Development Area – (Water bodies + Settlements)

3.5.1 Extraction of the main water bodies

The water bodies to be filtered out consisted of the areas covered by the main streams and rivers, especially the Ili itself and its main tributaries. Due to the technical procedure applied (see below), smaller streams and rivers were not considered. Any larger standing water bodies, (natural lakes, artificial dams) do not exist within the gross irrigation areas.

The main problem in extracting these water bodies was caused by the fact that the river water shows very similar spectral characteristics as (flooded) wetland rice fields in the early growing stages (cp. Fig. 17).[17] The diagram in Fig. 17 illustrates that - spectrally - there is no significant difference between a 'river pixel' and such a 'wetland rice' pixel. Visually, however, rivers and flooded rice fields can be distinguished easily, due to the respective typical forms and patterns (cp. Fig. 15). Spectrally, however, an open water surface is and remains an open water surface, no matter whether this is a river or a flooded wetland rice plot! As a consequence, spectral masking could not be applied, because every spectral procedure would always mask both types of water pixels.

Figure 17: Similarity of spectral signatures of river pixels and flooded wet rice

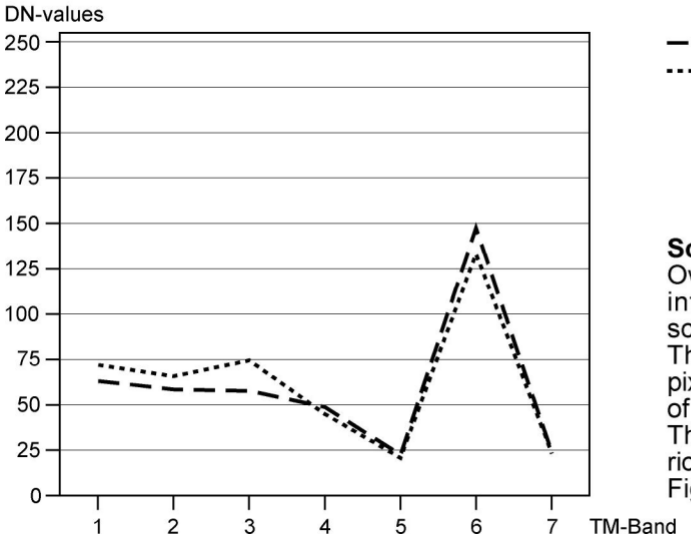

Source:
Own compilation, based on pixel value information extracted from Landsat 7 scene 147-29, 2001-05-27, area "NW". The spectral curves illustrate average pixel values of a flooded wet rice plot and of pixels of the central part of the Ili River. The values were extracted from the wet rice area and the adjacent river shown in Fig. 15.

Luckily, the ER-Mapper software supplies a special feature for his type of problem. ER-Mapper includes a tool which (spectrally) detects water bodies and creates a temporary Boolean map ("water" = 1, "no water" = 0). Using vector raster conversion, ER-Mapper then converts the detected "water" areas into polylines (line vectors). These polylines were then converted into DXF-format and exported to MapInfo 5.0. In MapInfo the polylines were converted to polygons.

Due to the spectral similarities shown above, these polygons still include both, rivers as well as flooded rice fields! However, fields and rivers can be easily discriminated visually by their typical form and pattern. Based on this visual assessment, the polygons were edited manually, to 'weed out' the non-river water areas. To facilitate and accelerate this time-consuming editing process, an area filter was applied to extract polygons whose sizes exceed a user-defined threshold value. By using this area filter, most of the river polygons could be selected, the remaining river polygons hat the selected and removed 'by hand'.

The "river" polygons were then re-converted (still in MapInfo) into polylines and these polylines were re-converted into DXF-format. Finally, the edited polylines in DXF-format were re-imported into ER-Mapper vector format and converted into so-called 'regions'.[18] Finally, a standard formula for a 'positive mask' was used to exclude the pixel values of the river areas from the raster data set of the gross development area. The result of this tedious procedure is a raster data set which covers the gross development area minus the (excluded) river areas.

---

[17] Which, in a way, are of course waterbodies too, although of a temporary nature only!

[18] In ER-Mapper, a ‚region' file corresponds to a vector polygon file, usually created by screen digitizing or by importing already existing vector data. The resulting polygons are linked to an existing raster image file by storing them in the raster image data set header. They define and delimit the areas of the raster data set for which subsequent processing steps will be performed: "A region is not an image, but rather an area you can use to calculate statistics for formulae or classification. The regions are defined as vectors but they are stored within the raster image dataset header file with the calculated statistics" (cp. ER-Mapper Online Hilfe). 'Regions' are typically used to define training areas for supervised classification, to calculate statistics for selected subunits of the raster image or – as in this case – to mask out areas of interest respectively areas of no interest.

3.5.2 Extraction of the main settlement areas

Masking the areas occupied by settlements is not a straightforward procedure either, especially if they are to be extracted as consolidated, coherent polygons. Settlements are characterised by a wide range of spectral reflectance values. A settlement typically consists of a complex assemblage of fairly small plots with different types of land cover (e.g. buildings, roads, gardens, parks, industrial areas etc.), all of which feature different spectral characteristics.

Hence, fixed spectral characteristics of 'the' typical settlement pixel do not exist! The problem is aggravated by the fact that settlement pixels give often so-called 'mixed pixel' signals. Depending on the spatial resolution of the pixel, the reflected signal of a specific pixel might be influenced by several different land cover types. A Landsat 7 pixel (30 x 30 m) could, for example, represent an area covered to 10% by a road, 40% by a building, and the remaining 50% by gardens. Therefore, a proper masking of settlement areas by digital classification procedures is difficult and will usually leave a certain percentage of unclassified and / or misclassified pixels within the settlement area.

Hence, a simple conventional technique was used instead. The settlement areas were mapped by screen digitising, based on the visual interpretation of the Landsat 7 satellite images (Pan and multispectral mode) and the Russian topographic maps:

- Using a suitable mode and band combination, the Landsat 7 image was displayed in combination with the respective Russian topographic map 1 : 200,000. With the help of these maps, the location of the settlement was identified.
- The exterior boundaries were then screen-digitised from the satellite image as polygon. Only settlements with a certain (subjectively defined) minimum area were mapped.
- Finally, the vector polygons were transformed into 'regions' as described for the 'water body areas'. These regions were then used again to mask out the respective data from the underlying Landsat 7 image data set.

3.6 DIGITAL IMAGE CLASSIFICATION OF THE NET IRRIGATION AREA

3.6.1 General Remarks

At the end of the above-described working steps, the gross development area had been – by and large - narrowed down to those pixels, which represent irrigated lands. Potential exemptions are the following:

- small water bodies and small settlements which were too small to be excluded by the filter procedure described above,
- fallow land,
- small miscellaneous areas which are neither water, nor settlements, nor fallow land (e.g. quarries, gravel and rubble areas along the riverbeds, little areas of bush and shrub)

Hence, the last working step now aimed at the following tasks:

- to filter out the latter two classes (fallows and miscellaneous areas respectively) and
- to sub-divide the irrigated areas further into different land use / land cover types.

In contrast to the working steps described before, this task now requires a digital image processing approach which makes use of the different spectral characteristics of the various land cover types. Hence, a supervised digital image classification of the remaining image pixels was performed.

Supervised image classification is a well-known standard image processing method which needs not be explained in detail.[19] The method uses the fact that different types of land cover,

[19] More detailed information on digital image classification is given in any remote sensing textbook, such as Mother (1999).

such as forest, pasture, water, bare soil, as well as different crop types feature different spectral characteristics. Once the correlations between different land cover classes and their respective spectral characteristics are established and verified for selected areas (the so-called 'training areas'), these correlations can be used to classify the image pixels of a satellite image into the respective 'most likely' land cover classes.

These 'training areas' are then used as decision reference for various classification algorithms ('classifiers'). During the classification procedure, the selected classifier compares the spectral characteristics of the (still unclassified) image pixel with the spectral characteristics of the previously selected training areas. Using statistical procedures and decision rules, the classifier then selects the most likely land cover class for each pixel. Standards classifiers are, for example, Minimum Distance, Parallelepiped ('Box') and Maximum Likelihood. Most digital image processing software packages offer several variants for each classifier.

The most critical limitation of standard digital image classification methods lies in the fact that they use only the spectral reflectance of a pixel. Other image characteristics, such as form, pattern, size or location of features, which are quite important decision criteria in visual interpretation, are not taken into account. The quality and reliability of the classification results depend on various factors, the most important being:

- data quality of the satellite images,
- quality, number and representativeness of the training areas,
- reasonably large coherent areas of uniform land cover,
- clear spectral differences between different land cover classes,
- reasonable spectral homogeneity within each land cover class,
- numerous and reliable ground truth data,
- selection of the most appropriate classifier.

In the case of this study, these conditions could be met to a limited degree only! Considerable constraints limited the degree of detail and the degree of accuracy of the information extracted from the satellite data. The most important constraints, partly interrelated with each other, were:

- poor data quality (Landsat 2 data),
- unfavourable recording date of the satellite scenes,
- very limited possibilities to conduct field checks.

In the following, some additional comments are given on these constraints.

Poor data quality

While the data quality of the selected Landsat 7 scenes is excellent, the data quality of the three Landsat 2 images was poor. All three satellite scenes were full of systematic and unsystematic data errors including faulty data lines etc. The errors were too numerous and too extensively distributed over the satellite scenes to be removed with error correction routines. While these Landsat images were still sufficient for the visual interpretation tasks described in Chapter 3.4 and 3.5, a supervised digital image classification would have been a futile exercise! Apart from the insufficient data quality, there would have been no reliable ground truth data of the land cover situation which existed in the area more than 25 years ago! Hence, the Landsat 2 images were used for visual interpretation only.

Unfavourable recording date of the satellite images

A second major constraint was that three of the four Landsat 7 images were recorded rather early, in fact at a much too early stage of the growing season. The selected satellite scenes (Landsat 7) were taken May 27 (scenes 147 / 030 and 147 / 029, June 5 (scene 146 / 030) and June 27 (scene 145 / 030) respectively. As outlined in Chapter 2.1, the growing season starts in April and ends in September. To discriminate different crops by digital image classification, the

spectral characteristics of the different crops should be as different as possible. This, however, requires that the crops have reached a sufficiently mature crop development stage. Hence, 'optimal' satellite images should have been recorded late in the growing season. Around end of July / mid-August would have been the best period.[20] Unluckily, such more suitable images were not available for the area for year 2000 or 2001.

A field check, conducted by Chinese colleagues in June 2003, showed that during the period end of May / middle of June the crop-specific spectral differences are not yet sufficiently developed to allow for a good discrimination of different crops. As illustrated by Photo 1 and 2, at that time most plants are still fairly small and a major part of the recorded pixel signal is still dominated by the reflectance characteristics of bare soil. Therefore, the spectral signatures of different crops are still very similar, which considerably limits the potential for detailed crop discrimination (cp. Fig. 18). This especially holds true for crops like maize and sunflower, which at that phase of the growing season hardly cover 10% of the soil surface. Fig. 18 shows the reflectance curve for different crops at this early growing stage. As can be seen from the small differences between the two lines, the spectral characteristics of the two crops - here sunflower and soybean - are more or less identical at this early stage.

Figure 18: Similarity of spectral signatures of different crops at early growing stage

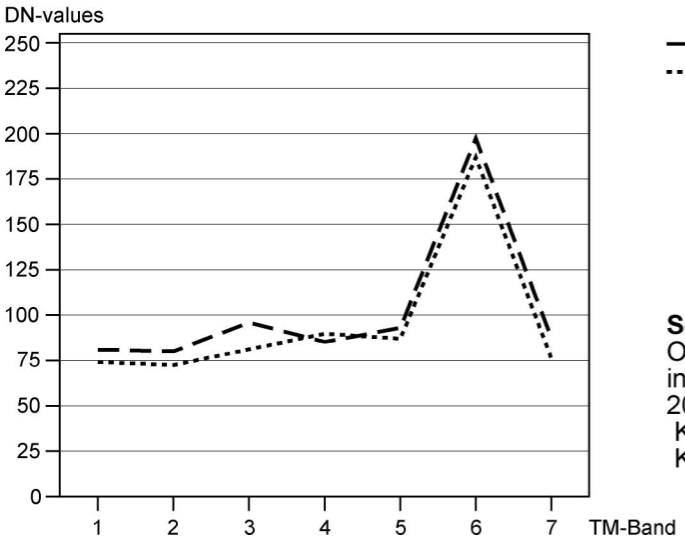

Source:
Own compilation, based on pixel value information from Landsat 7 scene 146/30, 2001-06-05, area "CEN", plots KL_146_6_3/KL_11 (soybean) and KL_146_6_2/KL_14 (sunflower)

Another problem of the early recording date is that crop development differences within a particular crop may be considerable, depending on the respective time of sowing. A comparison of the two sunflower fields shown by Photo 1 and Photo 3 illustrates this problem. On Photo 1 the sunflowers are hardly visible while on Photo 3 the crop leaves cover already most of the soil surface. While this problem is most prominent for sunflowers, to some lesser extent it also holds true for maize and soybeans.

Fig. 19 and 20 illustrate the consequences for the spectral signal. Fig. 19 shows the spectral variations between four individual pixels belonging to the same sunflower plot. As illustrated, the form of the curves for the four pixels is fairly similar. However, the absolute reflection values may vary up to 20 DN-values (cp. in particular bands 1, 2 and 3).

The variation becomes even worse if spectral signals from different fields (covered with the same crop) are compared. Fig. 20 shows average spectral values for three different soybean fields which are located within the same area and even fairly close together. The figure clearly shows that there are considerable variations of the spectral signal, even between fields within the same area. The spectral differences are caused by differences in the crop development stage which is mainly due to different sowing dates. If the satellite data were recorded at a later

[20] For a comparable land cover study of the lower course and the delta of the Amu-Darja, Ressl used Landsat scenes recorded in August (Ressl 1999, p. 73).

stage of the crop development cycle (e.g. in mid-July / early August) these 'in-field variations' and 'between-field' variations would have levelled out to a large extent.

Photo 1: Sunflower field at early growing phase

Even about two months after sowing crops like sunflower hardly cover 10% of the soil surface. Therefore the spectal signal is dominated by the bare soil.

Source: Photo taken in the central part of the study area during the field check campaign (Photo: Central_KI3-16, June 14, 2003)

Figure 19: Spectral signature of four pixels within the same soybean plot

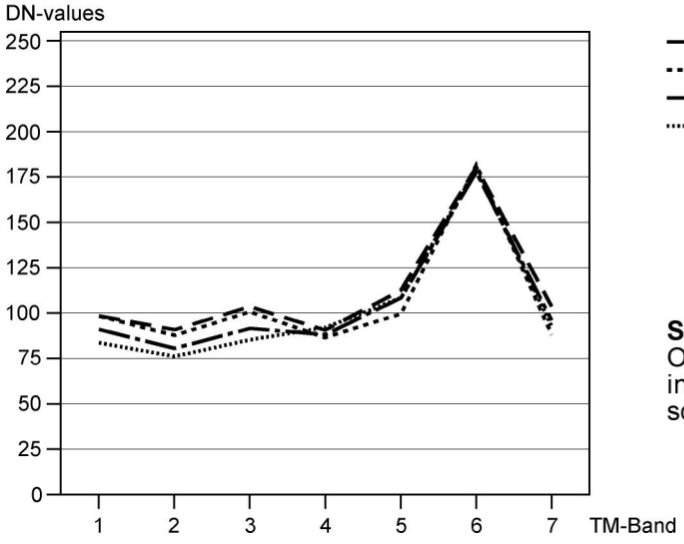

Source:
Own compilation, based on pixel value information extracted from Landsat 7 scene KL_147_N_5_3/KL_17

Photo 2: Sugar beet and maize field at early growing phase

In case of sugar beet (left field) and maize (right field), the soil coverage is somewhat higher but still rather low. Due to the oblique viewing angle, the photo actually overestimates the actual soil coverage considerably. If looked vertically from above, no more than about 20% of the soil surface is covered by the crop leaves.

Source: Photo taken in the central part of the study area during the field check campaign (Photo: NW_KI4-14, June 20, 2003).

Figure 20: Spectral variation between different soybean plots within the same area

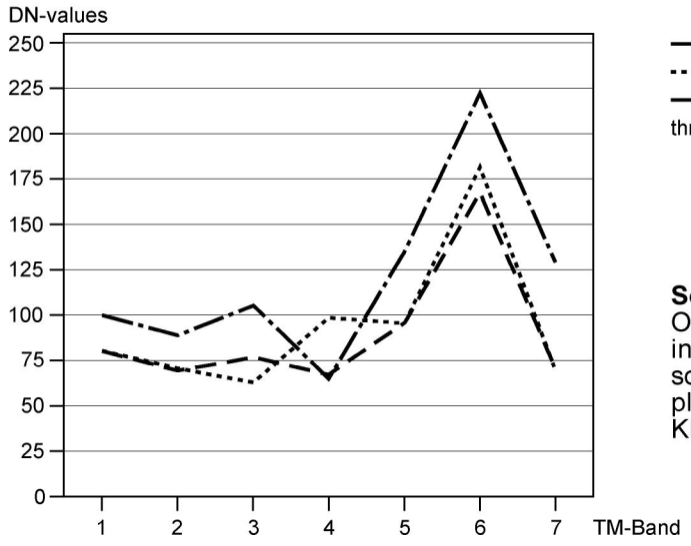

(KL 1)
(KL 4)
(KL 15)
three soybean plots are located fairly close together

Source:
Own compilation, based on pixel value information extracted from Landsat 7 scene 145/30, 2000-06-27, area "EAST", plots KL_145_1_1/KL_1, KL_145_4_1/ KL_4, KL_145_5_3/KL_15

Photo 3: Sunflower field at more advanced growing phase

Sunflower fields showed a considerable range of crop development. While the sunflower plants in Photo 1 are hardly visible, the plants in this field have already developed sufficiently to cover most of the soil surface. Naturally, the spectral signature of the two fields differs strongly!

Source: Photo taken during field check campaign in June 2003 (Photo-ID NW_KL-4-13)

It is clear that under these circumstances, crop-specific spectral reflectance signatures are very limited and, therefore, the crop discrimination potential as well. As a consequence, several little-developed crops had to be lumped together into one big land cover class.

Limitations regarding field check possibilities / limited ground truth

A third major constraint for the study was due to the fact that no team member actually visited the study area, neither for the usual pre-study reconnaissance trip, nor for the selection of the training areas, nor for the verification of the study results. The study area belongs to a region of China which is strategically and politically quite sensitive. For a foreigner, moving around freely in this area – as would have been required – is almost impossible and risky as well, in particular with 'suspicious' materials and instruments, such as satellite images and GPS. Apart from this problem, the field check would have caused considerable travel costs.

The cooperation with Chinese colleagues from the University of Urumqi offered an acceptable (though not fully satisfactory) way out. The Chinese colleagues were asked to compile ground truth data according to detailed prior instructions supplied by the authors. These instructions specified exactly where to go and what to check on each site. However, this assistance had logistic limitations regarding time availability, staff resources and the accessibility of the designated areas. As a consequence, only one field work campaign could be conducted at one selected moment during the study. This limited the number of the field check sites as well as their spatial distribution. It also ruled out the chance to interface field work and image processing more closely in order to adjust and optimise the processing results in an iterative way. More detailed information regarding the field check is given in Chapter 3.6.3.

3.6.2 Selection of Training Areas

The selection of training areas is usually based on a preliminary visual image interpretation in combination with a reconnaissance field trip. The information which is compiled during such a reconnaissance trip familiarises the image interpreter with the general nature of the area and in particular with the types and the visual appearance of the various land cover classes. By comparing land cover classes in the field with their respective characteristics on the satellite image, the interpreter then selects representative locations for training areas.

As described before, in the present study, this standard procedure could not be adhered to. The study team had to base the selection of the training areas on the visual interpretation and the spectral analysis of the satellite images. Using different colour composite combinations for optimal display, potential mapping units were selected. At potential training area sites, spectral curves were extracted and analysed. Based on these spectral characteristics first assumptions regarding the respective land cover type could be drawn, but – apart from very few clear land cover classes, such as water– no reliable identification was possible at that time.

For each of the spectrally different land cover classes several representative training areas were selected, usually using field plots which are easy to access and identify in the field. These training plots were marked on satellite image prints and on the digital topographic maps. Additionally, the exact geographic coordinates of the center of the respective plot were recorded from the screen, to enable the Chinese colleagues to verify the correct position by GPS.

In order to keep the staff and time resources for the fieldwork within acceptable limits, the number of training plots was limited to 85 only. For the same reason, the training sites were not distributed evenly over the entire study area, but concentrated in four easily accessible training area clusters. Each of the four clusters represented a certain section of the study area (Northwest, Southwest, Central, and East respectively). For each of these four clusters, a table was compiled with all data required to find and identify the selected training area plots and to verify their present and former land use. These tables were emailed to our Chinese counterparts who carried out the field check.

3.6.3 Field Check of Training Areas

The fieldwork campaign was conducted in June 2003. The timing of the fieldwork campaign was selected in such a way that the fieldwork period fell exactly into the same period during which the Landsat 7 images had been recorded in 2000 / 2001.[21] Hence, the crop growing stage recorded during the field check campaign is likely to be more or less comparable to the situation at the respective time of the image recording in 2000 / 2001.

Due to certain access restrictions, the Chinese colleagues could check only 70 out of 85 selected training sites. For these 70 plots, the following information was collected:

- land use / land cover at the time of field check (i.e. June 2003),
- land use / land cover at the time of image recording (i.e. in May / June 2000 / 2001)

To compile the information on the land use in 2000 / 2001, local farmers and farm managers were interviewed. It should be noted that this involves a considerable risk of compiling false information! Unlike the land use at the time of field check, the data regarding the land use in 2000 / 2001 could not be verified directly, but had to be based on the memory of the interviewed persons. Hence, for some training areas, this information was somewhat questionable.

Additionally, from each training site a digital photo was taken as reference. Of course, these photos in general do not show the 'same' situation as prevailing at the time of image recording. In most cases, the crop grown in 2003 was different from the crop grown in 2000 / 2001. Even if the same crop had been grown, a certain difference would have to be expected, due to (probable) slight differences in crop development. However, though the photos will not necessarily reflect the situation at the time of image recording for any specific location, all recorded photos together are nevertheless likely to give a fairly reliable overall impression of the crop development at the comparable growing stage in year 2000 / 2001.

---

[21] The four Landsat 7 images were recorded between May 27 and June 27, the fieldwork took place between June 12 and June 21, 2003.

3.6.4 Analysis of Field Check Results

The field check results revealed the problems described and discussed further above. Though it was clear that the early recording of the satellite images would cause certain problems, it was not expected that the crops are developed so little! It was also not expected that the growing differences within the same crop would be so pronounced.

As a result of the field check carried out in June 2003, various little-developed crops had to be lumped together into one land cover class. In this class "little-developed crops" the bare soil surface still dominates the reflectance signal. Therefore, this class may also contain a certain percentage of fallow area which could not be discriminated reliably from, for example, sunflower or maize at a very early growing stage (cp. for example Photo 1).

Photo 4: Flooded wet rice (paddy)

The rice plants on this photo are still fairly small and cover only a small fraction of the water surface. The characteristic spectral signature of 'open water' (very low signal values, especially in the infra-red bands) dominates the reflected signal and renders the flooded plots easily visible on the satellite image (cp. also Figure 15)

Source: Photo taken during field check campaign in June 2003 (Photo-ID NW_KL-4-02)

Another problem which became obvious from the field check concerns wetland rice ('paddy'). Initially it was unknown that paddy is grown in the study area in the first place. Though the irrigated paddy fields showed up clearly on the satellite images (cp. Fig. 15), Chinese colleagues who claimed to be familiar with the area, did not have any prior knowledge of the existence of paddy cultivation in this area! The field check eventually solved the mystery and verified our assumptions from the visual image analysis. However, the field check also illustrated two specific image classification problems for these rice areas. Photo 4 shows a typical irrigated rice field shortly after planting. In this growing stage, the vegetation cover is still very low and the open water still dominates the spectral signature. The paddy fields are thus easily identified by their characteristically low reflectance values, especially in the infrared bands 4, 5, and 7.

Photo 5: Wet rice field, temporarily dry

Temporarily dry paddy fields loose the characteristic spectral signature caused by water. The spectral characteristics become similar to those of open grassland and moderately developed winter wheat. Visually, however, the 'dry' paddy plots are fairly easy to identify because of their condierable size and their association with flooded paddy plots (cp. the big light blue pixel blocks in Fig. 15).

Source: Photo taken during field check campaign in June 2003 (Photo-ID NW_KL-4-24)

However, the flooded rice fields show – at this stage - more or less the same spectral characteristics as any other open water surface, such as rivers (cp. Chapter 3.5.1 and Fig. 15 and 17). Fig. 17 illustrated that 'river pixels' cannot be discriminated reliably from paddy field pixels on the basis of their spectral characteristics.

A second problem is illustrated by Photo 5. Some of the paddy fields were – for unknown reasons - temporarily dry at the time of image recording. In Fig. 15, these 'dry' paddy fields show up as large light blue plots in the immediate vicinity of (and always associated with) flooded paddy. During such a 'dry' phase, the spectral signature changes considerably and becomes very similar to certain grasslands and to winter wheat fields. In either of the two cases, flooded as well as 'dry' paddy, a normal pixel-based image classification alone will not separate paddy plots from other land cover types. Hence, the 'dry' paddy fields had to be mapped manually and added to the land cover class "paddy" 'by hand (cp. Chapter 3.5).

3.6.5 Final Definition of Mapping Classes

As described before, the early recording of the satellite images limited the potential for spectral discrimination of different crops. The following table summarizes the different types of crop / land cover, their growing stage and the resulting spectral characteristics for the different parts of the project area. The area had been covered by four satellite Landsat 7 scenes, taken at three different dates:

- The n**orthwest section** (NW) was covered by a scene recorded on May 27, 2001.

- The **southwest section** (SW) was recorded at the same day (May 27, 2001), but differs from the NW by a considerably higher altitude and a respectively cooler climate.
- The **central section** (CEN) is climatically similar to the NW, but the satellite scene was recorded nine days later (June 5, 2001).
- The **eastern section** (EA) is covered by a scene which was recorded still later in the growing season, but one year earlier (June 27, 2000).

To account for these differences, the image analysis of study area was subdivided into the above-described four sections. For each of these four sub-units, one representative cluster of training areas was selected on the respective scene and checked in the field as described in Chapter 3.6.3. Tables 5 – 8 summarise the appearance and the spectral characteristics of the various crop / land cover classes identified in these four sub-units, as verified 'on-site' during the fieldwork campaign. Hence, the data summarised in this table refer to and are based on the fieldwork findings in May / June 2003. They do not document the situation at the time of image recording! However, due to the comparable timing of both, the general situation at this time can be assumed to be more or less comparable.

The Tables 5 - 8 illustrate the dilemma for digital image classification. In many places the crops were too little developed to have already developed their crop-specific spectral signatures. As a consequence, the largely uncovered soil surface dominates the signal. As illustrates by Fig. 18 (cp. Chapter 3.6.1), the signature of this 'bare soil' signal is more or less the same, irrespectively of the cultivated crop! Hence, various different (but spectrally similar) crops / land cover types had to be lumped together into few big land cover classes.

Tables 5 - 8 also illustrates that the same crop may have fairly different spectral signatures, depending on the respective development stage in combination with the recording date of the image. For example, in Area East maize has already developed sufficient leaf cover to show a characteristic 'vegetation curve' with the typical 'red edge' between the 'red' band (TM-band 3) and the NIR band (TM-band 4). In Area Central, however, the maize plants were much less developed and thus the soil surface still dominated the signal. Therefore, in one part of the area, maize can be discriminated from bare soil and very small crops, but in another part it has to be lumped together with other similarly little developed crops like soybean or sunflower.

Finally, there was a third problem: In Area East, the maize fields show spectral reflectance curves which are almost identical to the spectral signature of winter wheat (cp. Fig. 21). Hence, although the two crops have already developed a typical vegetation signature, the signatures are too close together to allow for a reasonably reliable discrimination at this crop development stage. Therefore, again two crops had to be lumped together into one mapping unit.

Table 9 - 12 summarise the resulting mapping classes for the different sub-units of the study area and the crop / land cover types which form the components of these classes. It illustrates that the possibilities to discriminate individual crops vary from area to area but are – in general - disappointingly limited.

With regard to the planned assessment of the overall water consumption in the area, the most important discrimination is the separation of wetland rice (paddy) from other crops, because the (net) water consumption differs by a factor of about three to four (rice about 11,500 m^3 / ha / year, other crops 2000 – 3750 m^3 / ha)[22]. This discrimination was possible, although not solely on the basis of the spectral characteristics (cp. Chapter 3.5.1 and 3.6.4). The other field crops require (more or less) similar water allocations. Hence, an average water allocation per hectare and year could be assumed in the calculations presented in Chapter 4. A more detailed water consumption assessment which is based on a detailed crop-by-crop survey would have been nice to have, but was not crucial for the planned overall water consumption assessment.

[22] The irrigation rates were collected by Prof. Dr. Hamid Yimit and his team from the College of Resource & Environmental Science of the Xinjiang University in Urumqi during the fieldwork campaign in June 2003, based on interviews with local farmers and farm managers. These figures are 'net irrigation rates', i.e. they refer to the amount of water which actually reaches the field. The 'gross irrigation rates', i.e. the amount of water which actually has to be taken from the river, is roughly twice this rate, due to conveyance losses of 40 – 50% between the river and the fields (cp. the detailed discussion Chapter 4.3).

Table 5: Area Northwest: Crop types / land cover classes and their spectral characteristics

Area Northwest (Scene 147 / 29, May 27, 2001), field check conducted June 19 – 21, 2003 (3 weeks later than image recording in year 2001!)

General area information collected during field check:

Elevation ≈ 700 m, yearly **rainfall** ≈ 270 mm, Æ **temperature** ≈ 9° C., yearly **evaporation** ≈ 1600 mm, **main crops**: sunflower, wheat, rice, soybean

Sunflower sown between April 10 - May 5, yields ≈ 1,800 - 2,250 kg / ha.

Winter wheat sown September 2002, yields ≈ 4,500 -6,000 kg/ha.

Rice transplant seeding at May 5 - 20, yields ≈ 3,000 - 9,000 kg/ha.

Soybean sown in spring (April 15 - May 15) and in summer (July 10 - 15), yields ≈ 3,000 - 4,500 kg/ha.

Melon sown May 5-15.

Water consumptions for irrigation: rice ≈ 11,500-14,000 m^3 / ha (= 1,150 – 1,400 mm), other crops ≈ 2,500 – 3,500 m^3 / ha (= 250 – 350 mm); irrigation is applied twice or three times per growing season.

Crop / Land Cover	Description	Spectral Characteristics	spectrally similar to	Reference Photo(s)
paddy rice (flooded)	small crops, planted in rows, plants covering very little of the surface	water dominates the spectral characteristics, very low DN-values, especially in the IR-bands 5 and 7	open water (rivers)	Photo 4 (NW_KL-4-02)
paddy rice (temporarily dry)	small crops, planted in rows, plants covering parts of the soil surface, some rice straw at the soil surface	low signal in band 1 – 3, typical 'red edge' to band 4 already developed	grassland and winter wheat	Photo 5 (NW_KL-4-24)
soybean	different development stages: small plants, covering about 15 – 35 % of the soil surface	fairly similar values in bands 1 – 4 and 7; soil still dominates the signal, no 'red edge' yet	sunflower, little developed maize, melon	NW_KL-4-09 and 17
sunflower	at time of field check already fairly developed in this area, leaves covering most of the soil surface	not clear, none of the training plots had sunflower in 2001, (> new development?)	maize, soybean, melon	NW_KL-4-04, 05, 06a, 10, 13
maize	moderately developed at time of field check; much more bare soil at time of image recording	bare soil still dominating the signal, DN values 80 - 90 for band 1 – 4, no 'red edge' developed	sunflower, soybean, melon	NW_KL-4-16
melons (plastic-covered)	rows of transparent plastic foil, separated by bare soil; plants not yet visible	bare soil dominates the signal, DN-values between 80 – 90 for band 1 – 4	little developed sunflower, maize, soybean	NW_KL-4-23
grassland	typical grassland, green at time of field check (irrigated?)	characteristic 'red edge' from band 3 to band 4	winter wheat	NW_KL-4-03
open land / fallow	dry soil with dried up shrubs and plant remnants	typical fallow signature, DN Band 3 ≈ 110, dropping to ≈ 95 in band 4	little developed crops	NW_KL-4-06
winter wheat	well developed, about 70 cm high, covering most of the soil	characteristic 'red edge' from band 3 (DN ≈ 30) to band 4 (DN ≈120)	grassland	NW_KL-4-07, 16
sugar beet	little developed at time of field check	bare soil dominates the signal, no 'red edge'	little developed crops like maize, soybean, sunflower	NW_KL-4-14
sweet grass	lots of bare soil with little cover of grass sown in rows, surface cover 10 – 15 %	bare soil dominates the signal	fallow, little developed crop with bare soil	NW_KL-4-22
others	graveyard: lots of bare soil with some grass cover	bare soil dominates the signal	fallow , little developed crop with bare soil	NW_KL-4-21

Table 6: Area Central: Crop types/ land cover classes and their spectral characteristics

Area Central (Scene 146 / 30, June 5, 2001), field check conducted June 13 – 15, 2003 (almost the same time as the image recording in year 2001!)

General area information collected during field check:

Elevation ≈ 750 m, yearly **rainfall** ≈ 280 mm, Æ **temperature** ≈ 9° C., yearly **evaporation** ≈ 1400 mm, **main crops**: sunflower, rice, soybean and some wheat, rape and maize

Sunflower sown between May 15 - May 25, yields ≈ 900 - 2,250 kg / ha.

Winter wheat sown September 2002, yields ≈ 3,000 -9,000 kg/ha.

Rice transplant seeding at May 10 - 25, yields ≈ 3,000 - 9,000 kg/ha.

Soybean sown in spring (April 20 - May 20) and in summer (July 10 - 15), yields ≈ 3,000 - 4,500 kg/ ha.

Winter wheat sown September 25 – October 10, 2002, yields ≈ 3,000 - 4,500 kg/ha

Maize sown May 10 – June 15, yields. ≈ 7,500 – 13,500 kg/ ha

Water consumptions for irrigation: rice ≈ 10,500-12000 m^3 / ha (= 1,050 – 1,200 mm), other crops ≈ 2,000 – 3,000 m^3 / ha (= 200 – 300 mm); also some non-irrigated land

Crop / Land Cover	Description	Spectral Characteristics	spectrally similar to	Reference Photo(s)
paddy rice (flooded)	crops even less developed than in Area NW, planted in regular rows, plants still very small, covering little of the surface	water dominates the spectral characteristics, very low DN-values, especially in the IR-bands 5 and 7	open water (rivers)	CEN_KL-3-12, 15, 19
soybean	different development stages, similar to Area NW, covering about 15 – 35 % of the soil surface	similar values in bands 1 – 4 and 7; soil still dominates the signal, no 'red edge'	sunflower, little developed maize, melon	CEN_KL-3-04, 06, 11, 22
sunflower	at time of field check much less developed than in Area NW, soil surface almost completely bare	bare soil dominates signal, similar DN-values in bands 1 and 3 as well as in band 2 and 4	maize, soybean	CEN_KL-3-03, 07, 14, 16
maize	crops much less developed than in Area NW (very late sowing!), at time of image recording some fields may have not even been sown	bare soil dominates the signal, DN values between 80 and 90 for band 1 – 4, no 'red edge' developed	sunflower, soybean	CEN-KL-3-21
grassland	typical grassland, at time of field check still green	typical vegetation curve with characteristic 'red edge' from band 3 to band 4	winter wheat, winter rape	CEN_KL-3-05, 17, 18
winter wheat	well developed, about 70 cm high, covers most of the soil	characteristic 'red edge' from band 3 (DN ≈ 30) to band 4 (DN ≈120)	grassland winter rape	CEN_KL-3-06
winter rape	well developed, green, about 80 cm high	no direct reference plot, characteristics supposed to be typical for green vegetation	winter wheat, grassland	CEN_KL-3-08
wasteland / fallow	dry soil with dried up shrubs and plant remnants	no reference plot in this area, probably similar to fallow signature in Area NW, DN band 3 ≈ 110, dropping to ≈ 95 in band 4	sunflower, maize	none
swampy grassland	similar appearance as normal grassland	typical vegetation curve, abrupt increase from band 3 (DN-value ≈ 45 to band 4 (DN-value ≈ 120)	grassland winter rape	CEN_Kl-3-13

Table 7: Area East: Crop types / land cover classes and their spectral characteristics

Area East (Scene 145 / 30, June 27, 2000), field check conducted June 16 – 18, 2003 (about 10 days earlier than the image recording in year 2000!)

General area information collected during field check:

Elevation ≈ 800 - 900 m, yearly **rainfall** ≈ 500 mm, Æ **temperature** ≈ 9° C., yearly **evaporation** ≈ 1400 mm, **main crops:** wheat, sugar-beet, soybean and maize

Winter wheat sown September 2002, yields ≈ 4,500 -6,000 kg/ha.

Sugar-beet sown in April 10 – May 15, yields ≈ 30,000 – 45,000 kg/ha.

Soybean sown in spring (April 20 - May 5) and in summer (July 10 - 15, yields ≈ 3,000 - 4,500 kg/ha.

Maize sown April 10 - 30, yields. ≈ 7,500 – 13,500 kg/ha

Water consumptions for irrigation: rice ≈ 11,500-14000 m^3 / ha (= 1,150 – 1,400 mm), other crops ≈ 2,700 – 3,750 m^3 / ha (= 270 – 375 mm); irrigation two to three times per season, maize four to six times

Crop / Land Cover	Description	Spectral Characteristics	spectrally similar to	Reference Photo(s)
winter wheat	well developed, about 70 cm high, covering most of the soil	characteristic 'red edge' from band 3 (DN ≈ 30) to band 4 (DN ≈120)	grassland, some maize plots	EAST_KL-5-12
sugar-beet	plants about 35 cm high, covering about 30% of the soil surface	drop from band 3 (DN 100) to band 4 (DN ≈ 60)	soybean	EAST_KL-5-09, 28
soybean	different development stages, plants about 30 cm high, covering about 15 - 30 % of the soil surface	wide range of different spectral curves, no clear signature	partly similar to winter wheat, partly similar to sugar beet, depending on growing stage	CEN_KL-5-01, 02, 03, 04, 06, 07, 09, 12, 14. 15, 16, 17, 19, 22, 27, 31
maize	crops moderately well developed, crop about 50 cm high, covering about 40 - 50% of the soil surface	leaves dominate the spectral signature; curves similar but with differing absolute values	winter wheat	CEN_KL-5-05, 08, 23
lavender (planted Sept. 2002)	small plants, by wide strips of bare soil, very little soil cover	bare soil dominates spectral signature	soybean, fallow	CEN_KL-5-13 (
fallow land (salinized)	totally bare soil, uncultivated land due to salinization	bare soil dominates spectral signature	soybean, lavender	CEN_Kl-5-10

Table 8: Area Southwest: Crop types / land cover classes and their spectral characteristics

Area Southwest (Scene 147 / 30, May 27, 2001), field check conducted June 12 – 13, 2003 (about two weeks later than the image recording in year 2001!)

General area information collected during field check:

Elevation ≈ 1400 - 1600 m, yearly **rainfall** ≈ 500 mm, Æ **temperature** ≈ 3° C., yearly **evaporation** ≈ 1300 mm, **main crops**: wheat, rape, both crops not irrigated

Summer wheat sown April 10 - 20, yields ≈ 200 – 400 kg/ha.

Summer rape, sown April 10 – May 15, yields ≈ 140 – 200.

Crop / Land Cover	Description	Spectral Characteristics	spectrally similar to	Reference Photo(s)
Summer wheat	crop development varying; plants usually 30 – 50 cm high, covering most of the soil surface	clear vegetation signature, sharp 'red edge' developed	none	SW_KL-1-04, 06, 08, 10, 11, 12
Summer rape	crop still in initial stage, covering little of the soil surface	bare soil still dominating the spectral signature; no 'red edge' developed yet	none	SW_KL-1-01, 02, 03, 05, 09

Figure 21: Similarity of spectral signatures of maize and winter wheat in area East

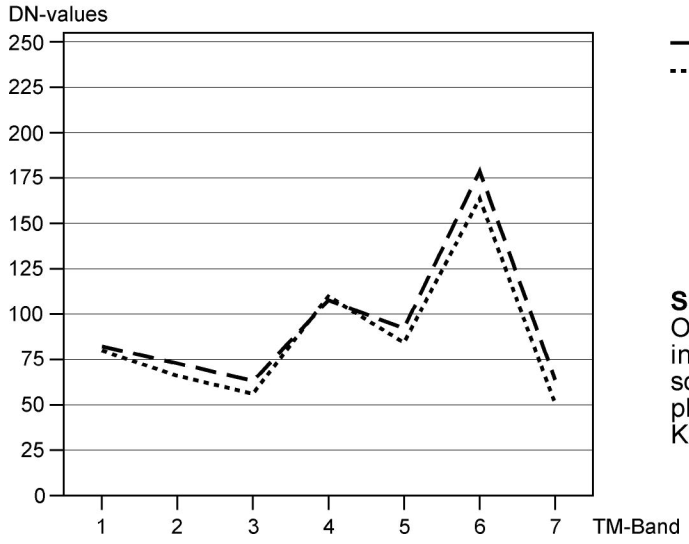

Source:
Own compilation, based on pixel value information extracted from Landsat 7 scene 145/30, 2000-06-27, area "EAST", plots KL_145_6_4/KL_28 and KL_145_9_2/KL_31

Table 9: Mapping classes: Area Northwest

Area Northwest (Scene 147 / 29, May 27, 2001)				
Class-ID	**Short Name**	**Description**	**Included Crops / land covers**	**Spectral Characteristics**
NW-1	wetland rice (paddy)	flooded, irrigated plots, large and rectangular, plants still fairly small, covering less than 10 - 20% of the surface	rice	typical water signature, very low DN-values, especially in band 5
NW-2	dried up wetland rice (paddy)	dried up irrigated, large rectangular fields, plants still fairly small, covering 10 - 20% of the surface; spatially always associated with NW-1	rice	clear 'red edge', spectrally similar to grassland and winter wheat
NW-3	grassland - wheat complex	pasture land / winter wheat field, crop covering most of the surface; large areas	grass winter wheat	clear 'red edge', spectrally similar to grassland and winter-wheat
NW-4	undeveloped crops + bare soil	bare soil, interspaced with little developed crops	soybean maize water melon unplanted fields (black fallow)	bare soil signature, no 'red edge' developed yet
NW-5	Open land / fallow	open, unused land, bare soil with shrubs and dried up plant remnants	unused land (> 1 year), graveyard	similar values in band 1, 2, 4 (DN ≈ 80)

Table 10: Mapping classes: Area Central

Area Central (Scene 146 / 30, June 5, 2001)				
Class-ID	**Short Name**	**Description**	**Included Crops / land covers**	**Spectral Characteristics**
CEN-1	wetland rice (paddy)	flooded, irrigated rice fields, large and rectangular, plants still fairly small, covering less than 10 - 20% of the surface	rice	typical water signature, very low values, especially in band 5

Area Central (Scene 146 / 30, June 5, 2001)				
Class-ID	**Short Name**	**Description**	**Included Crops / land covers**	**Spectral Characteristics**
CEN-2	grass-wheat complex	pasture land / winter wheat field, crop covering most of the surface; large areas	grass winter wheat winter rape swampy grassland	clear 'red edge', spectrally very similar to grassland and winter-wheat
CEN-3	winter rape (?)			
CEN-4	undeveloped crops + bare soil	bare soil, interspaced with little developed crops in juvenile growth stage	soybean maize sunflower unplanted fields (black fallow)	bare soil signature, no 'red edge' developed yet
CEN-5	open land / fallow	open, unused land, bare soil with shrubs and dried up plant remnants	unused land (> 1 year) graveyard	similar values in band 1, 2, 4 (DN ≈ 80)

Table 11: Mapping classes: Area East

Area East (Scene 145 / 30, June 27, 2000)				
Class-ID	**Short Name**	**Description**	**Included Crops / land covers**	**Spectral Characteristics**
EA-1	wetland rice	flooded, irrigated rice fields, large and rectangular, plants still fairly small, covering less than 10	rice	typical water signature, very low DN-values, especially in band 5
EA-2	progressed crop complex	mainly well developed winter wheat, about 70 cm high, covering most of the soil, includes some maize, soybean and grasslands	winter wheat maize, soybean (green leaf stage) grassland	characteristic 'red edge' from band 3 (DN ≈ 30) to band 4 (DN ≈120)
EA-3	undeveloped crops + bare soil	little developed crops, which leave most of the soil surface bar	soybean (some), lavender fallow	typical bare signature, similar DN-values from band 1 - 4
EA-4	sugar beet – soybean complex	different development stages, plants abut 30 cm high, covering about 15 - 30 % of the soil surface	sugar beet soybean	drop from band 3 (DN ≈ 100) to band 4 (DN ≈ 60)
EA-5	Others	miscellaneous other land covers	salinized fallow (?)	different spectral signatures

Table 12: Mapping classes: Area Southwest

Area Southwest ((Scene 147 / 30, May 27, 2001)				
Class-ID	**Short Name**	**Description**	**Included Crops / land covers**	**Spectral Characteristics**
SW-1	Summer wheat	crop development varying; plants usually 30 – 50 cm high, covering most of the soil surface	none	clear vegetation signature, sharp 'red edge' developed
SW-2	Summer rape	crop still in initial stage, covering little of the soil surface	none	bare soil still dominating the spectral signature; no 'red edge' developed yet
SW-3	Others	miscellaneous other land covers		different spectral signatures

Due to the above-described problems the classification potential for crop-specific discrimination is rather limited. Also, the mapping classes (cp. Table 9 - 12) which can in fact be discriminated differ somewhat from area to area and so does the usefulness of the respective classification results. Fairly disappointing results were achieved in Area East. Here, image classification can discriminate only between “little developed crops and bare soil” on the one hand and somewhat “more developed crops” on the other hand. In either class, different crops occur. Moreover, due to considerable differences in crop development within the Area East, some crops – like soy bean - may occur in the “little developed crop" class as well as in the “more developed crop" class”.

The best discrimination was achieved in area “Southwest”. This area is fairly homogeneous, and basically only two crops are grown (summer wheat and summer rape). These two crops, though again occurring in somewhat different growing stages, show sufficient spectral differences to allow a reliable discrimination (cp. Fig. 22).

Figure 22: Spectral differences between summer wheat and summer rape in area Southwest

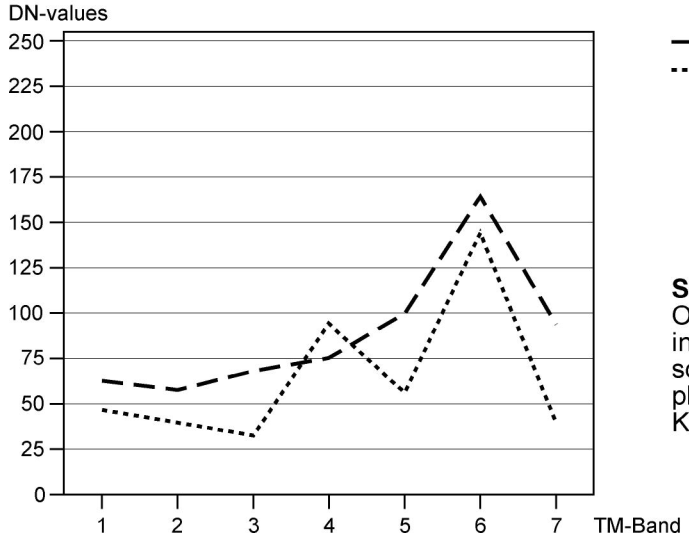

Source:
Own compilation, based on pixel value information extracted from Landsat 7 scene 147/30, 2001-05-27, area "SW", plots KL_147_S_1_3/KL_9 and KL_147_S_2_3/KL_10

3.6.6 Supervised Digital Image Classification of the Land Cover

The final step of the image interpretation procedure was the digital image classification of the ‘net areas’ which had been filtered out in the preceding working steps (cp. Chapter 3.4 and 3.5). The general principle of a supervised digital image classification has been discussed in Chapter 3.6.1. The same chapter also summarised the organisational and technical constraints which hampered the classification process and impeded better classification results.

ER-Mapper 6.2, the image processing software used for this study, offers the usual three standard classifiers (Minimum Distance, Parallel-epiped (‘Box’) and Maximum Likelihood Classifier) as well as another, less commonly used algorithm (Mahalanobis Classifier). The latter is similar to the minimum distance classifier with the difference that it takes into account the directional spread of the class data using the covariance matrix of the means.

Most of these classifiers can be fine-tuned to the respective application objective by selecting different variants of the algorithm and/or by choosing appropriate values for various processing parameters. However, whatever type, variant and parameters are selected, eventually each of these classifiers is basically an automated decision algorithm which allocates ‘unknown’ image pixels to certain (predefined) land cover classes. The decision to which class a specific image pixel will be assigned is always based on a comparison between the spectral characteristics of the (unclassified) pixel with clusters of reference pixels (training areas).

A vast number of research papers examine and compare the quality of the classification results of different image classifiers. With regard to the above-listed standard classifiers, research papers and text books generally agree that the (relatively) best classification results are usually

achieved with the Maximum Likelihood (MaxLike) method. However, it is common knowledge that for good results MaxLike crucially depends on numerous well-selected, representative training areas which are well-distributed over the entire study area. Compared to the MaxLike algorithm, Minimum Distance (MinDist) is usually second or third choice only. However, though this classifier is not as flexible as Maximum Likelihood, it may produce better results in cases where training areas are limited and less reliable (ER-Mapper 6.0 User Guide 1998, S. 381). The Parallelepiped (Box) classifier is a fairly simple classifier. It is well-suited to explain the principle of a classifier to students, but is rarely used for serious project work.

There are, of course, various more sophisticated classification methods which attempt to overcome the constraints inherent in standard pixel-based hard classifiers such as Minimum Distance, Parallel-epiped and Maximum Likelihood. To be mentioned in this context are:

- approaches with so-called 'soft' or 'fuzzy' classifiers' (cp. e.g. Mather 1999, p. 195 ff. or Eastman 2001, p. 66 ff.),
- texture-based classification approaches, as tested, for example, by Ressl for land cover mapping in the lower course of the Amur-Darja (cp. Ressl 1999, S. 94 and Lohmann 1991),
- object-oriented approaches using contextual information like the Delphi-based eCognition software as tested by Koch, Ivits, Jochum (2003, S. 12 ff.) for forest mapping, and
- methods which integrate external (i.e. non-spectral) data in the classification process or for post-classification procedures (cp. Mather 1999, p. 201 f.

Unluckily, as discussed before, the satellite data to be analysed were too weak and the compiled ground truth was too scarce to justify the application of any more sophisticated approach. If the information content of the data at hand is as limited as in this case, also more sophisticated classification approaches would not improve the result considerably. The image classification was therefore limited to the use of the above-mentioned standard methods.

To analyse which classifier or classifier variant is the best, numerous combinations were tested. Area Northwest, the most complex, the largest and also the most important part of the study area served as principle test area. Various methods and method variants were run and the results were compared until the ‘best’ match with the original image was identified. The quality of the respective results was assessed interactively, analysing the statistical data as well as the ‘purity’ and the plausibility of the respective classification maps shown on the computer screen.

As illustrated by Fig. 23, this visual evaluation was relatively straightforward. Due to the typical 'field pattern' in the irrigation areas, it can be assumed that within any field only one type of land use (i.e. one crop) occurs. Hence, a 'good' classification result should produce homogeneous results within each field and sharp, clear boundaries to the neighbouring fields. Thus, the output map should clearly reflect the 'field pattern' as well as the linear pattern of the transport and irrigation infrastructure (paths, roads, irrigation channels). Secondly, the classification results should make sense from a logical point of view. For example, temporarily dry ‘wetland rice’ plots should occur in association with flooded wetland rice.

The test runs quickly showed that the limited number of training areas which had been selected and field-checked, were neither sufficiently numerous nor adequately well-distributed to allow for good result with the MaxLike method. None of the different variants tested gave satisfactory results. The negative effects of:

- the relatively small number of training areas,
- their limited spatial distribution,
- the early growing stage of most crops and the resulting spectral variations within a specific land cover

together summed up to fairly disappointing classification results which did not fulfil the quality criteria given above. As expected, the Parallepiped (Box) Classifier did not yield any useful classification results either.

The MinDist classifier, which assesses the spectral similarity between pixels as distance in a multidimensional feature space, gave classification results which are at least reasonable. ER-Mapper offers two variants of the MinDist classifier module:

- Variant A measures the distance between the position of the unclassified pixel (in the n-dimensional feature space) and the centres (mean value) of the training areas directly in DN-values.
- Variant B measures the same distance in a 'normalised' way (i.e. in standard deviations). The user can further fine-tune the results by defining a threshold parameter measured in standard deviations from the class mean. The threshold defines which pixels may still be allocated to a certain class or, otherwise, should remain unclassified.

The best results were achieved with the standard deviation variant (Variant B), using 3.5 standard deviations as threshold. Using this value, the classification results were reasonably homogeneous within the individual fields and also reflected the characteristic 'field pattern'. Also, with this threshold value, a still reasonable 30 % of the pixels remained unclassified. As shown by Fig. 24, the unclassified pixels can be divided into three types:

- classification 'impurities', i.e. scattered single pixels or pixel clusters within a certain field which had not been classified 'correctly' as the respective crop,
- 'mixed pixels', especially at the field edges and along thin linear features such paths / roads etc.,
- consolidated blocky areas of unclassified pixels, indicating additional land cover classes which had not been covered by the training areas.

Figure 23: Visual comparison of the classification results of two different classifiers

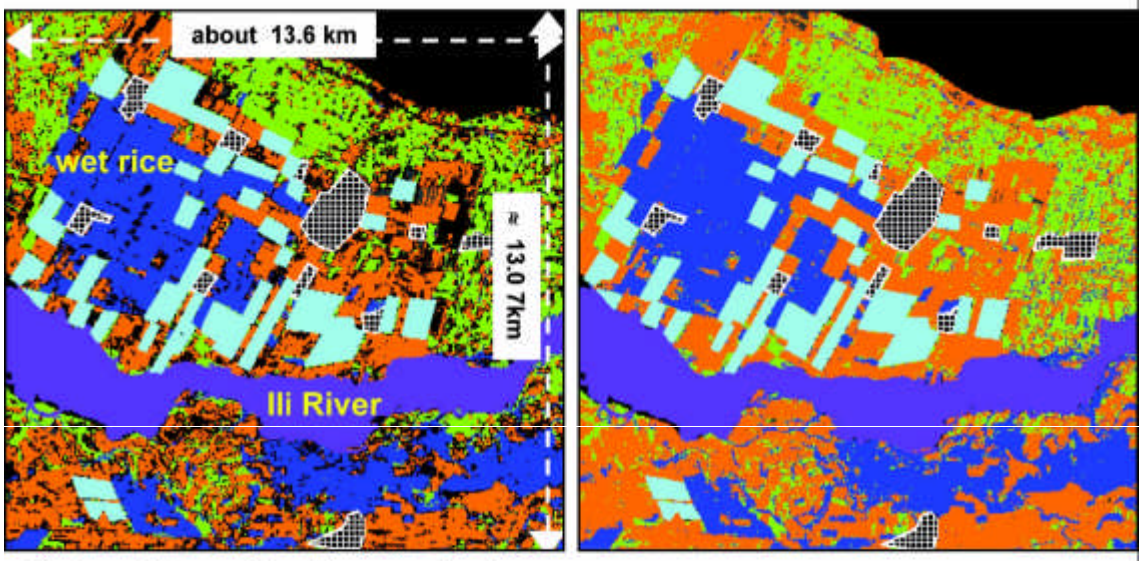

Minimum Distance Classifier, normalised, max. distance 3.5 standard deviations

Maximum Likelihood, standard method

Source: own compilation, classification of Landsat 7 ETM+, 147-29, 2001-05-27

The two images illustrate that different image classifiers will give different results. The minimum distance classifier (left side) was run in the normalised variant with a max. distance classification of 3.5 standard deviations. Despite this fairly big max. distance, the classification leaves certain areas unclassified (black pixels). The Maximum Likelihood method classifies all pixels. Please note that four areas of the images were not included in the classification process: The Ili River (violett colour), settlement areas (hatched areas) and the temporarily dry wet rice plots (light blue areas) were masked out by hand and re-added to the classified image as vector polygons. The consolidated black area in the upper right corner belongs to the mask which had been used to separate the irrigated from the non-irrigated areas (for details cp. Chapter 3.5.1 and 3.6.4).

A visual check of the unclassified pixels confirmed that most unclassified pixels belong to the first two categories. A closer look at the spectral characteristics of some randomly selected 'classification impurities' showed that in most cases the apparent 'misclassification' did make sense. For one reason or the other, many of these pixels do in fact deviate significantly from the typical class signature. 'Mixed pixels' are a method-inherent structural problem which cannot be

solved satisfactorily, except by using data with a much higher resolution. Large consolidated areas of unclassified pixels occurred rarely, which indicates that no major land cover was forgotten when selecting and defining the training areas.

If the threshold was set too narrow (i.e. to a value of 3 or lower), the percentage of unclassified pixels grew rapidly. In particular the 'salt & pepper' impurities within the individual plots increased. If the threshold was set too wide (value of 4 or higher), the salt & pepper effect gradually vanished, but so did the linear features separating the individual fields. Hence, a threshold of 3.5 standard deviations formed the optimal compromise.

Figure 24: Different types of unclassified pixels

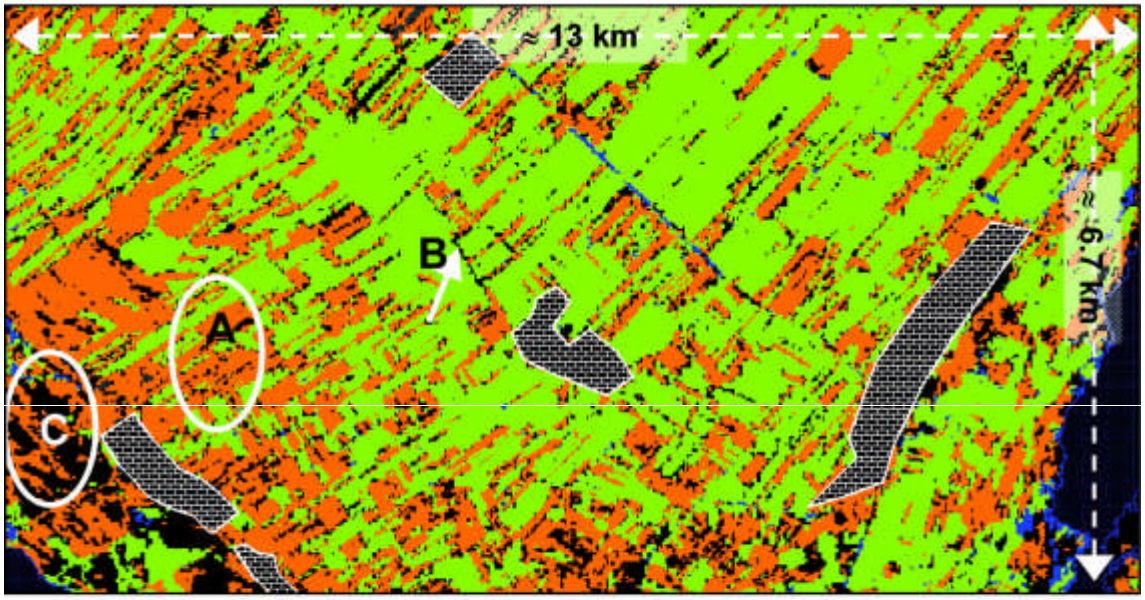

FCC 432 Landsat 7 ETM+, 147-29, 2001-05-27, minimum distance classifier

Source: own compilation

The image illustrates the different types of unclassified pixels. Area "A" is an example for the "salt and pepper" pixels, i.e. apparently randomly distributed unclassified pixels within a fairly homogeneous area. Area "B" shows the effect of 'mixed' pixels located along the edges of field plots. Area "C" shows larger, consolidated unclassified areas, probably caused by types or variants of land cover not properly covered by the selected training areas. The figure also illustrates that the general result of the classification is rather disappointing, as discussed further before in this chapter.

4. ANALYSIS RESULTS

The data and the methodical approach of this study have been described and discussed in detail in Chapter 2 and 3 of this report respectively. The present chapter now summarises and analyses the results and findings, following the sequence of workings steps as shown by the study flow chart (cp. Fig. 14 in Chapter 3.1).

4.1 GROSS DEVELOPMENT AREAS AND NET IRRIGATION AREAS IN THE UPPER ILI CATCHMENT

The cultivated areas in the Upper Ili Catchment were mapped by a combination of visual and digital satellite image interpretation. The first step consisted of the delineation of the exterior boundaries of the cultivated areas which form consolidated regions along the main rivers. Due to the aridity of the area, the outer boundaries of these cultivated areas form a sharp contrast to the surrounding arid land. By and large, the outer boundaries could thus be mapped easily by means of visual image interpretation (cp. Chapter 3.4.)

4.1.1 Gross Development Areas in 1975 / 1976 versus 2000 / 2001

Fig. 25 shows the extension of the gross development areas in 1976/77 as compared to the situation in year 2000/01. Fig. 25 also illustrates the subdivision of the project area into the four regions Northwest (NW), Central (CEN), East (EA) and Southwest (SW). These four regions have been evaluated separately in the digital image classification whose results will be presented in Chapter 4.2. The green parts illustrate the developed areas existing in 1976/77, covering a total area of about 7,300 sqkm. Please note that these areas still include a certain percentage of areas covered by settlements and water bodies as well as some fallow areas.

Fig. 25: Gross cultivation area in 1976 / 77 versus 2000 / 01

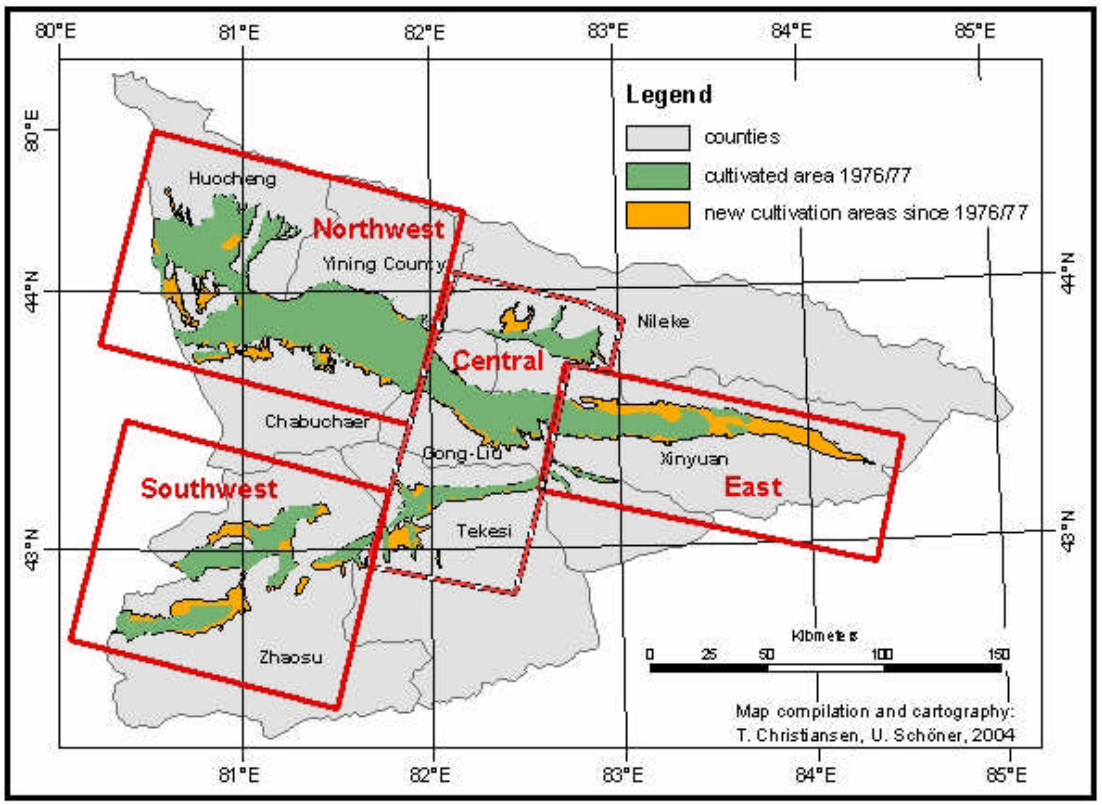

Source: own compilation, based on visual interpretation of Landsat MSS and Landsat 7 ETM+ data

As detected during the fieldwork, these areas also include some rainfed cultivation. This mainly refers to the cultivation areas in Zhaosu county in the south-western part of the study area. In this county considerably higher altitudes result in a cooler climate with higher rainfall, which allows for rainfed cultivation of summer wheat and summer rape. The orange parts of the map indicate areas which were taken under cultivation between 1976/1977 and 2000/2001. Old and new areas together total a gross area of about 9,300 sqkm. This corresponds to an increase of about 2,000 sqkm respectively 27% over 25 years. The map shows that the new development areas extend mainly along the outer edges of the 'old' development zones. These new areas are scattered over most parts of the Upper Ili catchment, but show some concentrations in the upper part of the Kunes catchment in the East and in the upper Tekes catchment in the southwest. As mentioned before, the areas shown in Fig. 25 still include areas covered by settlements, water bodies and fallow, as well as some rainfed cultivation.

4.1.2 Net Irrigation Areas in 2000 / 2001

As described and discussed in detail in Chapter 3.5, the gross development area for year 2000/2001 was then further refined by a stepwise exclusion of those areas which are covered by major settlements and rivers and by the exclusion of areas with rainfed cultivation. The results are shown in Fig. 26 and Tables 13 and 14.

Fig. 26: Net cultivation area 2000 / 01

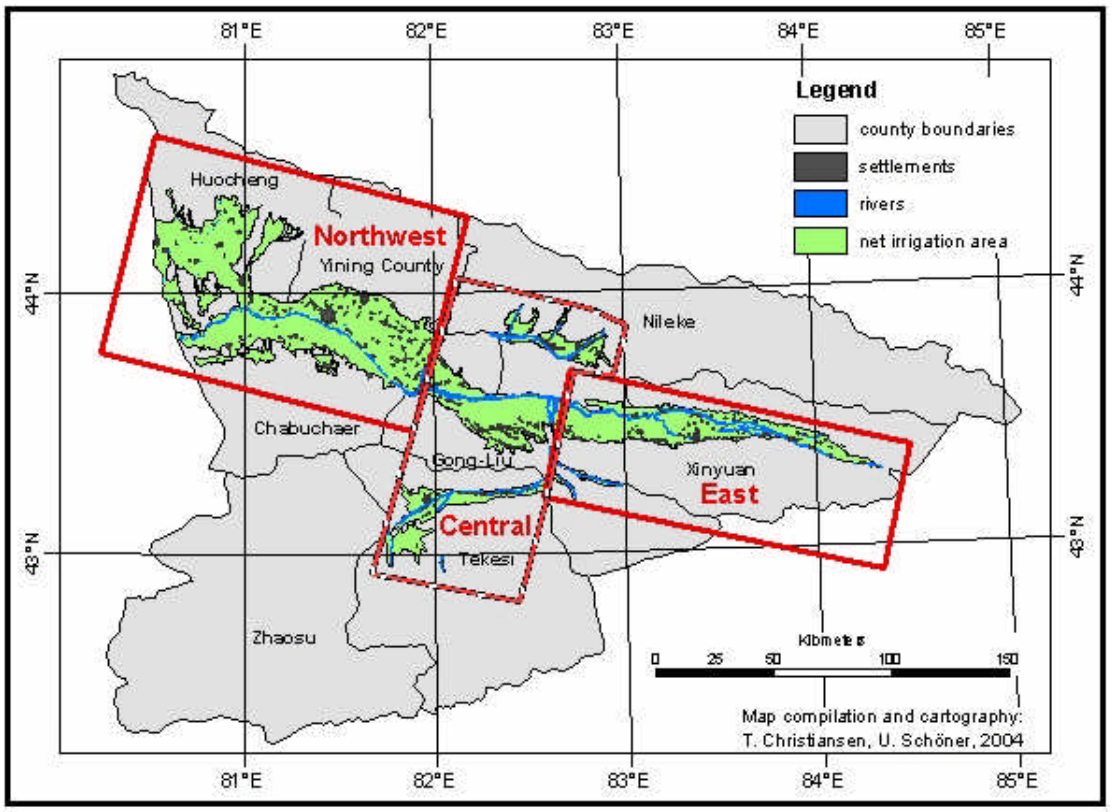

Source: own compilation, based on Landsat 7 ETM+ data

Table 13 shows that about 7% – 8% of the gross development area are occupied by water and settlements. The resulting 'net development area' of about 8,700 sqkm still includes:

- minor settlements (not excluded because of their too small size),
- areas covered by streams and rivers which are too small to be excluded,
- some rainfed cultivation (mainly area Southwest (Zhaosu))
- two types of fallow land

- open, unused land (partly used as pasture, partly wasteland) with bare soil, grass and scattered shrubs,
- 'black fallow' (uncultivated plots with bare soil)

Table 13: Net development area in year 2000 / 2001

	NW (sqkm)	NW (%)	Central (sqkm)	Central (%)	East (sqkm)	East (%)	SW (sqkm)	SW (%)	Total Area (sqkm)	Total Area (%)
gross development area	4006.0	100.0	2172.0	100.0	1531.0	100.0	1655.0	100.0	**9364.0**	**100.0**
river area	150.0	3.7	135.0	6.2	30.0	2.0	17.0	1.0	**332.0**	**3.5**
interrmediate sum	3856.0	96.3	2037.0	93.8	1501.0	98.0	1638.0	99.0	**9032.0**	**96.5**
settlement areas	160.0	4.0	109.0	5.0	66.0	4.3	31.0	1.9	**366.0**	**3.9**
net development area	**3696.0**	**92.3**	**1928.0**	**88.8**	**1435.0**	**93.7**	**1607.0**	**97.1**	**8666.0**	**92.5**

Table 14 illustrates an assessment of the actual 'net irrigation area', based on the figures given as 'net development area' in Table 13 and the following assumptions:

- alltogether all areas covered by smaller rivers and settlements total another 1% of the gross development area,
- the mapped agricultural development in area Southwest is dominantly rainfed agriculture and will thus be excluded completely,
- the areas classified as 'open land' is non-irrigated land and is thus to be subtracted from the gross area,[23]
- 10% of the 'unclassified pixels' (cp. Chapter 4.2) are non-irrigated land[24].

The figures in the second row of Table 14 correspond to the last row figures in Table 13 (excluding area Southwest). All percentage figures are based on the 'gross area' figures (cp. Table 13, first row) as 100% reference. The biggest reduction of these figures results from the exclusion of the cultivated areas in region Southwest (1,607 sqkm). According to the findings of the field check, crop cultivation of this higher elevated part of the study area is mainly depending on rainfall. This alone reduces the net development area from 8,666 sqkm to about 7,060 sqkm.[25]

Table 14 reduces these 7,060 sqkm further by applying the correction contingencies outlined above: non-mapped rivers / settlements, 'open land' area and 10% of the unclassified pixels. This results in an additional reduction of about 430 sqkm, which eventually results in a (likely) 'net irrigation area' of about 6,628 sqkm. Hence, the approximate 'real' net irrigation area of the

---

[23] 'Black fallow', i.e. uncultivated, bare soil can not be excluded due to its spectral similarity to cultivated fields in the initial growing stage (cp. Chapter 3.6).

[24] The figure of 10% is a 'best guess' estimation, thus eventually an arbitrary figure. The estimation is based on visual interpretation of the classification results. It is obvious that a certain percentage of the unclassified pixels belong to non-irrigated land, but with the limited ground truth data it is not possible to quantify this part exactly.

[25] According to Chinese land use statistics (cp. Statistical Bureau for Xinjiang (Ed.) (2002)) about 161 sqkm or 40% of the total cultivated area of Zhaosu county is irrigable land. However, the satellite image of this area does not show the typical patterns of irrigated land and the field check did not verify any irrigation in this area either! A possible explanation for this contradiction could be that some of the cultivated land receives temporarily supplementary irrigation (e.g. by sprinkler) to bridge drought periods. Furthermore, some 'normal' irrigation may occur in the transition zone between the cooler 'highlands' in the upper parts of the Tekes catchment and the lower lying areas at the boundary between Zhaosu and Tekesi. In order to keep the area estimations conservative and 'on the safe side', the entire Zhaosu cultivation area was excluded in the water consumption estimates presented in Chapter 4.3.

Upper Ili Catchment in year 2000/2001 totalled an area of about 6,600 sqkm! This figure equals roughly 70% of the originally mapped gross irrigation area (9,364 sqkm).[26]

Table 14: Net Irrigation Areas in Year 2000 / 2001

	NW (sqkm)	NW (%)	Central (sqkm)	Central (%)	East (sqkm)	East (%)	Total Area (sqkm)	Total Area (%)
gross development area (without area SW)	4006	100,0	2172	100,0	1531	100,0	**7709**	**100.0**
net development area	3696	92.3	1928	88.8	1435	93.7	**7059**	**91.6**
minus 1% allowance for un-mapped river and settlement areas	37	0.9	19	0.9	14	0.9	**70**	**0.9**
minus uncultivated 'open land'	159	4.0	19	0.9	0	0.0	**178**	**2.3**
minus 10% of unclassified pixels	109	2.7	25	1.2	49	3.2	**183**	**2.4**
Net irrigation area	**3391**	**84.6**	**1865**	**85.9**	**1372**	**89.6**	**6628**	**86.0**

On the basis of the available data, only rough estimations can be made about the extension of the actual net irrigation area in 1976/77. It can be assumed, however, that the excluded river areas are more or less the same as in 2000/2001. The areas covered by settlements have probably increased somewhat since 1976/77. Likewise, Fig. 25 illustrates that the excluded rainfed cultivation areas in Area Southwest have increased considerably since 1976/77. If all other calculation parameters (1% gross area allowance for unmapped river and settlement areas, 10% allowance for unclassified pixels) are kept the same as in the preceding calculation, it can be concluded that the percentage difference between the gross irrigation area and the actual net irrigation area will be slightly less for 1976/77 than it is for year 2000/01.

It can therefore be assumed that the percentage difference between the gross and the net irrigation area will be somewhat less for 1976/77 than the about 30% which have been calculated for year 2000/01 (see above). Assuming that the 'net irrigation area' percentage in 1976/77 totalled about 75% of the gross development area (7,300 sqkm, cp. Chapter 4.1), the net irrigation area in 1976/77 totalled about 5,475 sqkm. Comparing the (approximate) net irrigation areas figures for 2000/01 (6,600 sqkm) and 1976/77 (5,475 sqkm) respectively, an increase of about 1,125 sqkm (i.e. 20.5%) can be ascertained during these 25 years.

4.2 LAND USE / LAND COVER IN THE NET IRRIGATION AREA IN 2000 / 2001

As described in Chapter 3, the results of the image classification were – all in all - fairly disappointing. The two main reasons are the early recording date of the images and the limited number of training areas. Nevertheless, the results do still give a useful idea of the extent and spatial distribution of different types of land cover. As described in Chapter 3.6.5, the classification was split into four regions: Northwest, Central, East, and Southwest. In the following, the results for these areas will be presented and discussed one-by-one.

---

[26] As will be discussed in Chapter 4.3 in more detail, this figure contradicts official Chinese data which quote a total irrigation area of only 2,390 sqkm (this even includes the above-mentioned 161 sqkm in Zhaosu)! In other words: According to the satellite image interpretation, the actual irrigation area is 177% higher than given by the the official Chinese statistics!

4.2.1 Land Use / Land Cover in Area Northwest

Fig. 27 displays the result of the digital image classification for the northwestern part of the study area. Tab. 15 shows the respective absolute and relative area figures. The Landsat ETM+ scene used for this classification had been recorded on May 27, 2001. The field check for this area was conducted June 19 – 21, 2003. The mapping units and the spectral characteristics of the included crops are described in Table 5 and Table 9 (cp. Chapter 3.6.5).

The certainly most interesting – although not the biggest - mapping unit of this section of the Upper Ili Catchment are the wetland rice areas (NW-1 and NW-2) west and southwest of Yining City. The wetland rice is indicated by the colours dark blue (= flooded wetland rice) and light blue (temporarily dry wetland rice). An enlarged cut of the area can be seen in Fig. 15. The approximate situation of the growing stage of these units at the time of image recording is illustrated by Photo 4 and 5 respectively (cp. Chapter 3.6.4). It should, however, be kept in mind that these photos are taken about three weeks later in the growing period than the recording of the satellite image in 2001.

As discussed before, the wetland rice as well as the 'dry' wetland rice were spectrally very similar to other mapping units and could thus not be mapped out by digital image classification only. The techniques used to separate flooded wetland rice from other water-covered areas and to discriminate the temporarily dry wetland rice plots from similarly reflecting grassland and winter wheat plots had been outlined in cp. Chapter 3.5.1 and 3.6.4 respectively.

The wetland rice areas cover just about 168 sqkm or 2.6% of the area Northwest, but these areas are nevertheless rather interesting and important. Firstly, the old satellite image from 1977 shows only very little areas of (possible) wetland rice cultivation. Fig. 28 illustrates that in 1977 (at best) very few isolated wetland rice plots may have existed, while in 2001 large extended wetland rice cultivation complexes are clearly visible. This is likely to be a fairly new development, because none of our Chinese colleagues were aware of any wetland rice cultivation in this area in the first place! Secondly, the extension of the wetland rice areas is important because wetland rice requires about four times as much irrigation water as other field crops: 10,500 to 12,00 m^3/ha as compared to 2,000 – 3,000 m^3/ha for crops such as sunflower, wheat, soybean, maize (cp. Table 20 in Chapter 4.3.1).

The remaining crop-discrimination potential of the classification is rather limited. The two mapping units NW-3 (light green) and NW-4 (orange) basically reflect fields carrying a somewhat developed crop and fields with crops with little to almost no plant development. Most of these somewhat developed crops are apparently winter crops.

Mapping unit NW-3 includes winter wheat and (some) grassland. Spectrally, NW-3 already shows a clearly developed 'red edge', the characteristic signal increase from Band 3 (red) to Band 4 (NIR) which indicates healthy green vegetation. The field check indicated that these 'developed crop' areas are mainly covered by winter wheat. The approximate growing stage of winter wheat at the time of image recording is shown by in Photo 6. Besides winter wheat, other winter crops and some grassland / pastures may fall in this unit as well. Altogether the mapping unit NW-3 accounts for about 630 sqkm respectively 10% of the area Northwest.

The fourth mapping unit (NW-4, orange) consists of a variety of little developed crops in various initial growing stages (cp. Photo 1 and 2 in Chapter 3.6.1) all of which are summer crops. The field check results indicated that the range of crops is fairly limited: The mapping unit seems to consist mainly of soybean and maize and some sunflower, sugar beet and water melon. Due to the early growing stage and the resulting limited soil cover, the vegetation-typical red edge has not yet developed and bare soil still dominates the signal. Therefore a reliable discrimination from bare soil could not be made (cp. e.g. Photo 1). The unit may thus include some 'black fallow' plots, but the field check showed that black fallow plots are fairly rare. Altogether the 'undeveloped (summer) crops' account for the largest part of the total area (1,650 sqkm or 45%).

The last mapping unit (NW-5, grey colour) includes various open lands, fallow areas, and wasteland. It refers to areas which are – for whatever reason - presently not used for crop cultivation. This covers grasslands with some (dried-up) shrubs, some plant remnants on the soil surface and a varying percentage of bare soil. The Photo 7 illustrates one many variants of this land cover type which accounts for about 160 sqkm or 2.5% of the area Northwest.

Fig. 27: Classification results for area Northwest

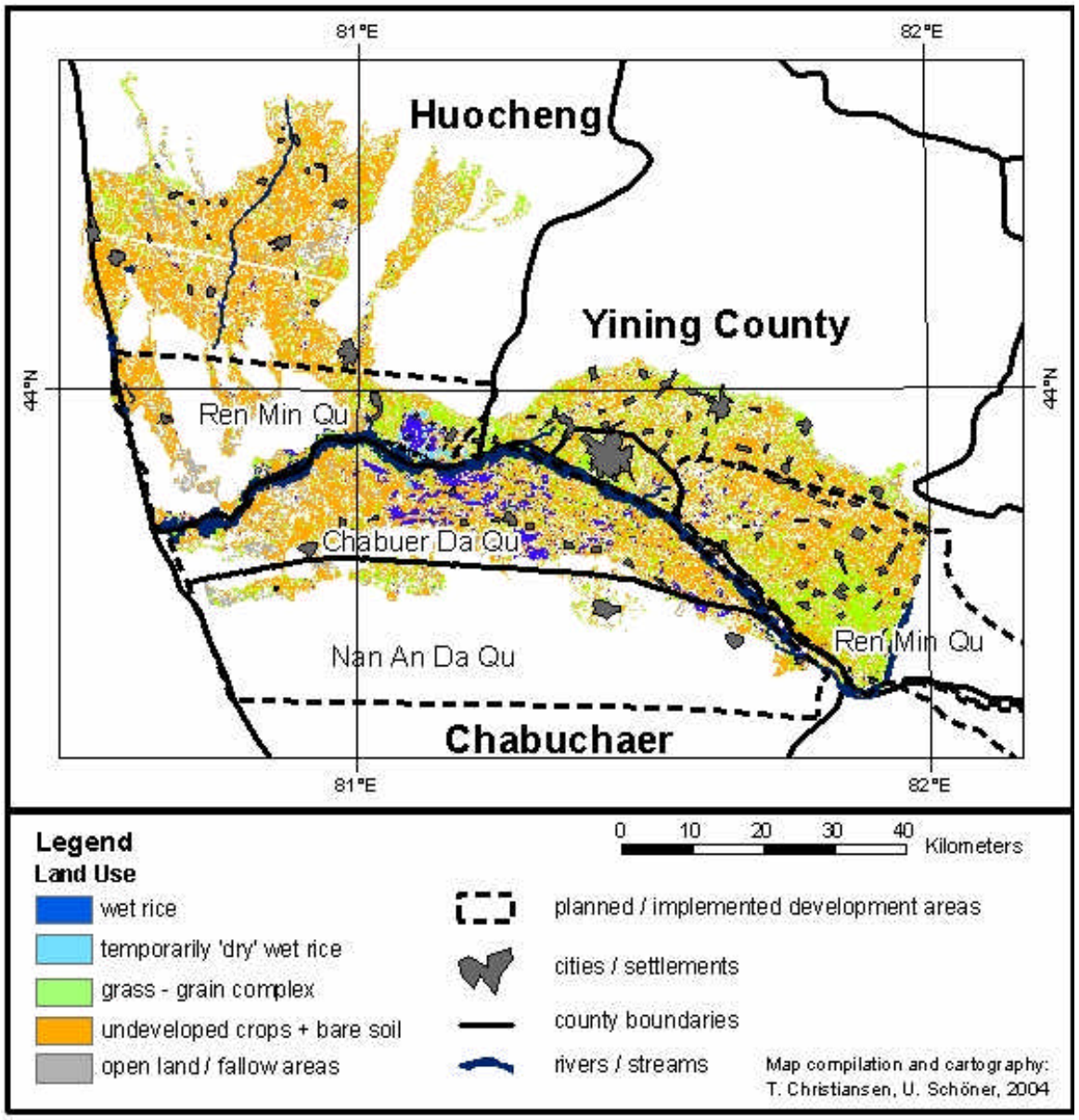

Source: own compilation, based on classification of Landsat 7 ETM+ data

Table 15: Area figures for the classification results of Area Northwest (Landsat7 ETM+ scene 147/29, 2001-05-27)

Mapping-Code	Mapping Unit	Area (sqkm)	Area (% of classified pixels)	Area (% of total area)	Remarks
NW-1	wetland rice	154.6	5.9	4.2	
NW-2	'dry' wetland rice	13.3	1.2	0.4	mapped out manually, cp. Chapter 3.6.4
	å NW-1 + NW-2	167.9	7.1	4.5	
NW-3	grass – grain complex (winter	630.4	24.2	17.1	

Mapping-Code	Mapping Unit	Area (sqkm)	Area (% of classified pixels)	Area (% of total area)	Remarks
	wheat, maize)				
NW-4	undeveloped crops (soybean, sunflower, maize, some sugar beet and water melon) + bare soil	1650.7	63.3	44.7	may include some fallow areas
NW-5	open land / fallow areas	159.1	6.1	4.3	
	å NW-1 to NW-5	2609.2	100.0	70.6	
	unclassified pixels	1086.3		29.4	
	å **Total Area (classified + unclassified pixels)**	3695.5		100.0	

Figure 28: Irrigation areas southwest of Yining

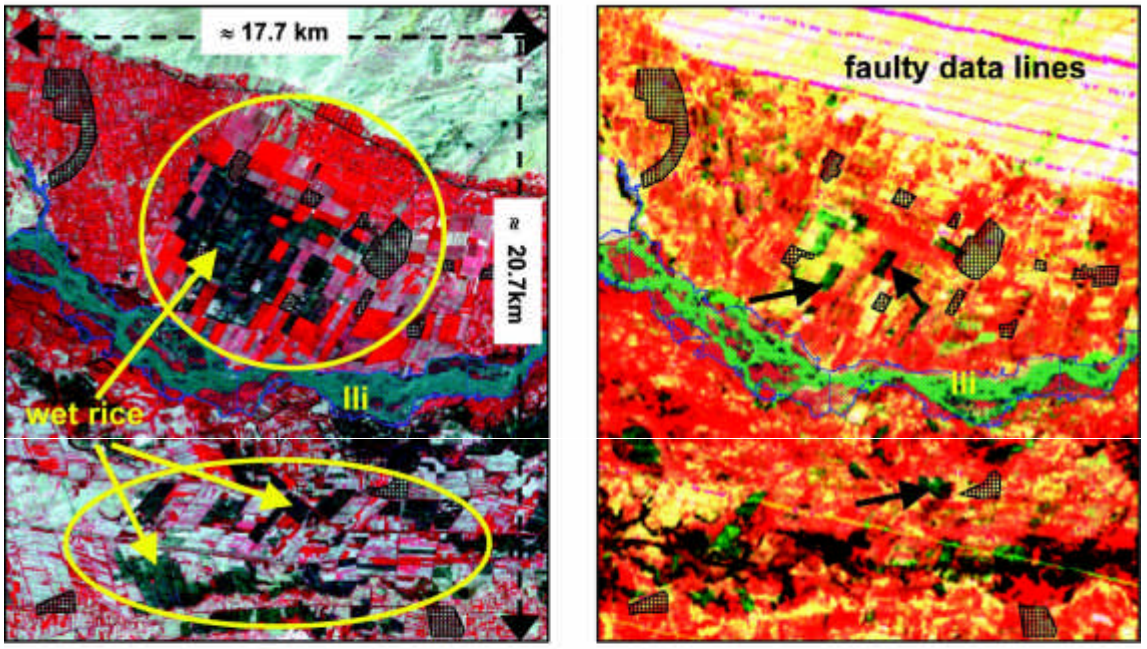

FCC 432 Landsat 7 ETM+,147-29, 2001-05-27 FCC 654 Landsat 2 MSS, 158-29, 1977-06-26

Source: own compilation

The images illustrate that large-scale wet rice cultivation complexes did not exist in this area in 1976/77. Despite the fact that the recording dates of the two scenes are about one month apart and that the Landsat 2 scene has a much lower spatial resolution and plenty of data errors, the large wet rice complex would have been clearly visible on the Landsat 2 image. Some few small, isolated wet rice plots, however, seem to have existed already (see black arrows in Landsat 2 image). The cross-hatched areas indicate the location of settlements as mapped from the Russian topographic maps and the Landsat 7 images.

Photo 6: Winter wheat in area Northwest

Source: Photo taken during fieldcheck campaign June 19-21, 2003. (Photo-ID NW_KL_147_N_7_1/KL_7)

With the selected variant of the minimum distance classifier (i.e. normalised, 3.5 standard deviations) roughly one third of the pixels (1,086 sqkm or 29%) remains unclassified. A certain number of unclassified pixels are caused by 'mixed pixels' along field boundaries (see also the discussion and Fig. 24 in Chapter 3.6.6). However, most of the unclassified pixels are 'infield' pixels, i.e. single, isolated unclassified pixels within an otherwise more or less homogeneously classified plot of maize, wheat, soybean etc. These pixels are distributed more or less evenly over the two major mapping units NW-3 and NW 4.[27]

This 'salt & pepper' distribution pattern of the unclassified pixels illustrate that the dominating land cover types had in fact been caught by the classification. However, the training areas were too few and the spectral variations of these classes are too wide and inhomogeneous to allow for a better (i.e. more homogeneous) classification result. Nevertheless, with regard to the calculations of the water consumption in Chapter 4.3, it can be assumed that the vast majority of the unclassified pixels do in fact belong to either class NW-3 or class NW-4.

[27] One exception is the white strip running WNW – ESE through the upper left corner of Fig. 27 which is caused by faulty lines in the original data.

Photo 7: Open land / waste land in area Northwest

Source: Photo taken during fieldcheck campaign June 19-21, 2003. (Photo-ID NW_KL_147_N_6_1/ KL_6)

4.2.2 Land Use / Land Cover in Area Central

Fig. 29 shows the results of the digital image classification for area Central. The respective areas of the mapping units are listed in Table 16. The Landsat ETM+ data (scene 146-30) for this classification was recorded on June 5, 2001. The field check for this area was carried out between June 13 and June 15, 2003. Hence, image recording and field check took place at about the same phase of the growing period. The mapping units and the spectral characteristics of the different land covers had been described in Table 6 and Table 10 (cp. Chapter 3.6.5).

Unlike area Northwest, which consists of one coherent piece of land, the irrigation areas in region Central consist of three separate sub-regions. The biggest of these three sub-regions is located along the northern and southern banks of the Ili (respectively Kunes) in the area of Gong Liu (cp. Fig. 3). This central irrigation complex actually forms the eastward extension of the irrigation area Northwest which has been described in the preceding subchapter. A second, smaller complex is located further north, along the Kash River near the city of Nileke. The third (again smaller) complex forms a relatively narrow, east-west extending band along both sides of the lower course of the Tekes River.

With some exceptions, the mapping units of area Central are similar to area Northwest. As in area Northwest, there is again one large, clearly visible area of wetland rice cultivation (CEN-1, blue colour), located somewhat northwest of Gong-Liu (cp. Fig. 30). A second, much smaller wetland rice cluster is located at the north-eastern outskirts of Gong-Liu. Also in this area in 1977 few isolated wetland rice plots existed at best.

The remaining parts of the central irrigation complex are covered either by somewhat developed crops, mainly winter wheat (CEN-2, grass – grain complex, light green colour) or by fields with crops in their initial growing stage (CEN-4, undeveloped crops, orange colour). CEN-2 accounts for about half of the total area (≈ 950 sqkm or 50%), CEN-4 for about one third (≈ 570 sqkm or 30%). The field check results indicate that within the mapping unit CEN-4, sunflower seems to

be the dominant crop. However, in mid-June the sunflower crops on the plots checked by the fieldwork team were still so little developed that the crops were hardly visible (cp. Photo 1 in Chapter 3.6.1.

A particularity of the area Central is indicated by the mapping unit CEN-3 (yellow colour). Unluckily the field data are too few and sketchy to be certain, but the spectral signature of these yellow pixels and Photo 8 give reason to the assumption that the yellow areas, especially in the Nileke section, consist of winter rape. This, however, was not verified because this area had not been visited during the fieldwork campaign.

Fig. 29: Classification results for area Central

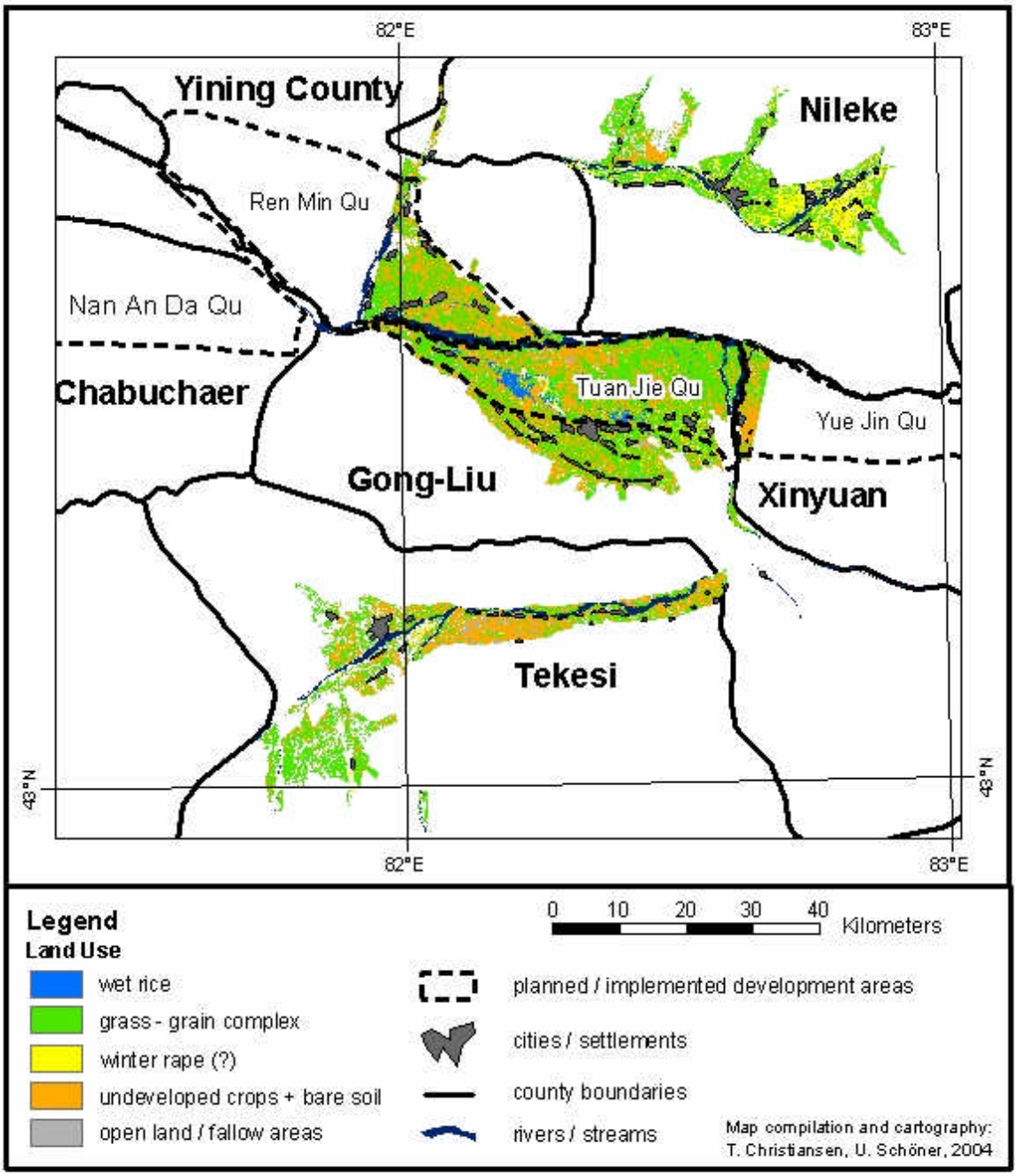

Source: own compilation, based on classification of Landsat 7 ETM+ data

Figure 30: Irrigation area near Gong-Liu

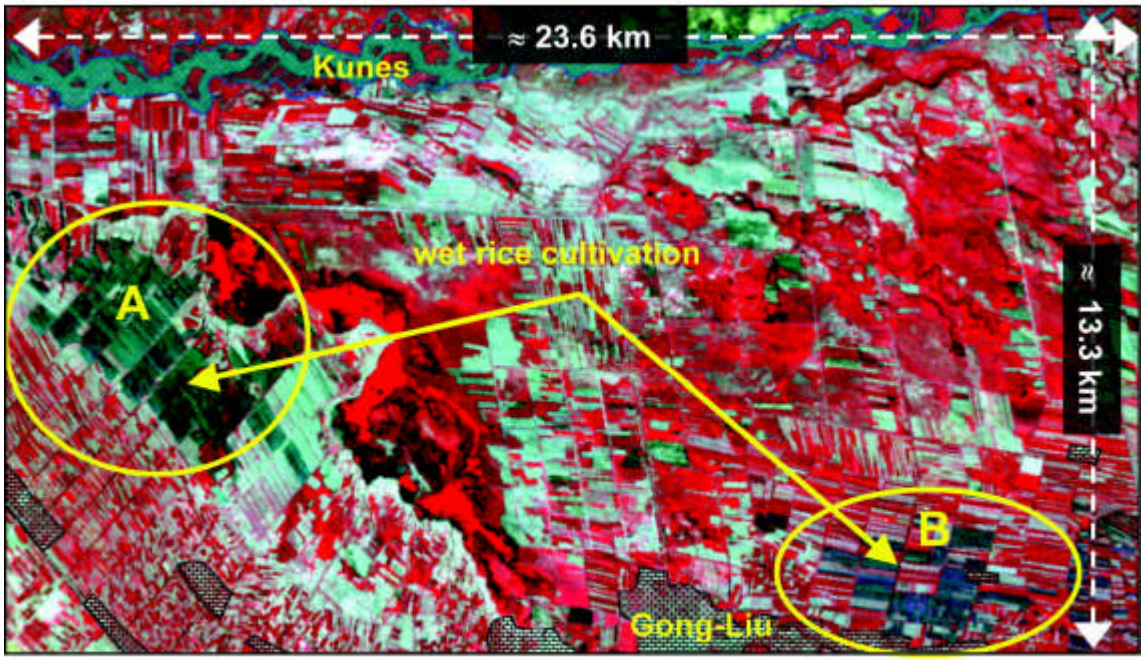

FCC 432 Landsat 7 ETM+, 146-30, 2001-06-05

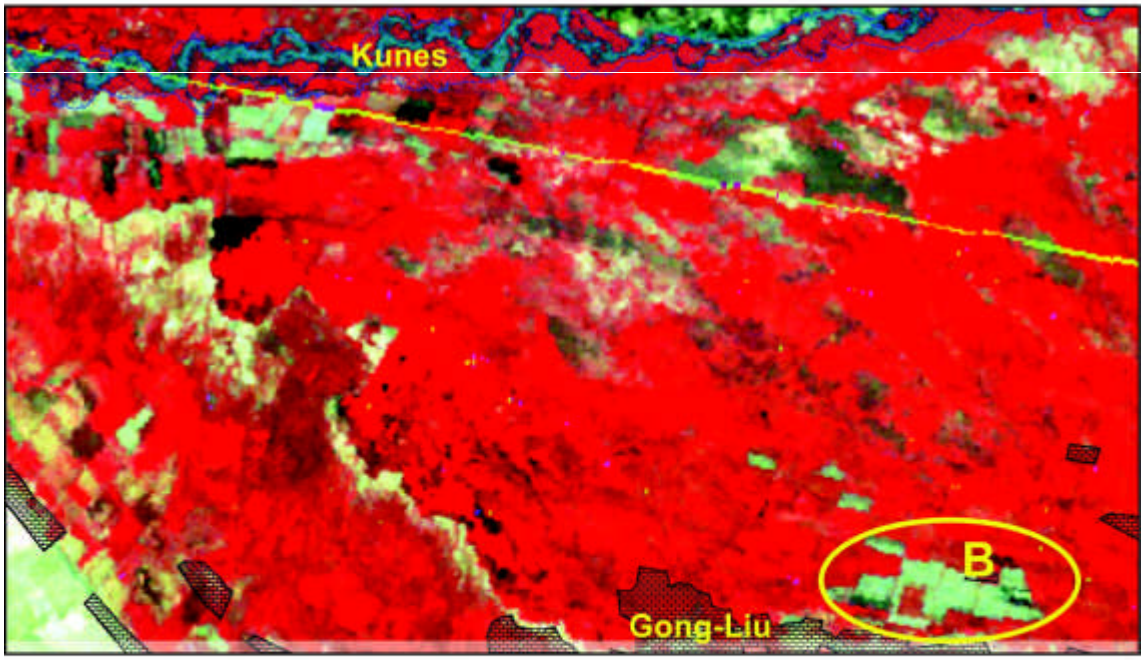

FCC 654 Landsat 2 MSS, 157-30, 1977-08-17

Source: own compilation

The two images show that large-scale wet rice cultivation in this area did not exist in 1976/77. The recording dates of the two scenes are about 10 weeks apart. Nevertheless, the wet rice plots would have shown clearly on the MSS 2 image, especially in area A. The plots visible in area B on the Landsat 2 image may possibly be a first rice cultivation complex, whose plots were already harvested at the time of image recording.

Table 16: Area figures for the classification results of Area Central (Landsat7 ETM+ scene 146/30, 2001-06-05)

Mapping-Code	Mapping Unit	Area (sqkm)	Area (% of classified)	Area (% of total area)	Remarks
CEN-1	wetland rice	27.4	1.6	1.4	
CEN-2	grass – grain complex	953.2	56.8	49.4	
CEN-3	winter rape	108.9	6.5	5.6	assumed crop, could not be verified
CEN-4	undeveloped crops (sunflower, soy-bean, maize,) + bare soil	569.2	33.9	29.5	
CEN-5	open land / fallow areas	19.4	1.2	1.0	
	å CEN-1 to CEN-5	1678.1	100.0	87.0	
	unclassified pixels	250.9		13.0	
	å Total Area (classified + unclassified pixels)	**1929.0**		**100.0**	

Photo 8: Winter rape in area Central

Source: Photo taken during the fieldwork campaign June 13 – 15, 2003 (Photo-ID CEN_KL146_7_2/KL_8)

The photo was taken in the central section of the area near Gong-Liu. At the time of image recording, this area was unused wasteland. The spectral signature of this rape field with its mature green vegetation would fit to the spectral values of the yellow pixels in the Nileke section.

4.2.3 Land Use / Land Cover in Area East

Fig. 31 shows the classification results for area East. The mapping units and their area are listed in Table 17. The Landsat ETM+ data of this area were not recorded in 2001, but one year earlier (scene 145-30, 2000-06-27). The field check for this area was conducted between June 16 and June 18, 2003, i.e. at the same time as the image recording three years earlier. As compared to the other three Landsat 7 satellite scenes, this scene was recorded three to four weeks later, which means, the crops had already reached a somewhat more matured stage of crop development. The mapping units and the spectral characteristics of the different land covers had been described in Table 7 and Table 11 (cp. Chapter 3.6.5). Unluckily, in area East almost 25% (8 of 31) of the training plots which had been earmarked for field check are located inside a huge prison farm and could thus not be accessed by the field-work team.

Fig. 31: Classification results for area East

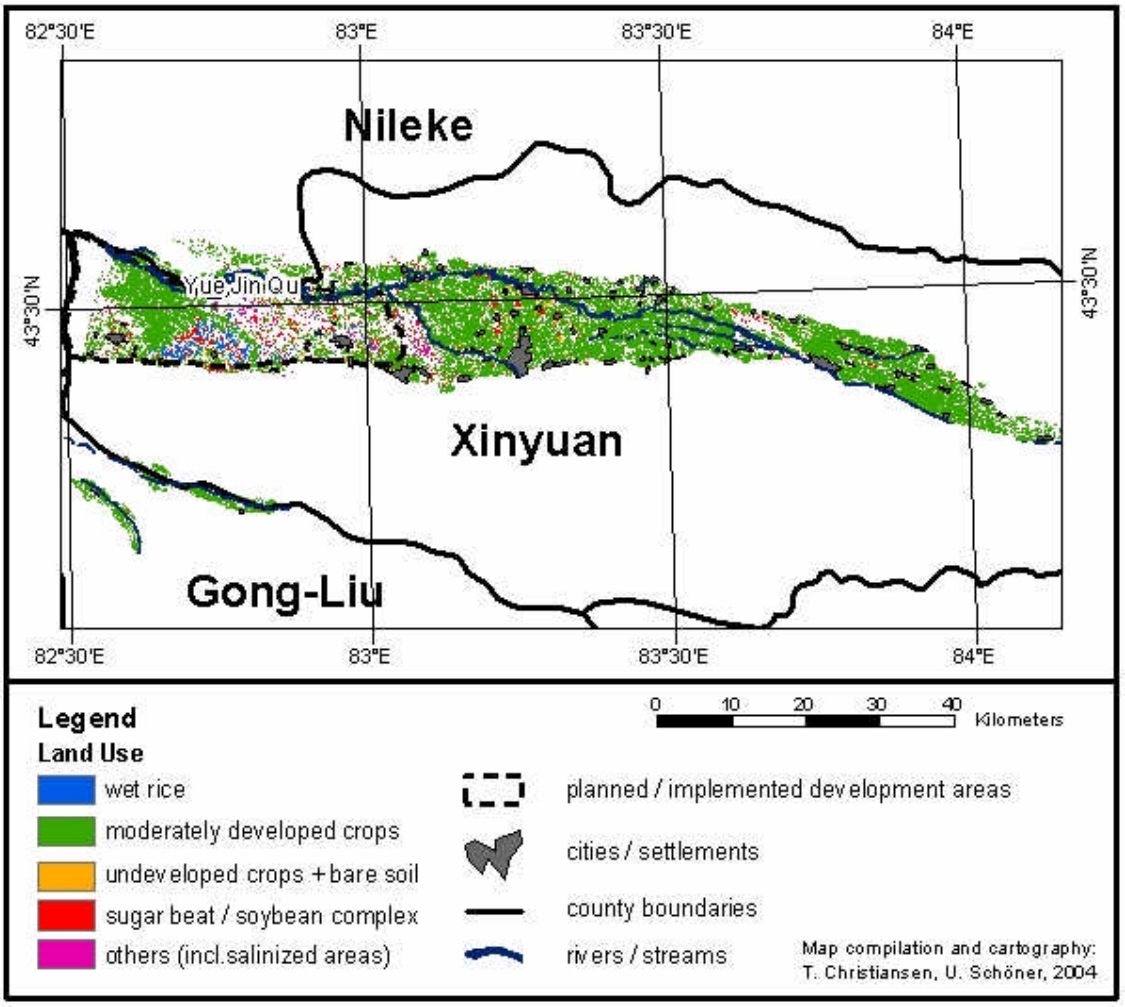

Source: own compilation, based on classification of Landsat 7 ETM+ data

Like area Northwest and area central, also area East includes one cluster of wetland rice cultivation (EA-1, cp. Fig. 31, blue colour). The cluster covers a total area of only 20 sqkm or 1.4% of the total area (cp. Table 17) and is located in the southern part of the Yue Jin Qu development scheme. Unluckily, all of the rice cultivation falls entirely into the above-mentioned prison and could therefore not be verified in the field. However, due to the clear spectral signature of the flooded plots, the areas are so prominent on the images that they can be identified reliably, even without field check. As illustrated by Fig. 32, in this particular case the extension of the rice fields during the last 30 years is fairly limited. Most of the rice cultivation already existed in 1976/77.

Table 17: Area figures for the classification results of Area East (Landsat7 ETM+ scene 145/30, 2000-06-27)

Mapping-Code	Mapping Unit	Area (sqkm)	Area (% of classified)	Area (% of total area)	Remarks
EA-1	wetland rice	19.8	2.1	1.4	
EA-2	moderately developed crops (winter wheat, maize, soybeans) + grassland	841.7	89.5	58.7	
EA-3	undeveloped crops (soybeans, lavender) + bare soil	8.4	0.9	0.6	may include some fallow
EA-4	sugar beet / soybean complex	59.7	6.3	4.2	
EA-5	others	11.3	1.2	0.8	probably including some salinized fallows
	å EA-1 to EA-5	940.9	100.0	65.6	
	unclassified pixels	494.1		34.4	
	å Total Area (classified + unclassified pixels)	**1435.0**		**100.0**	

Due to the relatively late recording date, the bulk of area East (almost 60% of the area) had to be classified as one big unit 'moderately developed crops' (EA-2). The sketchy field truth information indicates that the EA-2 class includes quite a variety of different crops, such as winter wheat, maize, and soybean as well as (possibly) some grassland. This unsatisfying discrimination of individual crops is also resulting from the fact that the late recording blurs the spectral differences between winter and summer crops. Without a second reference scene (e.g. taken in late March or early April) the winter crops can no longer be discriminated reliably from summer crops.

As a consequence of the late recording of the data, the percentage of pixels classified as 'undeveloped crops' (EA-3, orange colour) drops to less than 1% of the area. According to the field check findings, these 'undeveloped' plots include soybean (summer crop) and - somewhat unexpected – lavender and some bare soil. About 60 sqkm or 4% of the area are classified as sugar beat and soybean (EA-4, red colour). Most of it is located in the eastern part of the Yue Jin Qu development scheme.

The remaining mapping unit 'others' (EA-5, violet colour) covers 11 sqkm or almost 1% of the area, most of it as more or less consolidated pieces of land just east of the Yue Jin Qu boundary. Once again, field truth is too sketchy for verified conclusions. Unluckily, the most representative training plot of this unit fell again into the prison area. However, the spectral characteristics of the pixels of this unit and field observations at other parts of the area indicate that most likely the major part of EA-5 consists of plots which were left fallow due to salinization problems.

Due to the various classification constraints which were discussed in Chapter 3.6, a considerable part of area East (i.e. 34%) remained unclassified.

Figure 32: Irrigation area southwest of Xin-Yuan

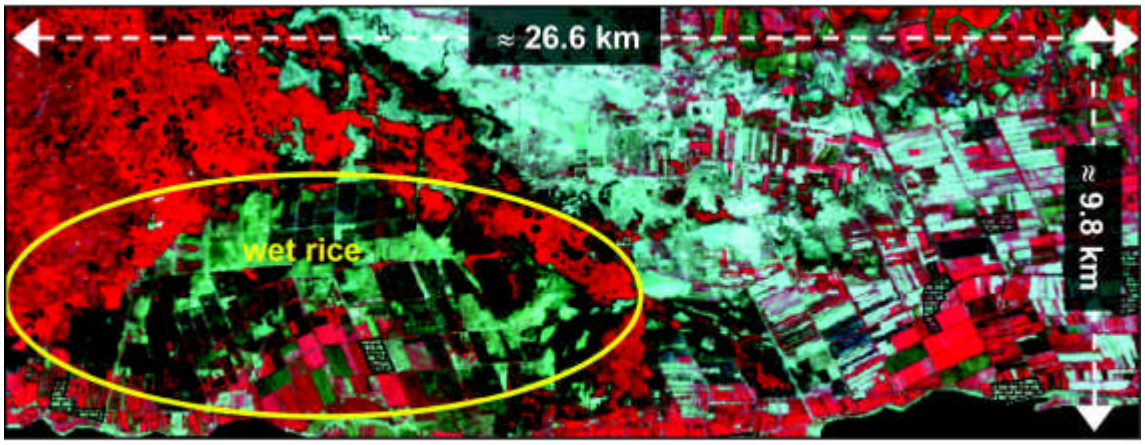

FCC 432 Landsat 7 ETM+, 145-30, 2000-06-27

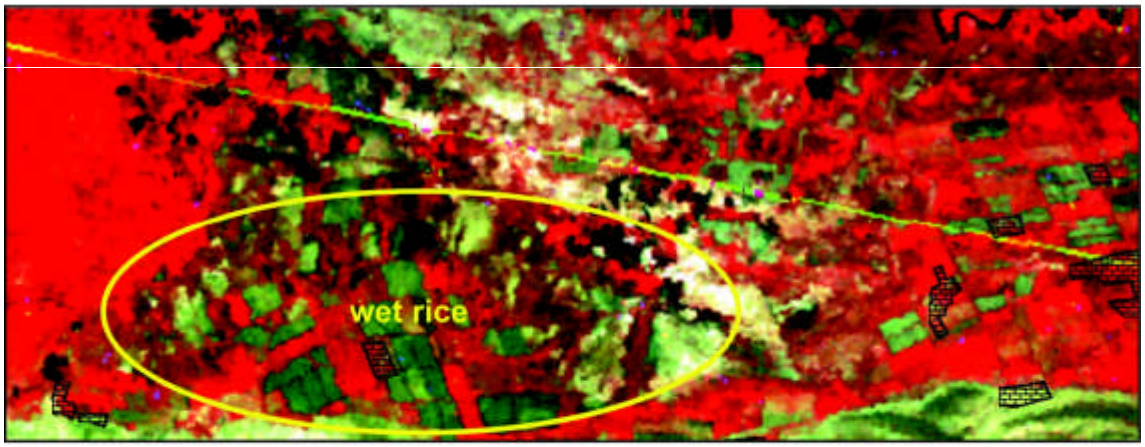

FCC 654 Landsat 2 MSS, 157-30, 1977-08-17

Source: own compilation

The image comparison shows that in this area large-scale wet rice cultivation was already present in 1977, but has been extended somewhat since then. The area belongs to a big prison farm and could thus not be visited during the fieldcheck. Although the recording dates of the two scenes (especially of the Landsat 2 scene) are much later in the growing period, the water-covered rice plots are still clearly visible.

4.2.4 Land Use / Land Cover in Area Southwest

Fig. 33 illustrates the classification results for area Southwest. The Landsat ETM+ data of this area were recorded on May 27, 2001. The field check was conducted between June 12 and June 13, 2003, i.e. about two weeks later than image recording two years earlier. The mapping units and the spectral characteristics of the different land covers had been described in Table 8 and Table 12 (cp. Chapter 3.6.5).

Apart from a negligible section at the eastern border, the cultivated parts of area Southwest fall entirely into Zhaosu County. During the fieldwork campaign, this region was verified as an area with almost exclusively rainfed agriculture (locally called 'glebe'). This finding is in line with the appearance of this area on the satellite images, but contradicts the figures for the Ili area given in the Statistical Yearbook (cp. Statistical Bureau for Xinjiang (Ed.) 2002). According to these figures, about 238 sqkm or 60% of the cultivated area is "glebe", while the remaining 40% (161 sqkm) is supposed to be "Irrigable Land". However, according to the satellite image analysis and the field check results, this can hardly be true!

Most of area Southwest is located at altitudes of about 1,400 – 1,600 m (cp. Chapter 2.1). Due to the cooler climate, the rainfall is considerably higher (about 500 mm) and the evaporation is

lower than in the lowlands along the Ili, Kash and Kunes. Hence, irrigation is not necessarily required to grow a reasonable crop. According to the fieldwork reports and the photos taken in the area, this region is dominated by large, rainfed summer wheat and summer rape fields on undulating terrain, with no sign of (permanent) irrigation (cp. Photo 9).

Photo 9: Typical summer wheat / summer rape landscape in area Southwest (County Zhaosu)

Source: Photos taken during the fieldwork campaign June 12 – 13, 2003 (Photo-ID SW_KL147_S_2_3/KL_10 (upper left), SW_KL147_S_1_3/KL_9 (upper right), SW_KL147_S_2_2/KL_7 (lower left), SW_KL147_S_1_1/KL_1 (lower right). The photos on the left side show (summer) wheat fields, the photos on the right side (summer) rape plots. Both crops are still in a fairly initial growing stage. Note the enormous field size, the slightly undulating terrain, and the lack of any indication for irrigation infrastructure.

The deviating figures of the statistical yearbook quoted above could be explained by one or more of the following points:

- The figures are simply wrong and overestimate the irrigation area. (Quite likely, see discussion further below!)
- A certain part of the rainfed rape and wheat fields receives supplementary irrigation (e.g. by transportable sprinklers) during drought periods. (Quite possible, but such fields cannot be distinguished from non-irrigated fields!).
- There really exist some smaller areas with permanent irrigation in the transitional region between the highlands and the lowlands in the eastern parts of Zhaosu, located along the borders of the Tekes River. (Possible and also in line with the satellite image.)

In order to be 'on the safe side' with the subsequent calculations of irrigation areas and water consumption (cp. Chapter 4.3), it was decided to exclude this area entirely from those calculations. Hence, the figures in Table 18 were not included in these calculations. The following classification results are thus mainly presented for the sake of completeness.

Photo 10: Summer rape field in area Southwest (County Zhaosu) in an early growing stage

Source: Photos taken during the fieldwork campaign June 12 – 13, 2003 (Photo-ID SW_KL147_S_3_1/KL_3. The photo proves that a certain part of the cultivated area was still in a fairly initial growing stage at the time of field check. It should noted that the Landsat ETM+ data were recorded even two weeks earlier (May 27, 2001) which mean the crops are likely to have been even less developed at that time.

In contrast to the other three areas, the land use in area Southwest is fairly homogeneous and easy to map. The two absolutely dominating crops are summer wheat and summer rape, covering 77% and 23% of the classified areas respectively (s. Table 18). As shown by Photo 9, at a first glance, the two crops seem to have a fairly similar appearance in this initial growing stage. However, the spectral characteristics of the two crops are (at least for a large percentage of the area) already sufficiently different to enable a good discrimination (see graph in Figure 22 in Chapter 3.6.5). 532 sqkm or 33% of the total input area remained unclassified. These unclassified areas fall into three main categories:

- The major part of the unclassified pixels, especially those scattered inside consolidated wheat and rape areas, is actually summer wheat and summer rape. These pixels have not been classified correctly because of a too early growing stage. As illustrated by Photo 10, some of the cultivated areas had not yet developed sufficient vegetation cover to show the typical spectral characteristics of wheat and rape respectively.
- A second, smaller part of the unclassified pixels probably corresponds to areas cultivated by rainfed crops other than wheat and rape. While wheat and rape are the dominating crops, it is unlikely that they are the only crops grown in this area. Since training areas for these 'minor' crops were not available, these pixels remain unclassified.
- A third part of the unclassified pixels may represent (permanently) irrigated areas which could not be sampled either. As discussed above, these areas are believed to be limited to a fairly small section in the transitional zone in the eastern part of the county (cp. Fig. 33, at about 81°30' E and 43° N)

Fig. 33: Classification results for rainfed land ("glebe") in area Southwest

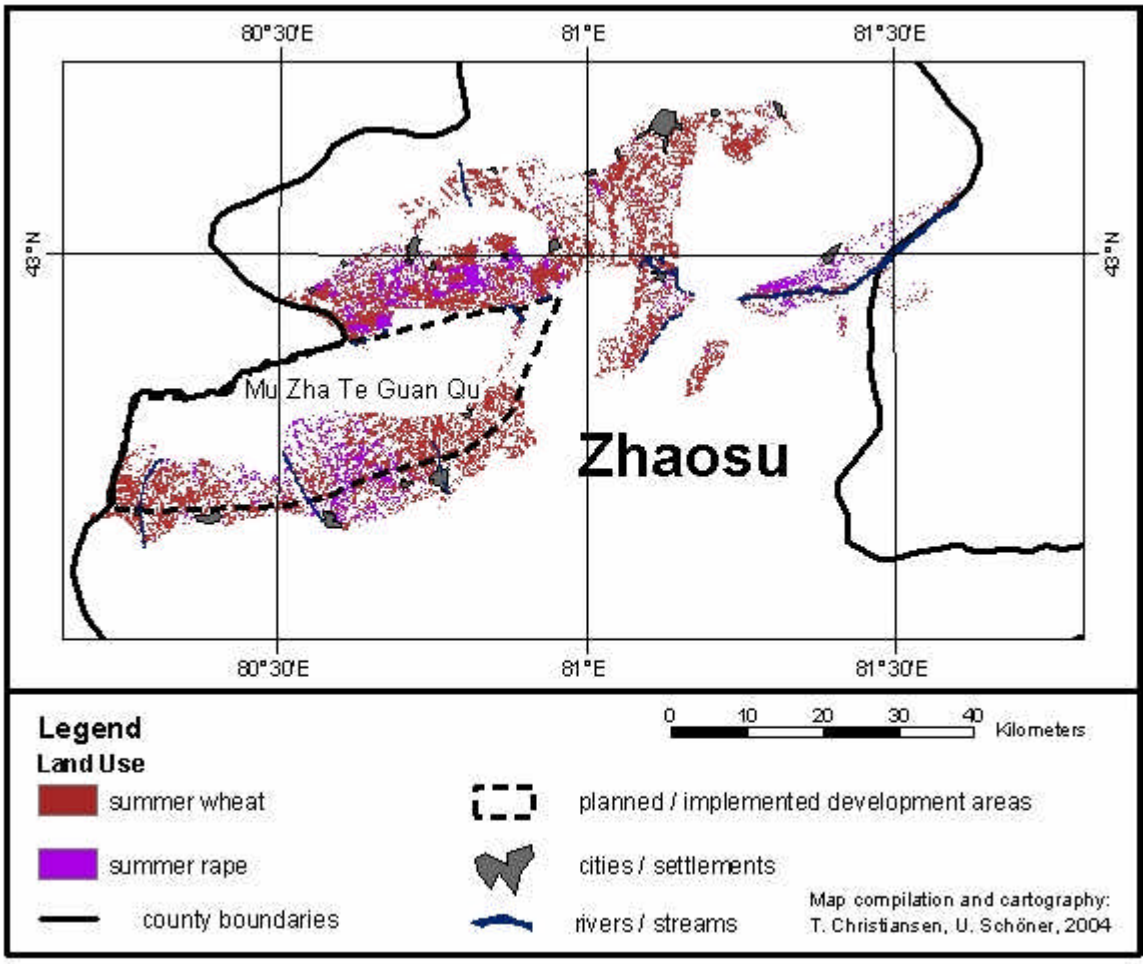

Source: own compilation, based on classification of Landsat 7 ETM+ data

Table 18: Area figures for the classification results of Area Southwest (Landsat7 ETM+ scene 147/30, 2001-05-27)

Mapping-Code	Mapping Unit	Area (sqkm)	Area (% of classified)	Area (% of total area)	Remarks
SW-1	summer wheat	830.1	77.2	51.6	
SW-2	summer rape	245.2	22.8	15.3	
	å SW-1 + SW-2	1075.3	100.0		
	unclassified pixels	532.3		33.1	probably includes some minor areas of irrigated land
	å Total Area (classified + unclassified pixels)	**1607.6**		**100.0**	

Table 18 shows that the official Chinese statistics strongly underestimate the actual total cultivation area. According to these figures, Zhaosu has total cultivation area of about 400 sqkm only. This would correspond to a consolidated piece of land of merely 20 x 20 km! Already a quick look at Fig. 33 reveals that this can impossibly be correct! Despite the limited amount of field truth data, the overall extension of the cultivated areas can hardly be mistaken visually on the satellite image. According to these figures, the classified areas alone total 1075 sqkm already! Moreover, as explained above, most of the unclassified areas are actually cultivated

land too. Hence, in reality, the actual total cultivation area in Zhaosu county is in the order of magnitude of about 1,500 – 1,600 sqkm, i.e. three to four times larger as given by the Chinese statistics!

4.2.5 Extension of Wet Rice Cultivation Areas

As outlined in the preceding chapters, the value of the results of the digital image classification is limited, the main reasons being:

- the early recording date of the satellite images,
- the lack of a second set of scenes at a later stage of the growing period,
- the limited number of training areas, which could be verified in the field,
- the fact that the field check could not be conducted by the team members themselves.

As a consequence, in general only 'crop groups', such as 'little developed crops' could be mapped rather than individual field crops. This restriction, however, does not apply for wetland rice cultivation! As illustrated by the Figures 28, 30, and 32, flooded wetland rice plots are striking features in the satellite images and the spectral signature is so clear that they can hardly be mistaken for anything else. Hence, even with the limited field truth data at hand, the mapped rice cultivation areas and the corresponding area figures can be taken as very reliable.

Fig. 34 shows the area figures which resulted from the satellite image classification as compared to the official statistics. The figure shows clearly that the Chinese statistics not only underestimate the overall irrigation area, but also the extent of this particularly water-consuming land use category. According to the Chinese statistics, the total wetland rice areas in the Upper Ili Catchment totals about 62 sqkm which corresponds to merely 29% of our mapping results (cp. Statistical Bureau for Xinjiang (Ed.) 2002).

Figure 34: Rice cultivation in the Ili area in 2001: Comparison of the figures of the Statistical Yearbook vs. the satellite image interpretation results

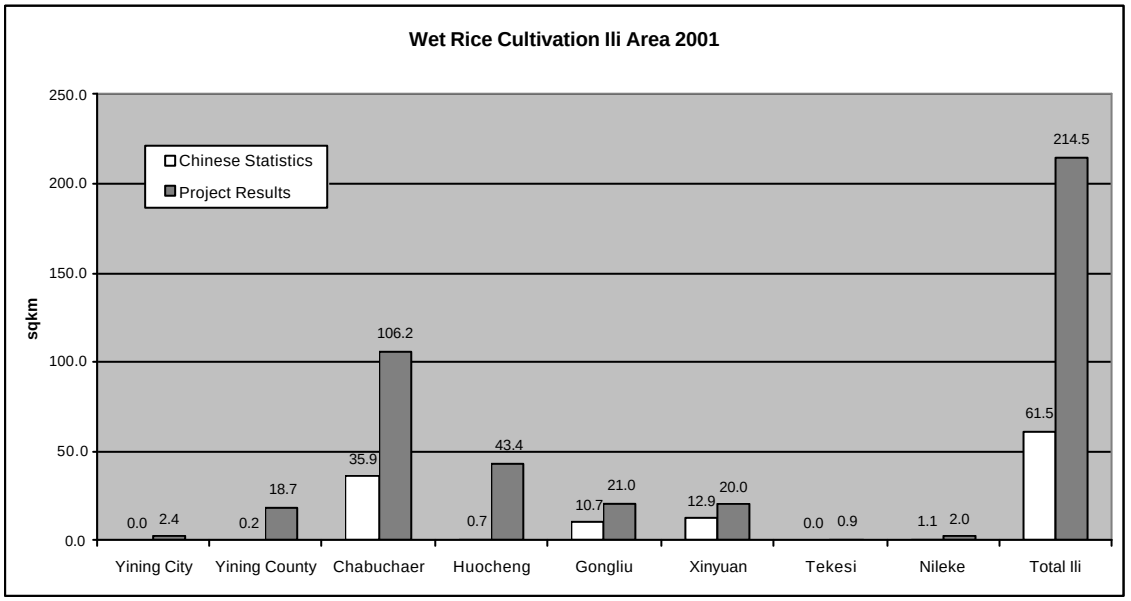

The difference is particularly striking in Huocheng, where (according to the statistics) paddy is supposed to be almost nil! However, as clearly visible in Fig. 27 and 28, Huocheng has the biggest single consolidated block of wetland rice cultivation of all counties! Also in four other counties (Yining County, Chabuchaer, Gongliu and Xingyuan) the survey proved that the rice cultivation areas are considerably larger than indicated by the Chinese statistics.

4.2.6 Conclusion

The digital image classification of the 'net irrigation area' gives only limited detail on the extension of individual field crops. Due to the early recording date of the used satellite images and the lack of a second set of images as reference for a later stage of the growing period, in most cases several irrigated crops had to be lumped together into bigger categories such as 'undeveloped crops', 'grass – grain complex' etc.

A further constraint resulted from the limited amount of field truth data, which was available for the classification process. The number of sample areas was fairly limited and the field work had to be 'outsourced' to Chinese colleagues, rather than having been conducted by the image interpreters themselves. Furthermore, a post-classification field check of the accuracy of classification results was not possible. Hence, the usual classification accuracy assessment by means of a confusion matrix had to be omitted.

However, despite these constraints, the classification procedure illustrates important facts. The wetland rice cultivation areas could be discriminated without difficulties. This provided accurate information on the location and the extent of those areas with the highest water consumption. Moreover, the classification procedure and field check gave a fairly reliable and comprehensive general overview over the (irrigated) crops in the Upper Ili Area and their spatial prevalence within.

The crop cultivation in the northern and eastern parts of the area (regions Northwest, Central and East) is based on full-scale permanent irrigation, due to the very dry and hot conditions during the vegetation period. According to information collected during the fieldwork, the (net) irrigation quantities vary between 2,000 and 3,750 m^3/ha for 'normal' crops and 10,500 – 14,500 m^3/ha for wetland rice.

According to Chinese statistics (cp. Statistical Bureau for Xinjiang (Ed.) 2002), rainfed agriculture ('glebe') is supposed to occur too. The figures indicate somewhat larger rainfed areas in Xinyuan (72.9 sqkm), Nileke (63.8 sqkm), Tekesi (41.1 sqkm), and Chabuchaer (35.9 sqkm). Even if these figures are approximately correct – which seems rather doubtful, given yearly rainfalls of 200 – 300 mm only - the bulk of these rainfed areas is most likely outside the consolidated blocks of irrigation land along the major rivers. Within this 'net irrigation area', the major crops are (winter) wheat, maize, soybean, sunflower. These main crops are supplemented by some sugar beet, water melon, and lavender and possibly some winter rape (area Central only).

The south-western part of the Ili catchment (region Southwest) is characterised by fairly different natural conditions. The area is located at about 1,200 -1,400 m altitude, i.e. 700 - 900 m higher than the northern parts of the project area. It is therefore considerably cooler and it receives about twice as much rainfall. As a consequence, there is no need for full-fledged irrigation. Hence, rainfed agriculture is by far the prevailing land use. The two dominating crops are winter wheat and winter rape, covering about 77% and 23 % of the classified areas respectively. According to the Statistical Yearbook 2001 (cp. Statistical Bureau for Xinjiang (Ed.) 2002), this south-western part of the Upper Ili Catchment is supposed to include a total of 161 sqkm of irrigated land. According to the appearance of this area on the satellite image and also according to the reports of the fieldwork team, this figure seems overestimated, at least if it refers to 'normal' (i.e. full-fledged) surface irrigation. Provided that the figure is approximately correct in the first place, it may possibly refer to land which receives some supplementary irrigation during drought periods, e.g. by transportable sprinklers. If 'normal' full-fledged surface irrigation does exist in this region, it is likely to be confined to small patches in the transition zone between the lower and higher altitudes in the east of Zhaosu county.

Table 19 and Fig. 35 give a summary of the most important classification results as compared with the respective 2001 figures quoted by the Statistical Yearbook (cp. Statistical Bureau for Xinjiang (Ed.) 2002). In Table 19, the columns which can be directly compared are marked with the same letter suffix. (E.g. columns "2b" and "3b" contain (approximately) comparable data.) It is evident that there are striking differences between the two figure sets. For all counties except Yining City proper, the satellite image interpretation resulted in considerably larger irrigated areas as indicated by the Yearbook. Alone the two identified crop categories (cp. columns 2a and 2b) already result in a total of about 5,020 sqkm. This is almost 3,000 (!) sqkm more than the 2,167 sqkm given by the Statistical Yearbook (column 3f). Moreover, it should be kept in mind that the bulk of the 'unclassified areas' (1,806.8 sqkm, see column 2e) actually belongs to some type of irrigated cropland too. If a realistic percentage of these 1,800 sqkm – let us say 70

- 80 % - is added, the figure for the 'likely' total irrigated areas even rises to roughly 6,300 - 6,500 sqkm. This is almost three times as much as given by the Yearbook![28]

Table 19: Overview: Most important classification results compared against the figures of the Statistical Yearbook Ili area 2001

	Total Area	Satellite Image Interpretation 2000 / 2001						Statistical Yearbook Ili Area 2001		
	(1) Area (Project Data)	(2a) Wet Rice	(2b) Other Irrigated Crops	(2c) Open Land, Fallow etc.	(2d) Total Classified Areas	(2e) Unclassified Areas	(2f) Total Net Irrigation Area	(3a) Wet Rice ("Paddy")	(3b) "Irrigable" Land (without "Paddy")	(3f) Total Irrigated Land
Yining City	120.4	2.4	55.2	2.0	59.6	26.9	86.5	0.0	102.8	102.8
Yining County	4880.3	18.7	963.2	14.4	996.3	308.9	1305.2	0.2	655.2	655.4
Chabuchaer	4505.3	106.2	560.4	51.7	718.3	298.9	1017.2	35.9	252.3	288.2
Huocheng	5413.9	43.4	896.2	92.1	1031.7	451.0	1482.6	0.7	345.9	346.6
Gongliu	4203.9	21.0	726.3	6.4	753.7	39.5	793.2	10.7	219.5	230.2
Xinyuan	6903.0	20.0	880.5	11.3	911.8	421.7	1333.5	12.9	296.7	309.6
Tekesi	8197.1	0.9	362.1	10.8	373.8	151.7	525.5	0.0	147.7	147.7
Nileke	10293.6	2.0	361.5	1.4	364.9	108.1	473.0	1.1	147.4	148.5
Total Ili	44517.4	214.5	4805.4	190.0	5210.0	1806.8	7016.7	61.5	2167.5	2229.0

[28] Furthermore, it should be remembered that all calculations assume that no major 'normal' irrigation areas exist in Zhaosu county. Hence, any actually existing irrigation areas in this county are not included in this assessment!

Figure 35: Summary of the most important classification results compared against the figures of the Statistical Yearbook Ili area 2001

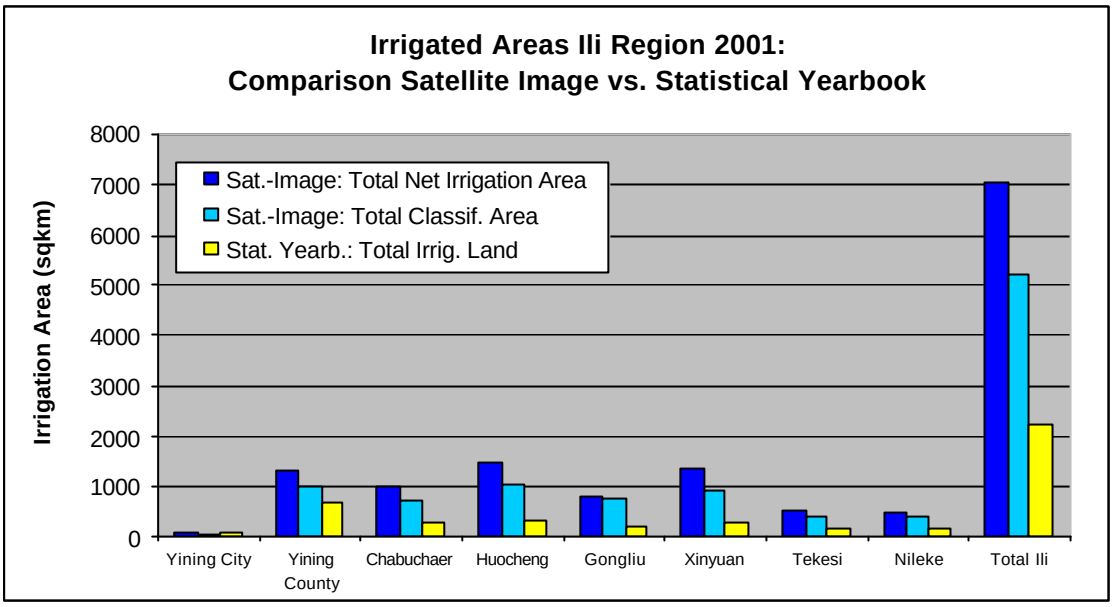

4.3 ESTIMATED WATER CONSUMPTION IN YEAR 2000 / 2001

4.3.1 Introductory Remarks and Assumptions

The final objective of the present study was to assess – as precise as possible - the amount of water which is used for irrigation purposes in the Upper Ili Area. To accomplish this task, two sets of parameters have to be known:

- the areas cultivated by different crop categories,
- the crop-specific (average) amount of irrigation water per area unit.

The latter factor consists of two components: The first component is 'net irrigation rate', i.e. the amount of water actually discharged on the field (in m^3/ha/year for each crop). These figures have been enquired accurately during the fieldwork (cp. Table 20). The second component is the amount of water which is lost during the transport from the point of withdrawal at the river to the point of discharge at the field (conveyance loss). Together, net irrigation rate and conveyance losses sum up to the 'gross irrigation rate', i.e. the figure which is actually asked for in this study! The so-called 'conveyance loss' is commonly given as percentage factor of the gross irrigation rate. Other terms are 'irrigation efficiency' (cp. Rogers et al. 1999) or 'conveyance efficiency' respectively 'distribution efficiency' (cp. ILACO 1981, p. 378 ff). For example, an irrigation efficiency of "0.6" signifies a conveyance loss of 40% of the extracted water, only the remaining 60% reach the field.

Table 20: (Net) irrigation rate per area unit in different parts of the study area

Area	Water consumption per season (m^3 / ha)	
	Wet rice	Other crops
Northwest	11,500 – 14,500	2,500 – 3,500
Central	10,500 – 12,000	2,000 – 3,000
East	11,500 – 14,000	2,700 – 3,750

Unlike the net irrigation rate data, which could be established very reliably (cp. Table 20), area-specific conveyance loss data could not be made available for the Ili region. However, fairly

reliable 'rules of thumb' figures are available from various standard textbooks and irrigation manuals. The range of 'rule of thumb' figures given by these sources then has to be evaluated carefully in order to select the 'most likely' parameter value for the following water consumption calculations. This evaluation has to be based on the physiographic conditions in the Ili area, in particular on the size and form of the irrigation areas and the respective distances from the water source.

As mentioned already in Chapter 1, standard textbooks such as the Agricultural Compendium (ILACO 1981) or Booker Tropical Soil Manual (Landon (Ed.) 1984) quote irrigation efficiency rates in the order of 0.5 (respectively 50% conveyance losses). According to (ILACO 1981, p. 380) the efficiency for poorly managed large surface irrigation schemes ranges between 0.5 and 0.7 (30% - 50% conveyance losses). With a range of 0.4 – 0.5 (50% - 60% conveyance losses) the Booker Tropical Soil Manual gives a somewhat more conservative figure (Landon (Ed.) 1984, p. 338). Both figures are based on general experience in numerous countries all over the world. They are, however, not specifically derived from irrigation schemes in Central Asia.

On the other hand, figures quoted by Ressl (1999, p. 156) prove that these rule of thumb figures hold true for Central Asia as well! According to Ressl, the irrigation efficiency in the Amu Darja delta ranges between 0.5 – 0.6 too! Hence, the conveyance losses are in the order of 40 – 50 %, which is fully in line with the figures quoted by ILACO and Landon (see above).

Comparing the situation between the Amu Darja delta and the Ili region, the physiographic characteristics are clearly more favourable in the latter. The irrigation areas in the Ili area form elongated, fairly narrow strips along the main rivers (cp. especially area East in Fig. 31). Hence, compared with the Amu Darja delta, the water transport distances in the Illi region are relatively short. In other words: There is just not enough transport time to loose very much of the extracted water.[29] Therefore, assuming a comparable technology and management level in both areas, the average efficiency rate in the Ili region will be at least as high as in the Amu Darja delta (and very likely even somewhat better). Taking these data and considerations into account, an efficiency rate of 50 – 60 % is a rather reliable and a fairly conservative assessment of the overall irrigation efficiency in the Upper Ili Area.

Once the above-discussed variables are established, the subsequent calculation is just a simple multiplication exercise. During the field check, our Chinese colleagues collected data on the net irrigation rates used for different crops in different parts of the study area (cp. Table 20). It turned out that – apart from rice – all other irrigated crops receive more or less similar water quantities. Wetland rice, on the other hand, requires about four times as much water as the 'normal' crops.

According to the figures given in Table 20, the irrigation rates vary somewhat from region to region. Based on these general figures for the three major irrigation areas of the Upper Ili Catchment, the applicable irrigation rates for each of the eight counties were established for different scenarios (cp. Table 21). The subsequent water consumption calculations are based on the area figures given in Table 19 and the per unit rates shown in Table 20. Based on these figures, four scenarios were calculated:

- **Scenario 1** – the 'Chinese Data Scenario' (CDS) calculates the water consumption per year based on the (clearly too low) area figures of the Statistical Yearbook (cp. Statistical Bureau for Xinjiang (Ed.) 2002) and on 'average' per unit rates as taken from Table 21.
- The **Scenarios 2, 3, and 4** represent different calculations based on the satellite image interpretation results. **Scenario 2** represents a 'best case scenario' (BCS), using very conservative assumptions regarding the areas and the per unit quantities. It thus estimates the 'lower end' of the potential range of water consumption. **Scenario 3** calculates the 'likely case scenario' (LCS), based on intermediate figures which are most likely to fit the real situation. Finally, **Scenario 4** represents the 'worst case scenario' (WCS), which uses area figures and per unit quantities which are on the 'high end' of the possible range.

Table 21 summarises the assumptions for the four scenarios CDS, BCS, WCS, LCS. Please note that the water quantities still refer to the 'net irrigation rates'! Hence, the contingency factor for the conveyance losses is not yet considered!

---

[29] This especially applies to the particularly water-consuming rice cultivation areas! As illustrated by Figure 27, 29, and 31 respectively, all wetland rice areas are in the immediate vicinity of a major stream!

Table 21: Assumptions used for the water consumption scenarios

	Area wetland rice (sqkm)	Area other crops (sqkm)	Fallow area assumed to be 'other crops' (%)	Fallow area assumed to be 'other crops' (sqkm)	Assumed water consumption per hectare wetland rice (m^3)	Assumed water consumption per hectare 'other crops' (m^3)
Assumptions Scenario 1: Chinese Data Scenario (CDS)						
Yining City	0.0	102.8	not relevant (n.r.)	not relevant (n.r.)	13,000	3,000
Yining County	0.2	655.2	n.r.	n.r.	13,000	3,000
Chabuchaer	35.9	252.3	n.r.	n.r.	13,000	3,000
Huocheng	0.7	345.9	n.r.	n.r.	13,000	3,000
Gongliu	10.7	219.5	n.r.	n.r.	11,250	2,500
Xinyuan	12.9	296.7	n.r.	n.r.	12,750	3,225
Tekesi	0.0	147.7	n.r.	n.r.	11,250	2,500
Nileke	1.1	147.4	n.r.	n.r.	12,750	3,225
S **ILI AREA**	**61.5**	**2167.5**				
Assumptions Scenario 2: Project Data > 'Best Case Scenario' (BCS)						
Yining City	2.4	55.2	50	13.4	11,500	2,500
Yining County	18.7	963.2	50	154.4	11,500	2,500
Chabuchaer	106.2	560.4	50	149.5	11,500	2,500
Huocheng	43.4	896.2	50	225.5	11,500	2,500
Gongliu	21.0	726.3	50	19.8	10,500	2,000
Xinyuan	20.0	880.5	50	210.9	11,500	2,700
Tekesi	0.9	362.1	50	75.9	10,500	2,000
Nileke	2.0	361.5	50	54.0	11,500	2,700
S **ILI AREA**	**214.5**	**4,805.4**		**903.4**		
Assumptions Scenario 3: Project Data > 'Likely Case Scenario' (LCS)						
Yining City	2.4	55.2	70	18.8	13,000	3,000
Yining County	18.7	963.2	70	216.2	13,000	3,000
Chabuchaer	106.2	560.4	70	209.3	13,000	3,000
Huocheng	43.4	896.2	70	315.7	13,000	3,000
Gongliu	21.0	726.3	70	27.7	11,250	2,500
Xinyuan	20.0	880.5	70	295.2	12,750	3,225
Tekesi	0.9	362.1	70	106.2	11,250	2,500
Nileke	2.0	361.5	70	75.7	12,750	3,225
S **ILI AREA**	**214.5**	**4,805.4**		**1264.7**		

	Area wetland rice (sqkm)	Area other crops (sqkm)	Fallow area assumed to be 'other crops' (%)	Fallow area assumed to be 'other crops' (sqkm)	Assumed water consumption per hectare wetland rice (m^3)	Assumed water consumption per hectare 'other crops' (m^3)
Assumptions Scenario 4: Project Data > 'Worst Case Scenario' (WCS)						
Yining City	2.4	55.2	90	24.2	14,500	3,500
Yining County	18.7	963.2	90	278.0	14,500	3,500
Chabuchaer	106.2	560.4	90	269.0	14,500	3,500
Huocheng	43.4	896.2	90	405.9	14,500	3,500
Gongliu	21.0	726.3	90	35.6	12,000	3,000
Xinyuan	20.0	880.5	90	379.6	14,000	3,750
Tekesi	0.9	362.1	90	136.6	12,000	3,000
Nileke	2.0	361.5	90	97.3	14,000	3,750
S **ILI AREA**	**214.5**	**4,805.4**		**1626.1**		

4.3.2 Water consumption by irrigation in 2000 / 2001

The following tables and figures show the results of the four scenarios outlined above. First, Tables 22 – 25 give the detailed results, separately for each scenario. Thereafter Table 26 and Fig. 36 summarise and compare the results of all four scenarios.

Scenario 1: Chinese Data Scenario (CDS)

Table 22 lists the yearly water consumption based on the area figures from the Chinese sources (i.e. the Statistical Yearbook) and 'average' irrigation rates as enquired on site during the fieldwork campaign. According to these figures, wetland rice plots receive irrigation rates between 11,250 and 13,000 m^3/ha and season (i.e. 1,125 - 1,300 mm). The respective figures for the other field crops range between 2,500 to 3,225 m^3/ha, corresponding to 250 – 322 mm respectively. The irrigation rate data collected during the fieldwork make sense: Together with the supply by rainfall (about 150 – 300 mm during the growing season) and the soil moisture storage, the overall water supply per season totals about 500 – 600 mm for 'normal' crops and 1,300 to 1,600 mm for wetland rice respectively.

Table 22: Water consumption according to Scenario 1: "Chinese Data Scenario (CDS)"

	Wet rice ("paddy")			Other crops			Wet rice + other crops
	Area (skm)	Irrig. rate (m^3/ ha)	Total water consumpt. (1,000 m3)	Area (sqkm)	Irrig. rate (m^3/ ha)	Total water consumpt. (1,000 m^3)	Total water cons. / year (1,000 m^3)
Yining City	0.0	13,000	0.0	102.8	3,000	30,840.0	30,840.0
Yining County	0.2	13,000	260.0	655.2	3,000	196,560.0	196,820.0
Chabuchaer	35.9	13,000	46,670.0	252.3	3,000	75,690.0	122,360.0
Huocheng	0.7	13,000	910.0	345.9	3,000	103,770.0	104,680.0
Gongliu	10.7	11,250	12,037.5	219.5	2,500	54,875.0	66,912.5
Xinyuan	12.9	12,750	16,447.5	296.7	3,225	95,685.8	112,133.3
Tekesi	0.0	11,250	0.0	147.7	2,500	36,925.0	36,925.0
Nileke	1.1	12,750	1,402.5	147.4	3,225	47,536.5	48,939.0
Total Ili	**61.5**		**77,727.5**	**2,167.5**		**641,882.3**	**719,609.8**

According to the 'totals' for the Upper Ili Area, the overall water consumption adds up to about 0.7 billion m^3 or 0.72 km^3/year, which are distributed over a total irrigation area of about 2,230 sqkm. 11% of the total water consumption is used for the (presumed) 61.5 sqkm wetland rice.

Scenario 2: Best Case Scenario (BCS)

Table 23 illustrates the figures which result from the BCS calculation, i.e. the most conservative estimation based on the project findings. The irrigation rates used are at the lower end of the range and only 50% of the unclassified pixels are assumed to be 'other crops'. According to these figures, the wetland rice areas and the respective water consumption is already more than three times higher than the CDS figures! The irrigation areas for 'other crops' and their respective water consumption are far more than twice as big as the figures calculated in the CDS.

The total irrigation water consumption for the Ili area adds up to 1.6 billion m^3 respectively 1.64 km^3/year which corresponds to 228% of the respective CDS total! About 245 million m^3 or 15% of the overall consumption is used for 214 sqkm of wetland rice.

Table 23: Water consumption according to Scenario 2: "Best Case Scenario (BCS)"

	Wet rice ("paddy")			Other crops			Wet rice + other crops
	Area (skm)	Irrig. rate (m^3/ ha)	Total water consumpt. (1,000 m^3)	Area (sqkm)	Irrig. rate (m^3/ ha)	Total water consumpt. (1,000 m^3)	Total water cons. / year (1,000 m^3)
Yining City	2.4	11,500	2,760.0	68.6	2,500	17,162.4	19,922.4
Yining County	18.7	11,500	21,505.0	1,117.6	2,500	279,408.0	300,913.0
Chabuchaer	106.2	11,500	122,130.0	709.9	2,500	177,466.3	299,596.3
Huocheng	43.4	11,500	49,910.0	1,121.7	2,500	280,422.5	330,332.5
Gongliu	21.0	10,500	22,050.0	746.1	2,000	149,213.8	171,263.8
Xinyuan	20.0	11,500	23,000.0	1,091.4	2,700	294,668.4	317,668.4
Tekesi	0.9	10,500	945.0	438.0	2,000	87,593.3	88,538.3
Nileke	2.0	11,500	2,300.0	415.5	2,700	112,196.6	114,496.6
Total Ili	**214.5**		**244,600.0**	**5,708.8**		**1,398,131.3**	**1,642,731.3**

Scenario 3: Likely Case Scenario (LCS)

Table 24 represent the assessment which is believed to be the most accurate and most realistic estimation. Also this LCS is based on the project findings, but it assumes that about 70% of the unclassified pixels actually represent (irrigated) areas of 'other crops'. Regarding the per unit irrigation rates, the same 'average' rates as for the CDS are used, which means the rates used are somewhat higher than in the (more conservative) BCS.

Due to the assumed higher irrigation rates, the water consumption for wetland rice rises slightly to 275 million m^3. The water consumption for 'other crops' rises considerably, because both factors increase, i.e. the assumed irrigation rates as well as the presumed cultivated area. According to these figures, the total irrigation water consumption of the Upper Ili Area adds up to about 2.07 billion m^3 or 2.07 km^3/year respectively. This corresponds to about 288% of the CDS total. About 12% of the irrigation water is used for 214 sqkm of wetland rice.

Table 24: Water consumption according to Scenario 3: "Likely Case Scenario (LCS)"

	Wet rice			Other crops			Wet rice + other crops
	Area (skm)	Irrig. rate (m^3/ ha)	Total water consumpt. (1,000 m^3)	Area (sqkm)	Irrig. rate (m^3/ ha)	Total water consumpt. (1,000 m^3)	Total water cons. / year (1,000 m^3)
Yining City	2.4	13,000	3,120.0	74.0	3,000	22,208.8	25,328.8
Yining County	18.7	13,000	24,310.0	1,179.4	3,000	353,821.4	378,131.4
Chabuchaer	106.2	13,000	138,060.0	769.7	3,000	230,895.4	368,955.4
Huocheng	43.4	13,000	56,420.0	1,211.9	3,000	363,565.9	419,985.9
Gongliu	21.0	11,250	23,625.0	754.0	2,500	188,494.2	212,119.2
Xinyuan	20.0	12,750	25,500.0	1,175.7	3,225	379,166.6	404,666.6
Tekesi	0.9	11,250	1,012.5	468.3	2,500	117,078.2	118,090.7
Nileke	2.0	12,750	2,550.0	437.2	3,225	140,984.1	143,534.1
Total Ili	**214.5**		**274,597.5**	**6,070.1**		**1,796,214.6**	**2,070,812.1**

Scenario 4: Worst Case Scenario (WCS)

Table 25 finally illustrates the results of the worst case scenario. In this calculation, the upper end of the irrigation rate ranges were used (cp. Table 20) and it was assumed that 90% of the unclassified pixels actually represent irrigated 'other crop' areas. Both assumptions are likely to be biased a bit to the high side. Hence, the results of this calculation mark the upper limit of the range of values within which the 'true' figure is located. According to these – probably somewhat high – figures, the overall irrigation water consumption for the Upper Ili Area rises by another 500 million m^3 to a total of 2.5 billion m^3 or 2.5 km^3 respectively.

Table 25: Water consumption according to Scenario 4: "Worst Case Scenario (WCS)"

	Wet Rice			Other Crops			Wet rice + other crops
	Area (skm)	Irrig. rate (m^3/ ha)	Total water consumpt. (1,000 m^3)	Area (sqkm)	Irrig. rate (m^3/ ha)	Total water consumpt. (1,000 m^3)	Total water cons. / year (1,000 m^3)
Yining City	2.4	14,500	3,480.0	79.4	3,500	27,793.3	31,273.3
Yining County	18.7	14,500	27,115.0	1,241.2	3,500	434,412.1	461,527.1
Chabuchaer	106.2	14,500	153,990.0	829.4	3,500	290,303.2	444,293.2
Huocheng	43.4	14,500	62,930.0	1,302.1	3,500	455,728.8	518,658.8
Gongliu	21.0	12,000	25,200.0	761.9	3,000	228,565.3	253,765.3
Xinyuan	20.0	14,000	28,000.0	1,260.1	3,750	472,521.0	500,521.0
Tekesi	0.9	12,000	1,080.0	498.7	3,000	149,597.8	150,677.8
Nileke	2.0	14,000	2,800.0	458.8	3,750	172,041.4	174,841.4
Total Ili	**214.5**		**304,595.0**	**6,431.5**		**2,230,962.9**	**2,535,557.9**

Summary & Comparison: Net Irrigation Quantities Scenario 1 – Scenario 4

Table 26 and Fig. 36 summarise and illustrate the most important results of Tables 22 – 25. In order to facilitate the correlation between the data in Table 26 and the graphical representation of these data in Figure 36, the respective components have been marked with the same colour For example, the values based on the official Chinese figures (CDS) are marked orange and the most realistic results (LCS) are marked green in table and figure alike. The less important lower and upper limits of the potential values (i.e. BCS and WCS) are marked medium grey and dark grey respectively. In contrast to the detailed results of individual scenarios in Table 22 – 25, all figures are given in million m^3.

Table 26: Comparison: Irrigation water consumption according to Scenarios 1 – 4

	Irrigation water consumption Ili area 2001 (million m^3)			
	CDS	**BCS**	**LCS**	**WCS**
Yining City	30.8	19.9	25.3	31.3
Yining County	196.8	300.9	378.1	461.5
Chabuchaer	122.4	299.6	369.0	444.3
Huocheng	104.7	330.3	420.0	518.7
Gongliu	66.9	171.3	212.1	253.8
Xinyuan	112.1	317.7	404.7	500.5
Tekesi	36.9	88.5	118.1	150.7
Nileke	48.9	114.5	143.5	174.8
Total Ili	**719.6**	**1,642.7**	**2,070.8**	**2,535.6**

Figure 36: Irrigation water consumption Ili area 2001 according to Scenarios 1 - 4

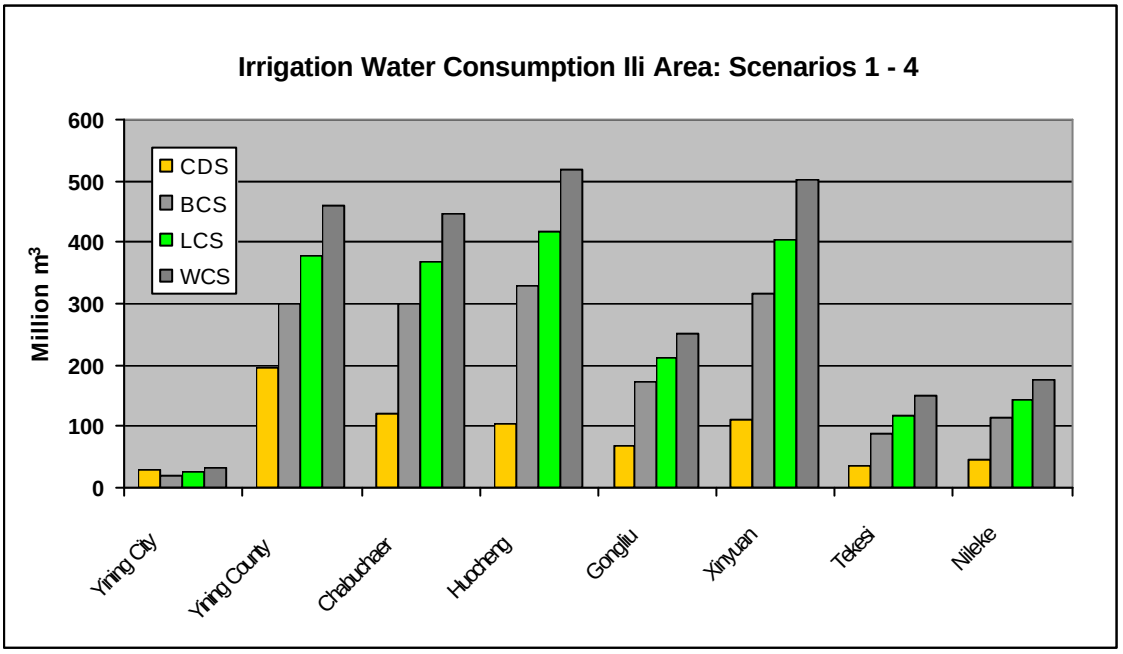

Estimation of the Gross Irrigation Quantities

As mentioned already several times, the results in Table 22 – 26 and Fig. 36 refer to the 'net irrigation ' consumption only, i.e. the water which actually reaches the fields! The conveyance losses as discussed in Chapter 4.3.1 have not yet been taken into account in these estimations! As outlined in Chapter 4.3.1, the irrigation efficiency in the Upper Ili Area can be assumed to be in the order of 50 – 60 % (and possibly even slightly higher). Hence, the quantities given in Tables 22 – 26 and Fig. 36 represent just 50 – 60 % of the 'gross irrigation' quantities, which specifies the 'true' amount of water extracted from the Ili and its major tributaries Tekes, Kunes and Kash for irrigation purposes.

Table 27 summarises different estimations of the resulting totals for the gross irrigation water consumption for the Upper Ili Area. The table presents the totals for the four different scenarios discussed above and assumed irrigation efficiency rates of 40%, 50%, 60% and 70% respectively. The two highlighted data in the LCS column are those which are (in the authors' opinion) the ones which are closest to the real situation.

Assuming realistic irrigation efficiency rates of about 50 – 60% and the Likely Case Scenario as assessment reference, the gross irrigation water consumption in the Upper Ili Area sums up to about 3.5 – 4.1 billion m^3/year. This quantity is used for about 6,000 sqkm of 'normal' crops and about 214 sqkm wetland rice. This corresponds to an average (gross) water consumption of 5,500 – 6,600 m^3/ha/year. These figures are believed to be fairly reliable and accurate and also make sense with regard to data from other sources. These 3.5 – 4.1 billion m^3/year are fairly well in line with the water extraction quantities conceded to by the Chinese in the Project 1515 report. This study numbers the gross water consumption for irrigation purposes at about 4.45 billion m^3/year (Forschungsteam "Projekt 1515 des Ili-Gebietes" und Wissenschafts- und Ingenieurverein vom Ili-Gebiet 1999: 37 -39).

The same study also indicates that the use of groundwater for irrigation purposes is negligible. According to this study, only 0.163 billion m^3 groundwater had been used in 1995 for this purpose. Furthermore, the study also mentions that irrigation water accounts for almost 98% of the extracted surface water! Hence, compared to the quantity of irrigation water, the extraction of water for industrial and other purposes is almost nil (cp. Forschungsteam "Projekt 1515 des Ili-Gebietes" und Wissenschafts- und Ingenieurverein vom Ili-Gebiet 1999: 37 -39).

Table 27: Estimations of the gross irrigation water consumption in 2000/2001 according to Scenarios 1 – 4 and different irrigation efficiency assumptions

	Gross Irrigation Water Consumption (million $m^{3)}$ Scenario 1 - 4			
Assumed Irrigation Efficiency	**CDS**	**BCS**	**LCS**	**WCS**
40%	1799.0	4106.8	5177.0	6339.0
50%	1439.2	3285.4	**4141.6**	5071.2
60%	1199.3	2737.8	**3451.3**	4226.0
70%	1028.0	2346.7	2958.3	3622.3

4.3.3 Water consumption by irrigation in 1976 / 1977

The water consumption in 1976/1977 can be estimated in an order of magnitude only. In Chapter 4.1.2 a first, rough estimation of the likely 'net irrigation area' had been conducted for both points in time, 1976/1977 and 2000/2001. This first assessment was based on various assumptions, one of which was that 90% of the unclassified pixels are actually 'other crop' areas.

Hence, the assumptions used in this first assessment are therefore more or less comparable with the assumptions in the WCS given above. Quite surprisingly, the two results for 2000/2001, which were calculated in very different ways, are almost identical. The first area assessment as given in Chapter 4.1.2 estimated the total irrigation area in 2000/2001 at 6,628 sqkm while the more detailed WCS calculation above came to a total of 6,646 sqkm (214.5 sqkm wetland rice plus 6,431.5 sqkm 'other crops').

This figure of the first, rough assessment of the net irrigation area equalled about 70% of the so-called 'gross irrigation area'. Based on this percentage established for the 2000/2001 situation, the net irrigation area for 1976/1977 was calculated at about 5,475 sqkm. Since this figure is based on WCS assumptions, the actual irrigation area in 1976/1977 area will have been somewhat less, probably in the order of about 5,000 sqkm.

As shown in Chapter 4.2, in 1976/1977 wetland rice cultivation was negligible at best. The very few square kilometres which might (or might not) have existed already at that time can thus be neglected. Hence, for calculation purposes, it can be assumed that the estimated 5,000 sqkm irrigated land had probably been used to 100% for 'normal' crops which receive net irrigation rates between 2,000 and 3,750 m^3/ha.

Multiplying the presumed 5,000 sqkm irrigated land in 1976/1977 with irrigation rates of 2,000 m^3/ha, 2,800 m^3/ha and 3,750 m^3/ha respectively, results in three different estimations of the net irrigation water consumption. Depending on the assumed irrigation rate, the total consumptions adds up to net irrigation rates of about 1.0 billion m^3 (1.0 km^3), 1.4 billion m^3 (1.4 km^3) and 1.875 billion m^3 (1.875 km^3) respectively.

As before, these figures still refer to the net irrigation water consumption only! To estimate 'gross irrigation' water consumption totals which are comparable with the figures calculated for 2000/2001, similar irrigation efficiency rates have to be assumed. Table 28 gives the resulting gross irrigation rates for the three net irrigation quantities quoted above and the assumed irrigation efficiency levels of 40 – 70 %. As in Table 27, the highlighted cells mark the two results which are presumably closest to the real situation.

Table 28: Estimation of the gross irrigation water consumption in 1976/1977 for three net irrigation quantities and different irrigation efficiency rates

Estimated Gross Irrigation Water Consumption (million m^3) 1976 / 1977			
Assumed Irrigation Efficiency	**Assumed net irrigation quantities / year**		
	1,000 mill. m^3	**1,400 mill. m^3**	**1,875 mill. m^3**
40%	2500.0	3500.0	4687.5
50%	2000.0	2800.0	3750.0
60%	1666.7	2333.3	3125.0
70%	1428.6	2000.0	2678.6

According to the highlighted figures, the gross irrigation water extraction in 1976/1977 has totalled between 2.3 and 2.8 mill. m^3/year. Assuming that this water was distributed over an area of about 5,000 sqkm, the average gross water consumption totals between 4,700 and 5,600 m^3/ha/year. The latter figure is well in line with the per hectare consumptions calculated for 2000/2001, especially if taking into account that wetland rice cultivation was negligible in 1976/1977.

4.3.4 Comparison of the gross water consumption in 1976/1997 versus 2000/2001

According to the calculations made in Chapter 4.3.2 and 4.3.3, the gross irrigation water consumption were estimated to total:

- about 2.3 to 2.8 billion m^3/year in 1976/1977 and
- about 3.5 to 4.1 billion m^3/year in 2000/2001.

From these figures it can be concluded that during the 25 years in between the yearly extraction of irrigation water has increased by approximately 1.0 – 1.5 billion m^3/year. This corresponds to an average yearly increase rate of about 40 – 60 million m^3 or a total increase of about 50 % in 25 years (based on the 1976/1977 figures as reference).

5. CONCLUSIONS

The principal objective of this study was to survey the extension of the irrigation areas in the Upper Ili Catchment and to assess the resulting water consumption. The main reason for this research was the fact that different sources give quite dissimilar figures for the water use in this area. Nobody really seems to know which figures are right and which are wrong! However, this is not just a scientific dispute about disagreeing research results. The actual background of these different figures has a political dimension: the disagreement between Kazakhstan and China over the use of the water resources of the Ili system.

The Kazakhs are suspecting that already now too much water is being extracted on the Chinese side of the Upper Ili Catchment and that even more will be extracted in the future. They are anxious that the ongoing extension of the irrigation areas on the Chinese side of the border might gradually run dry the Lake Balkhash further downstream (cp. Tursunov 2002a). Hence, this is the classical conflict of interest between the users at the upper and the users at the lower part of a river system. The technical reason of the dispute is that only part of the hydrological base data of such a large river system can be measured exactly, for example the river discharge at a given reading point. Other base data, such as the water renewal rate within the catchment are mainly based on indirect data (e.g. rainfall) and several estimated parameters (e.g. evapotranspiration, surface runoff, infiltration rate etc.).

As discussed in detail in Chapter 1, the Kazakhs at the lower end of the river system are afraid that they do not receive their full share of the Ili water. Consequently, their estimations of the water resources tend to assess the renewal rate relatively low and the water extraction on the Chinese side comparably high. As also outlined in Chapter 1, the Kazakhs are also likely to extrapolate the effects of the planned irrigation projects in the most pessimistic way, using high area figures and somewhat inflated unit water consumption rates (cp. the authors' comments in Chapter 1, Footnote 1).

The Chinese, on the other hand, want to keep as much Ili water as possible on their side of the border as resource for their ambitious land development and irrigation projects. Hence, their estimations of the water resources and the water extraction totals will tend to be just the other way round! Their estimations of the water renewal rate of the Ili system will be on the high side and the assessment of their own water extraction might possibly be biased to the low side. However, the data presented by the Chinese side are even more complicated, because they are rather inconsistent! Different Chinese sources give quite different figures and – see again Chapter 1 – even within the same source unaccountably big differences occur for the extent of irrigation areas as well as regarding the amount of water extracted from the Ili system.

The present study attempts to clarify this situation. The dispute on a just distribution of the Ili water resources and efficient ways of using these resources should stick to facts and rely on figures which are based on evidence rather than on vague assumptions or claims which cannot be verified. Despite some limitations of the used satellite imagery and despite some technical and organisational constraints, the authors believe that this study provides such 'hard' figures!

A systematic and transparent approach was followed to obtain water consumption data which are believed to be fairly accurate and reliable. In a first step, the net irrigation areas were mapped from satellite images, using a combination of visual interpretation and digital image processing. As second step, area-specific net irrigation rates for different crops were enquired from local farmers in the area. Finally, as third step, the irrigation efficiency rate was estimated to account for the water conveyance losses. The parameters used in the subsequent calculations were estimated on the basis of data taken from standard textbooks (ILACO 1981, Landon (Ed.) 1984) and verified by the respective data for comparable irrigation systems in the Amu Darja Delta (cp. Ressl 1999). Based on these key data, the approximate water consumption could be calculated fairly accurately for each county. Finally the county sub-totals were added up to calculate the overall total water consumption for the Upper Ili Catchment.

Of course, the results of this study cannot be 100% correct either! The visual mapping of the irrigation areas are likely to include minor errors, especially due to the fairly limited fieldtruth data which could be compiled during the study. Likewise, the digital image classification will include some misclassified areas. Finally, also our calculations had to include certain (sensible) assumptions on various levels of the calculation process. However, despite these potential error sources, the overall result is likely to be fairly accurate and probably provides the most reliable figures presently available for the Upper Ili Area!

The potential error of the presented calculations can, of course, be estimated only. The authors reckon that the area figures resulting from the satellite image based irrigation survey do not deviate from the reality by more than 10 – 15 % at most. The net irrigation rates are probably even more accurate because they were directly enquired from the farmers. The third calculation parameter, the irrigation efficiency percentage, is less verified than the other two and may thus bear the biggest error potential. For this reason, not a single figure but a range of results has been presented in Chapter 4.3.2, based on different assumptions about the irrigation efficiency. Nevertheless, even in this case, some of the assumptions (i.e. efficiency rates of 50 - 60%) are much more likely than others (40%, 70%).

The results of our investigations clearly show that the Chinese data on the extension of their irrigation areas in the Upper Ili Region are almost useless! The data are inconsistent and, in any case, far off the reality! According to Chinese sources, the irrigation area totals either 1,842 sqkm (year 1995, Project 1515 report) or 2,229 (year 2001, Statistical Yearbook) or 3,450 sqkm (year 1995, Project 1515 report) (cp. Statistical Bureau for Xinjiang (Ed.) 2002, Forschungsteam "Projekt 1515 des Ili-Gebietes" und Wissenschafts- und Ingenieurverein vom Ili-Gebiet (Hrsg.) 1999). However, not one of these three figures is anywhere close to the real situation! According to our survey and the resulting calculations, the correct extension of the irrigation areas was about 6,000 – 6,500 sqkm in 2000/2001. Even if this result were overestimating the real situation somewhat (e.g. 10 – 15%) it would still be more than 50% higher than even the highest of the three Chinese figures and more than 100% higher than the two other data quoted!

A comparison of the figures on wetland rice cultivation provides concrete and verifiable evidence how far off the Chinese data are from the real situation! Unlike the calculated figures for the overall irrigation area, which had to include certain assumptions, the wetland rice cultivation could be mapped directly, accurately and reliably. According to this satellite image survey, the wetland rice area totals 214.5 sqkm, more than three times as much as the 61.5 sqkm given by the Statistical Yearbook (cp. Statistical Bureau for Xinjiang (Ed.) 2002)!

Somewhat surprisingly, the water consumption figures are by far more realistic than the data on the irrigation areas. Again, different sources give different figures for the amount of Ili water extracted by the Chinese, ranging between about 2.35 km^3 and about 4.404 km^3 per year (cp. Project 1515 report, Forschungsteam "Projekt 1515 des Ili-Gebietes" und Wissenschafts- und Ingenieurverein vom Ili-Gebiet (Hrsg.) 1999, p. 34-35). While the lower figure is obviously unrealistic, the bigger of the two figures is well in line with the results of this study! As presented and discussed in Chapter 4.3.2 (cp. Table 21), the most likely calculation – i.e. 'Likely Case Scenario' assuming an irrigation efficiency of 50 – 60% - results in a total gross water consumption of about 3.45 – 4.15 km^3/year. This fits almost exactly the 4.404 km^3 given by the Project 1515 report. The study thus more or less confirms the commonly quoted water extraction rate of about 40 – 4.5 km^3 per year. This figure is also well in agreement with sensible, realistic (gross) water consumption rates of about 5,000 – 6,000 m^3/ha.

Summarising it can thus be concluded that the Chinese are (at present) probably not yet extracting more than the 4.5 km^3/year which they concede already! However, it should be kept in mind that the Chinese plans for new irrigation areas in the Ili catchment are not yet fully implemented (cp. Fig. 3, 27, 29 and 31). It is also possible that in particular the extremely water-consuming wetland rice areas will be extended further. In the last 25 years, the still ongoing extension of the Chinese irrigation areas resulted in an average increase of the water extraction rate of 40 – 60 million m^3/year (cp. Chapter 4.3.4). Assuming similar yearly increases for the future, the total water extraction for irrigation may soon reach the 5.0 km^3/year threshold.

The only feasible solution to resolve the problem of the dwindling water resources seems to be an increase of the – at present - relatively low irrigation efficiency rate. As illustrated by Table 28, increasing the average irrigation efficiency from 50% to 60% would result in a water saving in the order of 0.47 km^3/year. Assuming a gross irrigation rate of 5,500 m^3/ha, the water saving would be sufficient to irrigate another 850 sqkm.

6. LITERATURE

Dostaj, Ž.D. (1999): Naucnye osnoy upravlenija gidroekologiceskim sostojaniem besstocnych bassejnov Centralnoj Azii (na primere bassejna oz. Balchaš). Dissertacija na soisk. uc. st. doktora geograficeskich nauk. Almaty, 306 pp.

Eastman, J.R. (2001): IDRISI 32 Release 2: Guide to GIS and Image Processing. Volume 2. Manual Version 32.20. Clark Labs, Clark University, Worcester (MA), USA.

Earth Resource Mapping Pty Ltd (1998): ER-Mapper 6.0 User Guide**.** Revision 6.0, 30. Sept. 1998, Release 6.0.

Hamid, Y. (2003a): Zwischenbericht über die Forschung im Ili-Tal. Unveröffentlichter Projekt-zwischenbericht. Gießen.

Hamid, Y. (2003b): Fieldcheck results for the satellite image interpretation. Unpublished fieldwork report with data collected from various sources (in particular personal communication in the field).

ILACO (1981): Agricultural compendium for rural development in the tropics and subtropics. Produced and edited by ILACO B.V., International Land Development Consultants / Arnheim. Elsevier Scientific Publishing Company. Amsterdam, Oxford, New York.

Koch, B., Ivits, E., Jochum, M. (2003): Object-based versus Pixel-based. Forest classification with eCognition and ERDAS Expert Classifier. In: GIM International 12 (Vol. 17), p. 12 – 15.

Landon, J.R. (Ed.) (1984): Booker Tropical Soil Manual. A handbook for soil survey and agricultural land evaluation in the tropics and subtropics. Compiled by Booker Agricultural International Ltd., Longman Inc., New York.

Lohmann, G. (1991): An evidential reasoning approach to the classification of satellite images. In: DLR-Research Report 91.29, Deutsche Versuchsanstalt für Luft- und Raumfahrt, Köln.

Mather, P.M. (1999): Computer-processing of remotely-sensed images. 2nd edition. John Wiley & Sons, Chichester, New York, Weinheim, Brisbane, Singapore, Toronto.

Ressl, R. (1999): Fernerkundungs- und GIS-gestützte Optimierung des Bewässerungsfeldbaus am Amu-Darja-Unterlauf und in seinem Delta. Dissertationsschrift an der Fakultät für Geowissenschaften Ludwig-Maximilians-Universität München. Deutsches Fernerkundungsdatenzentrum (Hrsg.), Oberpfaffenhofen und Köln.

Rogers, D.H., Lamm, F.R., Alam, M. et al. (1999): Efficiencies and water losses of irrigation systems. Irrigation Management Series. MF-2243. Cooperative Extension Service, Kansas State University, Manhattan.

Statistical Bureau for Xinjiang (Ed.) (2002): Statistical Yearbook Xinjiang. Uygur Autonomous Region. Urumqi.

Tursunov, A.A. (2002a): Ot Arala do Lobnora. Gidrologija besstocnych bassejnov Centralnoj Azii. Almaty, 383 pp.

Tursunov, A.A. (2002b): Sovremennaja ocenka vodnych resursov transgranicnoj reki Ili s ucetom klimaticeskich izmenenij i principov sovmestnogo ispol'zovanija. Almaty. 16 pp. (unpublished paper)

Forschungsteam "Projekt 1515 des Ili-Gebietes" und Wissenschafts- und Ingenieurverein vom Ili-Gebiet (Hrsg.) (1999): Forschungen zur Erschließung des Ili- und Irtysch-Einzugsgebietes (Yili He e Erqisi He Liuyu Kaifa Yanjiu). Xinjiang Renmin Verlag, Urumqi.

Bisherige Veröffentlichungen in dieser Reihe:

No. 1 HERRMANN, R., KRAMB, M. C., MÖNNICH, Ch. (12.2000): Tariff Rate Quotas and the Economic Impacts of Agricultural Trade Liberalization in the WTO. (etwas revidierte Fassung erschienen in: "International Advances in Economic Research", Vol. 7 (2001), Nr. 1, S. 1-19.)

No. 2 BOHNET, A., SCHRATZENSTALLER, M. (01.2001): Der Einfluss der Globalisierung auf staatliche Handlungsspielräume und die Zielverwirklichungsmöglichkeiten gesellschaftlicher Gruppen.
(erschienen in: "List-Forum für Wirtschafts- und Finanzpolitik", Bd. 27(2001), H. 1, S. 1-21.)

No. 3 KRAMB, M. C. (03.2001): Die Entscheidungen des "Dispute Settlement"-Verfahrens der WTO im Hormonstreit zwischen der EU und den USA – Implikationen für den zukünftigen Umgang mit dem SPS-Abkommen.
(überarbeitete Fassung erschienen in: "Agrarwirtschaft", Jg. 50, H. 3, S. 153-157.)

No. 4 CHEN, J., GEMMER, M., TONG, J., KING, L., METZLER, M. (08.2001): Visualisation of Historical Flood and Drought Information (1100-1940) for the Middle Reaches of the Yangtze River Valley, P.R. China.
(erschienen in: Wu et al. (eds) Flood Defence '2002, Beijing, New York 2002, pp. 802-808.)

No. 5 SCHROETER, Ch. (11.2001): Consumer Attitudes towards Food Safety Risks Associated with Meat Processing.
(geänderte und gekürzte Fassung ist erschienen unter Christiane SCHROETER, Karen P. PENNER, John A. FOX unter dem Titel "Consumer Perceptions of Three Food Safety Interventions Related to Meat Processing" in "Dairy, Food and Environmental Sanitation", Vol. 21, No. 7, S. 570-581.)

No. 6 MÖNNICH, Ch. (12.2001): Zollkontingente im Agrarsektor: Wie viel Liberalisierungsfortschritt? Ergebnisse und Diskussion einer Auswertung der EU-Daten.
(gekürzte Fassung erschienen in BROCKMEIER, M., ISERMEYER, F., von CRAMON-TAUBADEL, S. (Hrsg.), Liberalisierung des Weltagrarhandels - Strategien und Konsequenzen. "Schriften der Gesellschaft für Wirtschafts- und Sozialwissenschaften des Landbaues e.V.", Bd. 37(2002), S. 51-59.)

No. 7 RUBIOLO, M. (01.2002): EU and Latin America: Biregionalism in a Globalizing World?

No. 8 GAST, M. (02.2002): Zollkontingente bei US-amerikanischen Käseimporten.
(gekürzte Fassung erschienen in: "Agrarwirtschaft", Jg. 51, H. 4, S. 192-202.)

No. 9 BISCHOFF, I. (08.2002): Efficiency-enhancing Effects of Private and Collective Enterprises in Transitional China.

No. 10 KÖTSCHAU, K. M., PAWLOWSKI, I., SCHMITZ, P. M. (01.2003): Die Policy Analysis Matrix (PAM) als Instrument zur Messung von Wettbewerbsfähigkeit und Politikeinfluss - Zwischen Theorie und Praxis: Das Fallbeispiel einer ukrainischen Molkerei.

No. 11 HERRMANN, R., MÖSER A. (06.2003): Price Variability or Rigidity in the Food-retailing Sector? Theoretical Analysis and Evidence from German Scanner Data.

No. 12 TROUCHINE, A. (07.2003): Trinkwasserversorgung und Armut in Kasachstan: Aktueller Zustand und Wechselwirkungen.

No. 13 WANG, R.; GIESE, E.; GAO, Q. (08.2003): Seespiegelschwankungen des Bosten-Sees (VR China).

No. 14 BECKER, S.; GEMMER, M.; JIANG, T.; KE, CH.. (08.2003): 20th Century Precipitation Trends in the Yangtze River Catchment.

No. 15 GEMMER, M.; BECKER, S.; JIANG, T (11. 2003): Detection and Visualisation of Climate Trends in China.

No. 16 MÖNNICH, Ch. (12.2003): Tariff Rate Quotas: Does Administration Matter?

No. 17 GIESE, E.; MOßIG. I. (03.2004) Klimawandel in Zentralasien

No. 18 GIESE, E.; Sehring, J. Trouchine, A. (05.2004) Zwischenstaatliche Wassernutzungskonflikte in Zentralasien

No. 19 Dikich, A.N.; Hagg, W. (09.2004) Gletscherwasserressourcen in Zentralasien

No. 20 CHRISTIANSEN, T. GIESE, E.; Schöner, U. (11.2004) Das obere Ilital

Stand 28. Oktober 2004
Die Diskussionsbeiträge können im Internet unter:
http://www.uni-giessen.de/zeu/Publikation.html eingesehen werden.